THESIS FOR THE DEGREE OF LICENTIATE OF ENGINEERING

# Grid Reinforcing Wind Generation

NAYEEM RAHMAT ULLAH


Department of Energy and Environment
Division of Electric Power Engineering
CHALMERS UNIVERSITY OF TECHNOLOGY
Göteborg, Sweden 2006

**Grid Reinforcing Wind Generation**
NAYEEM RAHMAT ULLAH



Technical Report at Chalmers University of Technology

Division of Electric Power Engineering
Department of Energy and Environment
Chalmers University of Technology
SE-412 96 Göteborg
Sweden
TEL: + 46 (0)31-772 1000
FAX: + 46 (0)31-772 1633
http://www.elteknik.chalmers.se/

Chalmers Bibliotek, Reproservice
Göteborg, Sweden 2006

Grid Reinforcing Wind Generation
NAYEEM RAHMAT ULLAH
Division of Electric Power Engineering
Department of Energy and Environment
Chalmers University of Technology

# Abstract

In this thesis, effects of some grid assisting possibilities that wind turbines could be equipped with, are investigated. The background is that concerns regarding the stability of the already existing power system in the presence of large wind farms have been risen. Variable speed wind turbines have power electronic based frequency converters already included in their design and the idea used in this thesis is to utilize the fast controllability of these converters to assist the grid.

It is found that the transient stability of conventional synchronous generators located nearby a wind farm, can be increased if a suggested contingency operational mode is incorporated into the control of the wind farm. Another finding is that large wind farms integrated into the transmission level with their control properly modified, can increase the steady state power transfer limit of the transmission line as well as assist the grid to delay or even prevent a voltage collapse event. It is also shown that wind farms integrated into the grid in the distribution level together with different loads, have the possibility to increase the short term voltage stability of the network provided that their controls have been modified accordingly.

Finally, the suggested grid assisting methods are incorporated into the control of two large planned wind farms in the southern part of the Swedish grid and tested in the CIGRÉ Nordic32 test grid, which is taken as a representation of the Swedish transmission network. It is concluded that care has to be taken if voltage control mode of operation is utilized in a wind farm located close to a conventional synchronous generator. The interaction between the operational mode of a wind farm and the overall synchronous generator control may interact with each other and could lead to a reduction of damping of power oscillations in nearby transmission lines instead of increasing the damping.

**Keywords:** variable speed wind turbine, frequency converter, transient stability, long term voltage stability, short term voltage stability.

# Acknowledgements

This work has been carried out at the Division of Electric Power Engineering, Department of Energy and Environment at Chalmers University of Technology. The financial support provided by E.ON Sverige is gratefully acknowledged. The author would also like to express his gratitude towards Dan Andersson and Åke Juntti from E.ON Elnät Sverige AB for their valuable technical assistance.

The author would like to thank his supervisor Dr. Torbjörn Thiringer for his kind patience, constant guidance, encouraging comments and revising the thesis manuscript to give it a better shape. In addition, the author acknowledges the motivational words from his examiner Professor Tore Undeland, especially when they were mostly needed.

The author expresses his sincere gratitude towards Dr. Daniel Karlsson from Gothia Power AB for his valuable technical comments.

The author also express sincere appreciation to Dr. Pablo Ledesma from Universidad Carlos III de Madrid for his kind assistance in helping writing user defined models in PSS/E. Special thanks are due to Dr. Andreas Petersson for helping with the research by providing support to compare wind farm models and giving practical tips to get started with the LaTeX.

Finally, the author would like to thank all his colleagues at the division of Electric Power Engineering.

# Table of Contents

# Chapter 1

# Introduction

Wind power as an energy source has been used for a long time. Wind turbines date back many centuries for irrigation and corn grinding. Denmark was the first country to utilize wind energy to produce electricity [1]. By 1910, wind turbines with capacities of 5 to 25 kW were in operation in Denmark [1].

The present interest in commercial green power in the developed world started in the mid-1970s after the first oil crisis [2]. At that time, the green power activities were driven by the goal to reduce the dependency on fossil fuels. In today's perspective, the goals of the green power activities is to reduce the $CO_2$ emission resulting from the burning of fossil fuels as well as to reduce the dependency on oil [2].

Today, the capacity of larger wind turbines has grown to 2-3 MW and more. Some of the manufacturers have already developed prototype turbines having a rating as high as 4 to 6 MW [3], [4], [5], [6].

## 1.1 Current wind power status

On a percentage basis, wind power is the fastest growing electricity generation source in the world with a fascinating 20% annual growth rate for the past five years [7]. During 2005, 10 GW of wind turbines were installed worldwide. In total, the worldwide installed capacity, by the end of 2005 was roughly 58 GW [8]. According to [8], these turbines can produce 140 billion kWh of energy which is 1% of the global electric energy requirements.

The EU member states are leading the wind energy sector hosting 70% of the world's installed wind capacity [9]. With over 40 GW of installed wind turbines by the end of 2005, which will produce 83 TWh in an average wind year, the EU can meet 2.8% of its electricity consumption from wind energy [9].

The U.S. is hosting 16% of the world's installed wind energy capacity (9.2 GW) [10]. According to [7], the U.S. capacity could reach 100 GW by 2020, meeting 6% of the electricity demand.

By the end of 2005, the total installed capacity in Sweden was 500 MW [9]. An annual growth of 13% was observed. According to [11], 0.5% (0.82 TWh) of the Swedish electricity consumption was met by the wind energy during 2005. The Swedish National Energy Agency has proposed a planning target of 10 TWh/year of wind energy expansion in the coming 10-15 years [12]. Several large wind farm projects, totalling nearly 2 GW of installed capacity, are under planning stage which could be realized in the next 5 to 10 years

[13], [14].

## 1.2 Demands from utilities on wind turbines

Besides connecting a single wind turbine scattered into the network with a rating of 0.5 to 2 MW, wind turbines are more and more being connected as groups of turbines with a total capacity ranging from tens of MWs to hundreds of MWs. With increasing penetration level of wind power, it is important to assure that the power system stability will not be endangered by a large scale wind power integration into the network. Due to the intermittent nature of the wind, existing grid codes which were established for the dispatchable generating resources, could not be fully applied to wind power. The German grid operator E.ON Netz first proposed the changes to its grid code regarding wind turbines in 2003 starting with the low-voltage ride-through issue. The modification of the grid codes of many other countries in Europe and other parts of the world have built on E.ON's work [7]. A comparison of some international connection regulations for wind energy installation can be found in [15].

## 1.3 Possible interaction of wind turbines with the utility network

As the integration level of wind energy is increasing into the power system, the issues related to the stability of the power system operation are becoming of utmost importance, as mentioned earlier. In certain parts of the grid, where the wind power penetration level is significant, disconnection of wind turbines due to a minor grid disturbance would cause serious power system operational problems. Accordingly, it would be beneficial for the grid if wind turbines can *ride-through* the voltage dip.

As an important member of the power system world, the wind generators should react *responsibly*. Which means, wind generators should not degrade the stability of the power system, instead they should contribute to an increase of the stability of the system while considering the intermittent nature of the wind.

Today wind turbines of variable speed type has become more common than traditional fixed-speed turbines [16]. For a variable speed wind turbine, the generator is controlled by a power electronic converter. In 2002, the total market share of variable speed turbines equipped with a power electronic converter was 67% [16]. Fast control of active and reactive power can be achieved using these types of turbines.

A variable speed, pitch-regulated wind turbine system with a full power electronic converter and a synchronous/induction generator is a commonly used system today [16]. In 2002, the worldwide market share of this type of turbine was over 20% [16]. From power system point of view, this particular configuration is interesting because the power electronic interface completely isolates the generator from rest of the power system and only the converter characteristic is seen by the grid [17]. The fast controllability of the power electronic converter can be utilized to shape the response of the wind turbine against various network disturbances and thus making the wind turbine to react *responsibly*.

A well known method to improve the steady-state power transmitted by the existing transmission line and also to improve the voltage stability limit is to inject reactive power into the

system near load centers [18], [19], [20]. Power electronic based reactive power compensators like the variable impedance type SVC (Static Var Compensator) and the converter based STATCOM (Static Synchronous Compensator) can control the voltage in a fast and continuous manner, unlike mechanically switched capacitors/reactors [21]. Several technical papers are available showing the applicability and effect of these power electronic based var compensators on the steady-state and transient voltage stability of electric power systems [22], [23], [24], [25]. Some utility applications of these devices are listed in [21].

An interesting possibility is to incorporate the SVC/STATCOM function into the control of variable speed pitch regulated wind turbine systems which have power electronic converters already included in their design. By doing so, this type of wind turbine system could also be seen as a reactive power source like a STATCOM besides being an intermittent power source.

A recent draft version of a technical regulation for wind farms connected to the transmission grid in the Danish system, provides guidelines for reactive power control of wind farms [26]. This regulation requires wind farms to have the capability for altering active and reactive power production via remote control, and locally, on demand by the system operator, depending on the network situation. This implies that the system operator would have the potential to utilize the reactive power injection capability of a modern wind farm to increase the system security and the wind farm owners would have the opportunity to trade with the built-in reactive power injection facility in the deregulated market environment.

## 1.4 Purposes of the work

The main purpose of this thesis is to investigate how the power electronic controllability of modern wind turbines can be utilized to improve the power system stability. In addition, a purpose is to investigate how the transient stability of the Swedish transmission system will be affected by the connection of several large wind farms in the southern part of the network. Finally, a goal is to discuss algorithms for the active and the reactive control of a wind installation to obtain a grid reinforcing property.

## 1.5 Publications

The publications related to this thesis are listed below:

1. **N. R. Ullah**, J. Groot, T. Thiringer, "The Use of a Combined Battery/Supercapacitor Storage to Provide Voltage Ride-Through Capability and Transient Stabilizing Properties by Wind Turbines," in Proc. *1st European Symposium on Super Capacitors and Applications ESSCAP'2004*, 2004.

2. **N. R. Ullah**, T. Thiringer, "Improving Voltage Stability by Utilizing Reactive Power Injection Capability of Variable Speed Wind Turbines," *International Journal of Power and Energy Systems*, 2006 (accepted for publication).

3. **N. R. Ullah**, "Small Scale Integration of Variable Speed Wind Turbine into the Local Grid and Its Voltage Stability Aspects," in Proc. *IEEE International Conference on Future Power Systems FPS 2005*, 2005.

4. **N. R. Ullah**, T. Thiringer, “Effect of Operational Modes of a Wind Farm on the Transient Stability of Nearby Generators and on Power Oscillations: A Nordic Grid Study” In Proc. *Nordic wind power conference NWPC’06*, 2006.

5. O. Carlson, A. Perdana, **N. R. Ullah**, M. Martins and E. Agneholm, “Power System Voltage Stability Related to Wind Power Generation” in Proc. *European Wind Energy Conference and Exhibition*, *EWEC 2006*, 2006.

6. Å. Larsson, A. Petersson, **N. R. Ullah**, O. Carlsson, “Krieger’s Flak Wind Farm” in Proc. *Nordic wind power conference NWPC’06*, 2006.

Some selected publications are appended at the end of the thesis.

# Chapter 2

# Overview of the wind energy conversion system (WECS)

The main components of a modern wind energy conversion system (WECS) are the tower, the rotor blades and the nacelle, which accommodates the transmission mechanism, the electricity generating system, the wind measuring device, and for a horizontal-axis device, the yaw systems. Switching equipments and the protection system, lines and the step-up transformers are also required to supply the extracted wind energy to the end users. This chapter will start with a brief description of the aerodynamic power conversion and control principle of a wind turbine. Later, some commonly used generator systems for a wind turbine are discussed.

## 2.1 Aerodynamic power conversion

### 2.1.1 Lift and drag forces

Airflow over a stationary airfoil produces two forces, a lift force perpendicular to the airflow and a drag force in the direction of the airflow, as shown in Fig. 2.1 [1], [27]. A good lift to drag ratio depends on the existence of laminar flow over both the sides of the airfoil. When the airfoil is allowed to move in the direction of the lift, a relative direction of the airflow is established as shown in Fig. 2.1. To maintain a desired lift to drag ratio, the airfoil has to be reoriented to suit the wind situation. Important to note is that the lift force is perpendicular to the relative wind but is not in the direction of airfoil motion [1], [27]. The lift and drag forces can be split into two components parallel and perpendicular to the undisturbed wind direction. Force $F_Q$, perpendicular to the undisturbed wind direction is the available force to do the useful work. Force $F_T$, in the direction of the undisturbed wind, is the force that the airfoil support should withstand [1].

One way to utilize the torque force $F_Q$ is to connect three such airfoils or blades to a central hub and allow them to rotate around a horizontal axis. This type of arrangement is known as horizontal-axis wind turbine (HAWT). The force $F_Q$ causes a torque that rotates the rotor blades and this rotational motion is utilized to drive the rotor of a generator to produce electricity [1].

The overall performance of a wind turbine depends on the construction and the orientation of the blades [1]. One important parameter is the pitch angle $\beta$, shown in Fig. 2.2. This

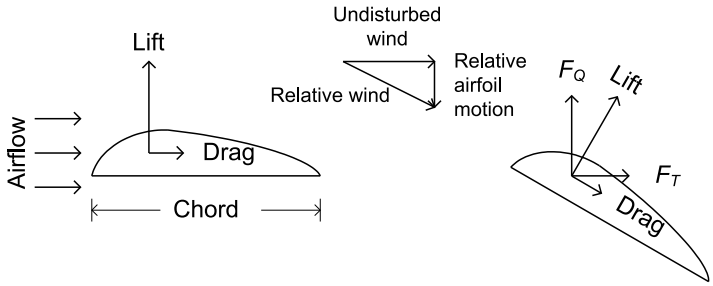


Fig. 2.1: Lift and drag forces on a stationary and translating airfoil.

is the angle between the cord line of the blade and the plane of rotation. The cord line is the straight line connecting the leading and trailing edges of an airfoil. The pitch angle is a static angle and depends only on the orientation of the blade. Another important parameter is the angle of attack $\gamma$, shown in Fig. 2.2. This is the angle between the chord line of the blade and the relative wind direction. It is a dynamic angle, depending on both the speed of the blade and the speed of the wind [1] for a given pitch angle.

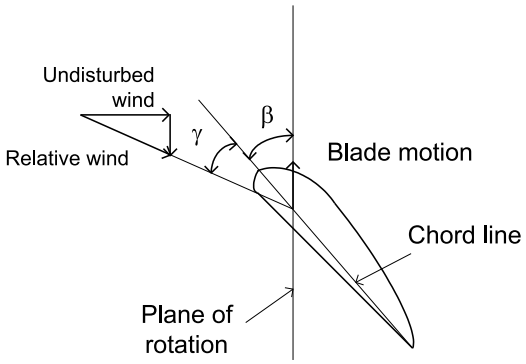


Fig. 2.2: The pitch angle $\beta$ and the angle of attack $\gamma$.

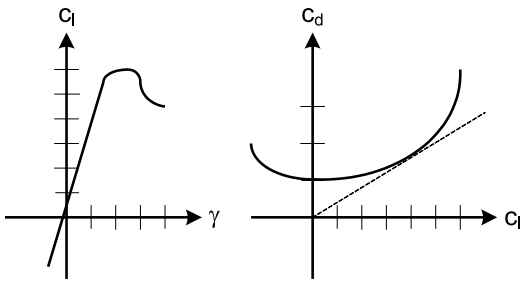


Fig. 2.3: lift and drag co-efficient of an airfoil.

The lift coefficient ($c_l$) against the angle of attack and the drag coefficient ($c_d$) against the lift coefficient for a airfoil is shown in Fig. 2.3. A line through the origin of the $c_d$-$c_l$ curve tangent to it gives the point of maximum lift to drag ration. This maximum establishes the best angle of the resultant aerodynamic force vector for the generation of torque [27].

### 2.1.2 Power output from a wind turbine

The fraction of power extracted from the available power in the wind by a wind turbine is given by the aerodynamic efficiency coefficient $C_p$. The aerodynamic efficiency coefficient can be determined either by measuring the power from the turbine or by the lift and the drag coefficients. The mechanical power output can be written as [1]

$$P_m = C_p(\lambda, \beta)(\frac{1}{2}\rho A_r \omega^3) \tag{2.1}$$

$$\lambda = \frac{\Omega_r r_r}{\omega}, \tag{2.2}$$

where $\beta$ is the pitch angle, $\lambda$ is the tip speed ratio, $\omega$ is the wind speed, $\Omega_r$ is the rotor speed (low speed side of the gear box), $r_r$ is the rotor blade length, $\rho$ is the air density and $A_r$ is the area swept by the rotor. The coefficient of performance $C_p$ is not a constant number, instead it varies with the wind speed, the rotational speed of the turbine and turbine blade parameters such as angle of attack and pitch angle. A typical $C_p(\lambda)$ curve and wind speed - power curve for different pitch angles are shown in Fig. 2.4 and Fig. 2.5, respectively.

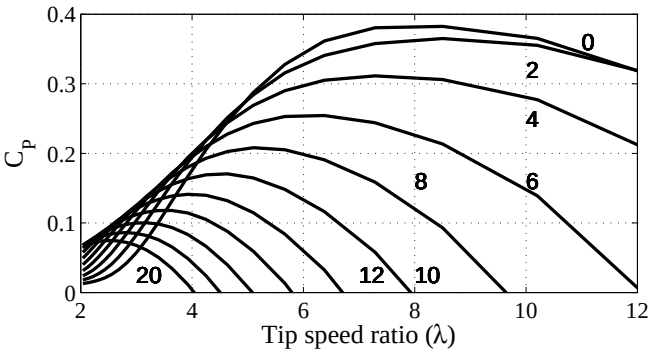


Fig. 2.4: A typical $\lambda$-$C_p$ curve for different pitch angle (from $0^o$ to $20^o$).

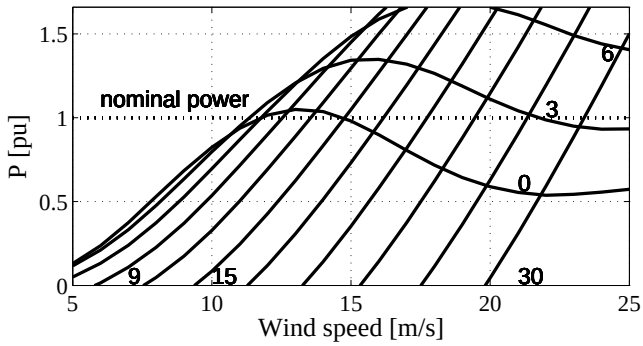


Fig. 2.5: A typical wind speed - power curve of a wind turbine operating at a fixed speed for different pitch angles.

## 2.2 Aerodynamic power control

The operation of a wind turbine involves starting the wind turbine from the rest, stopping the turbine under a wide range of normal and abnormal conditions and modulating the system power and load while the turbine is running [28]. The starting of many stalled controlled wind turbines is accomplished by turning the generator by a starter motor. For pitch controlled turbines, the aerodynamic control surface is employed to assist the startup process [28]. Aerodynamic control is particularly attractive for stopping the rotor and almost all horizontal axis wind turbines employ some sort of aerodynamic control to prevent rotor over speed. The third control function of regulating power output has been accomplished historically by use of aerodynamic control surfaces [28].

The power output from a wind turbine is determined by the value of $C_P$ which depends on wind speed, turbine rotational speed and the blade pitch angle. As the speed of the wind can not be controlled, the power output from a wind turbine can only be controlled by varying the rotational speed and/or the pitch angle. Based on this fact different control strategies can be employed to regulate the output power of the turbine.

### 2.2.1 Stall control

When no blade pitching mechanism is available i.e. when the pitch angle of the blade is constant, the so-called stall control is employed to limit the power extraction. In normal operation, laminar flow is obtained at the rotor blades [29]. A high lift to drag ratio is achieved in partial loading ranges and thus a high degree of aerodynamic efficiency is attained [29]. On the other hand, when the wind speed approaches the value at which the generator reaches its rated power, further torque development should be avoided [29]. Wind speeds exceeding rated value cause higher angle of attack (note Fig. 2.2) and thus to stalling. According to the characteristics of lift and drag as a function of the angle of attack, as shown in Fig. 2.3, this causes lift to diminish in certain areas and drag to increase [29]. When the turbine is under full load and the wind speed increases to the range beyond, this results in a lower rotor torque and a lower performance coefficient.

The main advantage with stall control is the fixed connection of the rotor blades to the hub. One drawback, however, is the maximization of the power production at a certain wind speed which is determined by the geometry of the rotor blade.

Wind turbine manufacturers like Made and Ecotecnia use this type of control method for their MW range turbines [16]

### 2.2.2 Active stall control

Referring to Fig. 2.2, during high wind speed situations when the angle of attack is higher, increasing the pitch angle during those situations will reduce the angle of attack i.e. the stall point could be pushed into a higher wind speed region. It is shown in Fig. 2.5 that during high wind speeds, varying the pitch angle in a narrow range ( $0^o$ to $4^o$) can push the stall point $actively$ towards a higher wind speed. This control method is called active stall control [16].

Besides the better exploitation of the wind turbine system during high wind speed situations, this pitching method makes emergency stopping and starting of the wind turbine easier.

This control method is used for larger fixed speed turbines (upto 2.4 MW). Manufacturers like NEG Micon and Bonus use this type of control.

### 2.2.3 Pitch control

This control method is, in principle, same as the active stall control method. But in this method, the pitch angle is varied in a wider range. During high wind speed situations, the angle of attack can be maintained to a lower value by varying the pitch angle in a wider range. In this way laminar flow over the rotor blades can be maintained for higher wind speeds and thus the thrust force can be reduced.

The advantage of this control method is the better exploitation of the system during high wind situations, decrease in thrust force on the turbine, starting and emergency stopping of the turbine. One drawback is the need of a pitching mechanism. Another drawback is the high slope of the power curve at high wind speeds which will cause a large output power variation for a small variation in wind speed.

This control method is used for larger variable speed turbines (up to 5 MW).

## 2.3 Common wind turbine generator systems

### 2.3.1 Fixed speed

The rotor of a fixed speed wind turbine system operates at an almost fixed rotational speed determined by the frequency of the supply grid, the gear ratio and the generator design, regardless of the wind speed. In the fixed speed wind turbine system, the stator of the generator is directly connected to the grid, as shown in Fig. 2.6. Since an induction generator always draws reactive power from the grid, a capacitor bank for reactive power compensation is used in this type of configuration [16]. The output power is limited by the aerodynamic design of rotor blades in the case that the stall control method is used. This is the conventional concept earlier used by many Danish wind turbine manufacturers [16]. As mentioned earlier, for larger units up to 2.4 MW, the control often is modified slightly using the active stall control. In order to increase the power production, the generator of some fixed-speed wind turbines has two sets of stator winding. One is used at low wind speeds and the other is used at medium and high wind speeds. Manufacturers like NEG Micon, Bonus, Made and Ecotecnia produce this type of fixed-speed wind turbine.

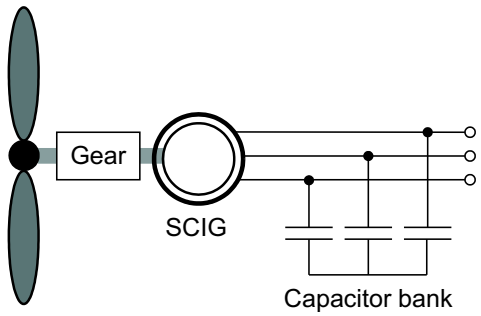


Fig. 2.6: Fixed-speed wind turbine. SCIG = squirrel cage induction generator.

As the rotor speed is constant, the mechanical power on the generator shaft can not be kept constant due to the variation in the wind speed. The mechanical power fluctuation due to the wind variation will be transmitted into the electric output power. A variable speed system, on the other hand, keeps the generator torque fairly constant by changing the generator speed in response to variations in the wind speed. Variations in the incoming wind power are absorbed by rotor speed changes. The aerodynamic power control method almost exclusively used with a variable speed system is the pitch control method [16].

### 2.3.2 Limited variable speed using external rotor resistance

This configuration uses a wound rotor induction generator (WRIG) (Fig 2.7) and has been produced by the Danish manufacturer Vestas since the mid-1990s. The generator is directly connected to the grid and a capacitor bank provides reactive power compensation in exactly the same way as for a standard fixed speed system. The unique feature of this configuration is that it has a variable additional rotor resistance which can be changed by an optically controlled converter mounted on the rotor shaft. This gives a small variable speed range. Typically the speed range is 0-10% above synchronous speed [16].

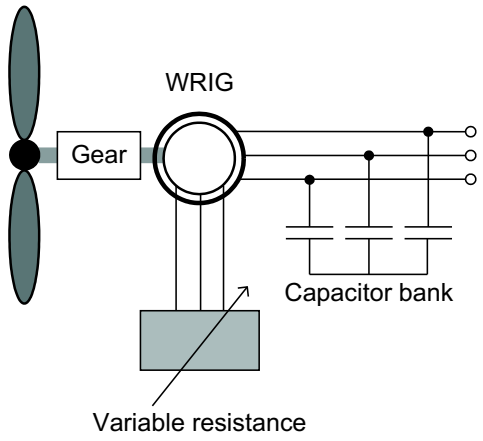


Fig. 2.7: Limited variable speed wind turbine. WRIG = wound rotor induction generator.

### 2.3.3 Variable speed with small scale frequency converter

Fig. 2.8 shows the variable speed wind turbine with a small scale frequency converter located in the rotor circuit, which is known as the DFIG (Doubly-Fed Induction Generator) system. In this type of configuration, the stator is directly connected to the grid while the rotor windings are connected via slip rings to the converter. The frequency converter is rated at approximately 30% of the generator power [16]. Typically, the variable speed range is -40% to +30% of the synchronous speed [16]. The converter also allows for control of the reactive power.

### 2.3.4 Variable speed with full scale frequency converter

This type of wind turbine concept has a full variable speed range, with the generator connected to the grid through a full scale power converter, as shown in Fig. 2.9. The generator

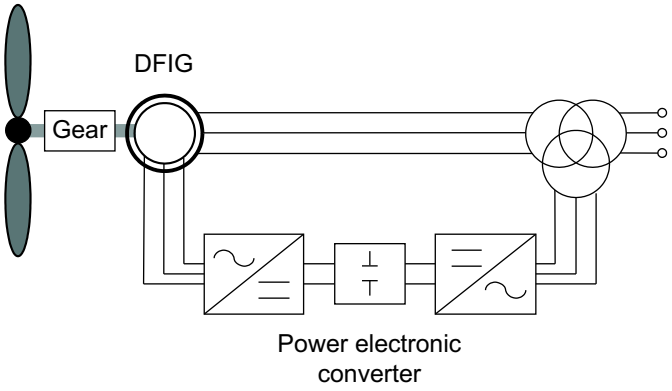


Fig. 2.8: Variable speed wind turbine with a doubly-fed induction generator (DFIG) and a partial scale frequency converter.

can either be an induction machine or a synchronous machine. In case the generator is of synchronous type, it can be excited either by electrically or by permanent magnets. The gearbox is designed so that the maximum rotor speed corresponds to the rated speed of the generator. Some full scale power converter variable speed wind turbine systems have no gearbox. In those cases, a direct driven multiple pole generator with a large diameter is used. The German wind turbine manufacturer Enercon is successfully manufacturing this type of wind turbines [5]. Its worldwide market share is 15.8% (based on the total installed capacity by the end of 2004) [5].

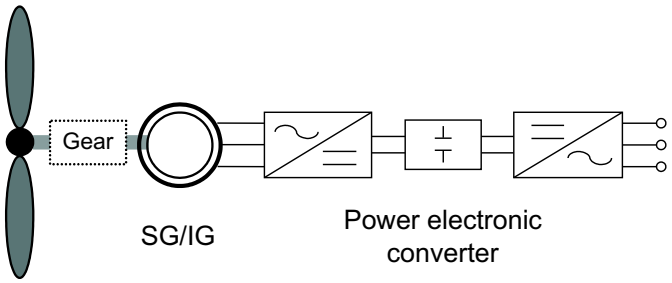


Fig. 2.9: Variable speed wind turbine with a full-scale frequency converter. SG = synchronous generator, IG = induction generator.

# Chapter 3

# Investigated WECS

In this thesis the main focus is on variable speed turbines equipped with a full scale power electronic converter. For the purpose of comparison, a traditional fixed speed wind turbine set-up is also considered. The wind turbine systems investigated in this thesis are described in this chapter.

## 3.1 System A

The system A set-up is shown in Fig. 3.1. It is a traditional fixed speed wind turbine system with a squirrel cage induction generator (SCIG) directly connected to the grid. Since the SCIG always consumes reactive power from the grid, a capacitor bank for reactive power compensation is used in this set-up. Here it is assumed that the no load reactive power compensation is provided by the capacitor bank which means at rated power operation system A consumes reactive power from the grid. It should be mentioned that full reactive power compensation during operation at higher wind speeds is also possible by utilizing switched capacitor bank.

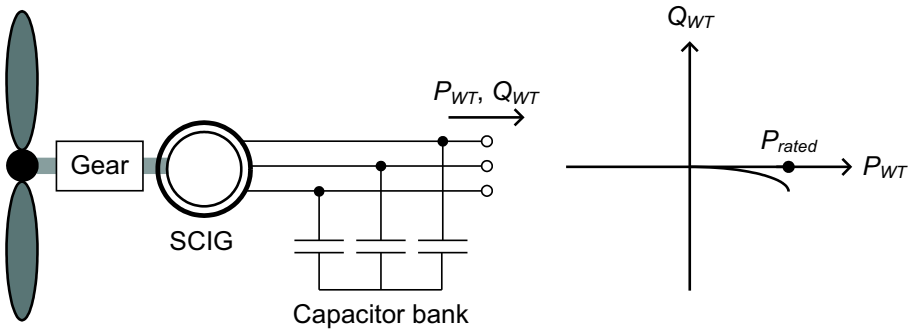


Fig. 3.1: System A and its capability curve at nominal voltage.

## 3.2 System B

This system is a variable speed wind turbine system with the generator connected to the grid via a full scale frequency converter and is assumed to be equipped with voltage ride-through

capability. The layout of system B turbine is shown in Fig. 3.2. Enercon is the largest manufacturer of this type of WECS [16], [5]. This system is capable of producing active power at a certain power factor. A preferable operation is at unity power factor. But in cases where a wind farm is connected to the grid by a large cable, it has to be operated at a lagging power factor angle to keep the reactive power exchange to zero at the grid connection point. In this case the grid side converter has to be overrated so that it can provide the necessary reactive power during high wind speed situations. The capability diagram of this system is shown with a bold horizontal line in Fig. 3.3 in the case when it is operating at unity $pf$. At unity $pf$ operations, the grid side converter has the same power rating as the turbine.

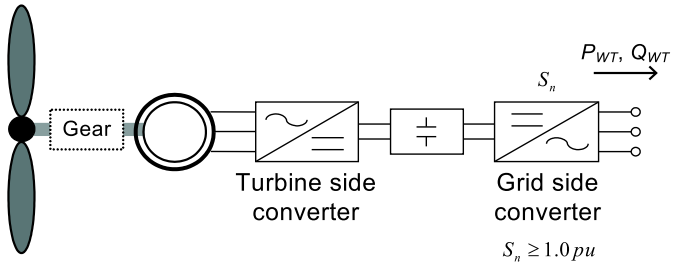


Fig. 3.2: Wind turbine systems B, C and D.

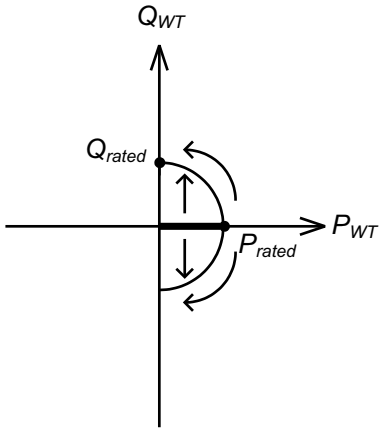


Fig. 3.3: Capability diagram of wind turbine systems B and C at nominal voltage.

## 3.3 System C

The hardware set-up of a system C turbine is similar to that of a system B type turbine (see Fig. 3.2). But the control of the grid side converter is modified so that this wind turbine system can inject/absorb reactive power into/from the grid while producing active power (observe the straight arrows in the capability diagram shown in Fig. 3.3), as long as the current rating of the converter is not violated (the border is represented in the figure by the circle). During a high wind speed situation, this system is able to reschedule its active production, to provide emergency reactive support to the grid (observe the curved arrows in the Fig. 3.3) when the rated operation of the system is at unity $pf$. In cases where the rated

operation of a wind farm is at a lagging $pf$, it can provide emergency reactive power support to the grid to some extent without rescheduling its active power production during high wind speed situations. So in principle system C is able to operate anywhere in the first and the fourth quadrant of the capability diagram.

## 3.4 System D

The wind turbine system D is assumed to have a larger grid side converter (over-dimensioned) (see Fig. 3.2). The capability diagram of this system is shown is Fig. 3.4. During a high wind speed operation, reactive power support to the grid is possible without reducing the active production from the turbine (observe the arrows in Fig. 3.4) in cases rated power $pf$ of the turbine is 1.0.

From a hardware point of view, systems C and D are quite similar to that of system B. But in systems C and D, a SVC/STATCOM function is incorporated in the control of the frequency converter.

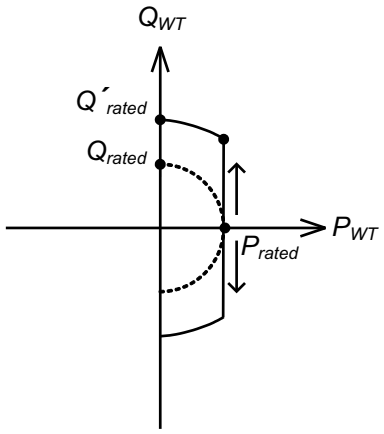


Fig. 3.4: Capability curve of the wind turbine system D at nominal voltage.

## 3.5 System E

The wind turbine system E is a variable speed wind turbine with a full-scale frequency converter where an energy storage device is added in parallel with the conventional DC-link capacitor and the grid side converter is made over-rated. The system layout is shown in Fig. 3.5. The capability diagram of this system is also shown in the figure. With this system, it is possible to operate the WECS at a power lower/higher than the rated power (observe the arrows in Fig. 3.5). This is achieved by the charging/discharging of the energy storage device mounted to the DC-link. It is assumed that the energy storage device associated with system E is capable of injecting active power equal to the rated power of the turbine at the rated voltage for a time duration sufficient for counteracting a power oscillation in the range of 0.1 to 2 Hz. [30] presents a detail description of the energy storage device.

The modeling and the operation of these investigated systems will be discussed in Chapters 4 and 5.

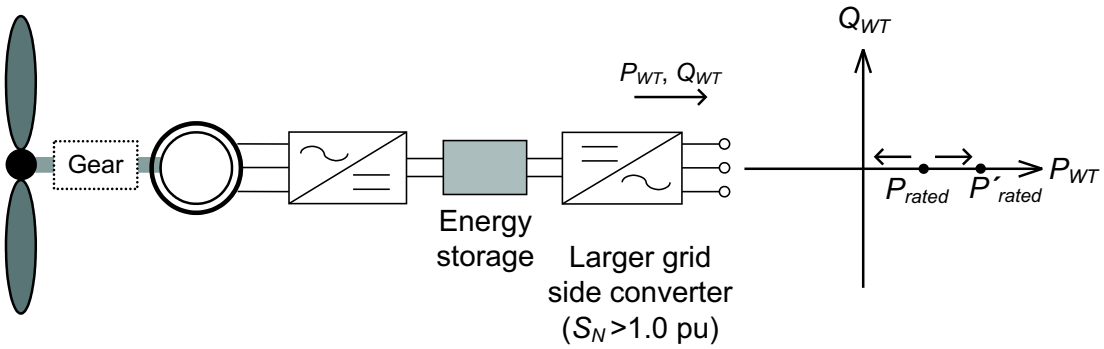


Fig. 3.5: The wind turbine system E and its capability curve at nominal voltage.

# Chapter 4

# Models and case studies

Different simulation tools used during the calculation phase of this thesis will first be mentioned in this chapter. A short description of investigated power systems and the modeling of different components will follow later. Different cases that have been investigated in this thesis will be mentioned. Finally, operating principles of different wind turbine systems for different case studies will be discussed briefly.

## 4.1 Simulation tools used

Calculations presented in this thesis are done using the commercial power system simulator PSS/E®. Both the load flow module (psslf4) and the dynamic simulation module (pssds4) are used for this purpose. Matlab® is also utilized to read different output files generated by PSS/E.

## 4.2 Investigated power system models

### 4.2.1 Set-up-1

In Chapter 6 of this thesis, the transient stability aspect of different WECSs is investigated using the power system layout shown in Fig. 4.1. It is a one machine - infinite bus system augmented with a WECS near the machine. The values of different components of this setup are given in Appendix A.1. A three-phase to ground fault (200ms duration) is applied at the middle of the line (F) as a grid disturbance, resulting in a power oscillation. The power from the hydro generator is 50 MW and the WECS rating is 20% of the hydro generator, i.e. 10 MW.

### 4.2.2 Set-up-2

In Chapter 7, analysis of the steady state and long term voltage stability aspect of different WECSs are performed using the power system model shown in Fig. 4.2. Values of different components of this setup are given in Appendix A.2. The selection of this example grid is inspired from the Swedish transmission system which is characterized by large scale power transfer through several 400 kV transmission lines from northern hydro generation sites to the load centers located mainly in the southern region. Coming wind generation sites are

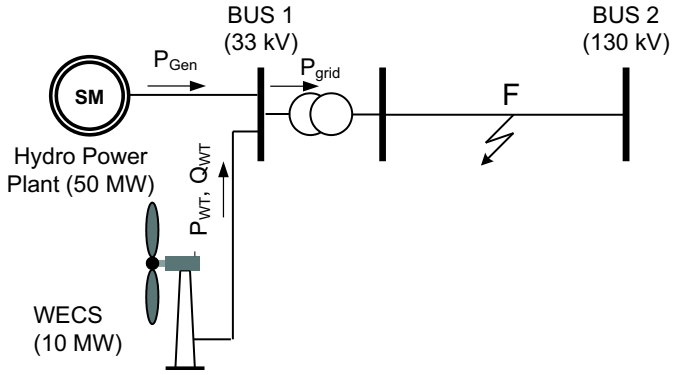


Fig. 4.1: Investigated power system, setup-1.

primarily located in the southern region which corresponds to the left part in the figure. This test system consists of a wind farm installation connected to the 400 kV transmission grid (BUS3) and load connected at a load bus (BUS4). Part of the load is supplied by the wind farm and the rest comes from the main grid through long transmission lines. The wind farm rating is 200 MW. For a given wind speed situation, the maximum amount of load that can be supplied by the transmission line depends on the line properties. Transformers T1 and T3 have fixed ratios, while T2 is a tap changing transformer.

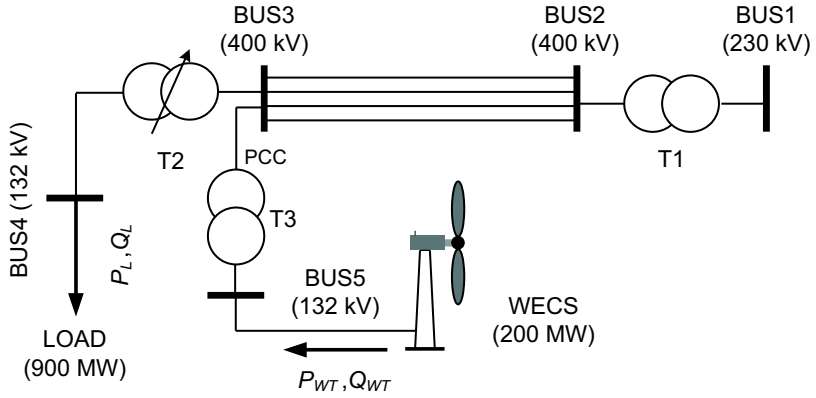


Fig. 4.2: Investigated power system, setup-2.

### 4.2.3 Set-up-3

The short term voltage stability aspect of a WECS, as discussed in Chapter 8, is investigated using the power system model shown in Fig. 4.3. Values of different components of this setup are given in Appendix A.3. The short circuit capacity ($S_k$) of the grid is 144 MVA and the grid impedance angle ($\psi_k$) is $85^o$. This small distribution network is assumed to have three feeders serving local loads of different types with embedded wind generations in all feeders. The distribution network is supplied by a 10 MVA transformer. The amount of load and wind generation at different feeders are - 2.5 MW of load and 4.3 MW of wind generation in feeder-1, 3.5 MW of load and 6.5 MW of wind generation in feeder-2 and 3.5 MW of load and 5.9 MW of wind generation in feeder-3. Further discussion regarding the setup will be provided in Chapter 8.

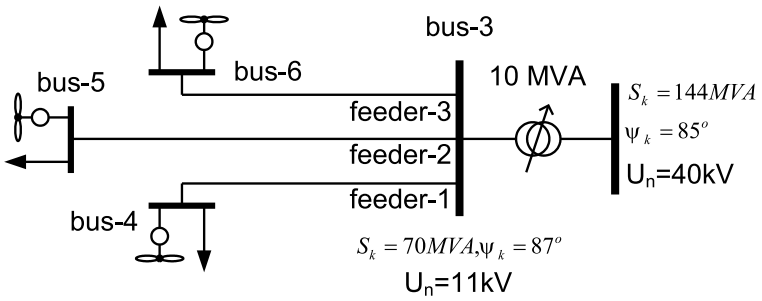


Fig. 4.3: Investigated power system, setup-3.

### 4.2.4 Set-up-4

In Chapter 9 of this thesis, the transient stability of Swedish transmission system in presence of several large wind farms is investigated where CIGRÉ Nordic32 test grid [31] is utilized as a representation of the Swedish transmission network. The original Nordic32 grid is shown in Fig. 4.4. In this thesis the original grid setup has been modified to incorporate the current network situation into account. Further description of the modified Nordic32 system will be given in Chapter 9.

## 4.3 Load models

Both static and dynamic load models are used in the calculation. Static loads of constant impedance type (Z load), constant current type (I load), constant power type (P load) and the combination of these three types (ZIP load [20]) are used in calculations. The dynamic load is modeled as an induction motor using a standard PSS/E® library model.

## 4.4 WECS modeling

The PSS/E® library model for an induction generator (CIMTR3) with a shunt capacitor is used to represent system A. Rest of the investigated WECSs (B, C, D and E as discussed in Chapter 3) are implemented using an owner-defined model in PSS/E. They are modeled as a negative load at the connection point with negative conductance and positive susceptance, as shown in Fig. 4.5. The WECS acts like a constant MVA source within the converter's current limit. The conductance ($G_{WT}$) and susceptance ($B_{WT}$) are given by

$$\hat{Y}_{WT} = -G_{WT} + jB_{WT} = \frac{P_{WT} + jQ_{WT}}{\hat{V}_{WT}^2} \tag{4.1}$$

where $P_{WT}$ and $Q_{WT}$ are the wind farm's active and reactive power production, respectively, $V_{WT}$ is the wind farm connection point voltage. Current injection from the wind farm is

$$\hat{I}_{WT} = \sqrt{(P_{WT} + jQWT)\hat{Y}_{WT}}. \tag{4.2}$$

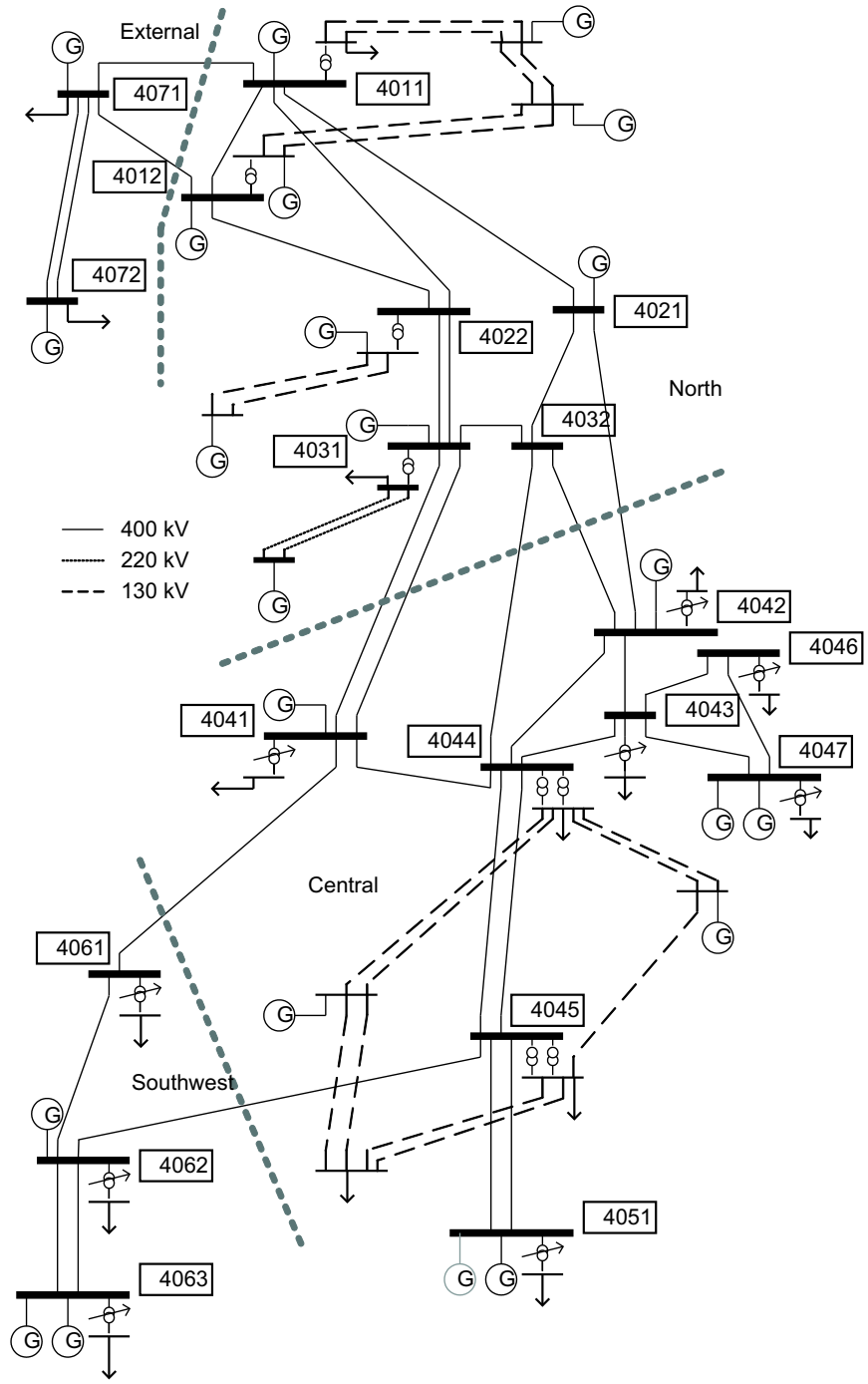


Fig. 4.4: CIGRÉ Nordic32 test system as considered a representation of the Swedish transmission network, setup-4.

When the converter current limit is reached, it operates as a constant current source and the conductance and the susceptance vary according to

$$\hat{Y}_{WT} = -G_{WT} + jB_{WT} = \frac{I_{max} \angle arctan(\frac{Q_{WT}}{P_{WT}})}{\hat{V}_{WT}} \tag{4.3}$$

where $I_{max}$ is the converter maximum current rating. The current injection at this stage is

$$\hat{I}_{WT} = I_{max}\angle arctan(\frac{Q_{WT}}{P_{WT}}). \tag{4.4}$$

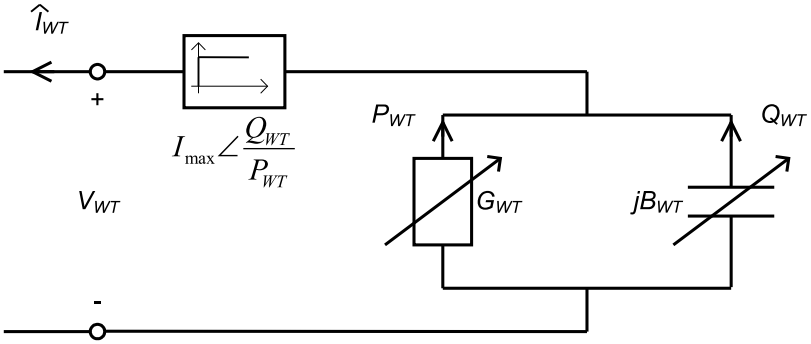


Fig. 4.5: Modeling representation of systems B, C, D and E.

## 4.5 Comparison of the simplified PSS/E® model of the WECS with a detail EMTDC® model

The suggested owner-defined PSS/E model of the variable speed wind turbine with a full scale power electronic converter, shown in section 4.4, is verified against a more detailed EMTDC model where the grid side converter is modeled including the converter switching. The EMTDC modeling details are presented in [32] .The EMTDC model of the wind turbine is shown in Fig. 4.6. In Fig. 4.7, the response of the two wind farm models to a grid fault is presented. Voltage, active and reactive power are shown both at the transformer platform of the wind farm and at the grid connection point. Good agreement between these two modeling approaches of the variable speed wind turbine with a full scale power converter is achieved as can be noted from Fig. 4.7.

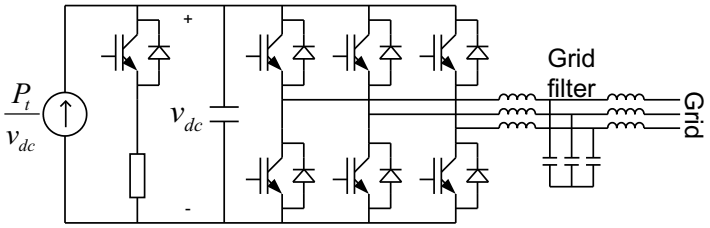


Fig. 4.6: EMTDC model of the variable speed wind turbine with a full scale power electronic converter.

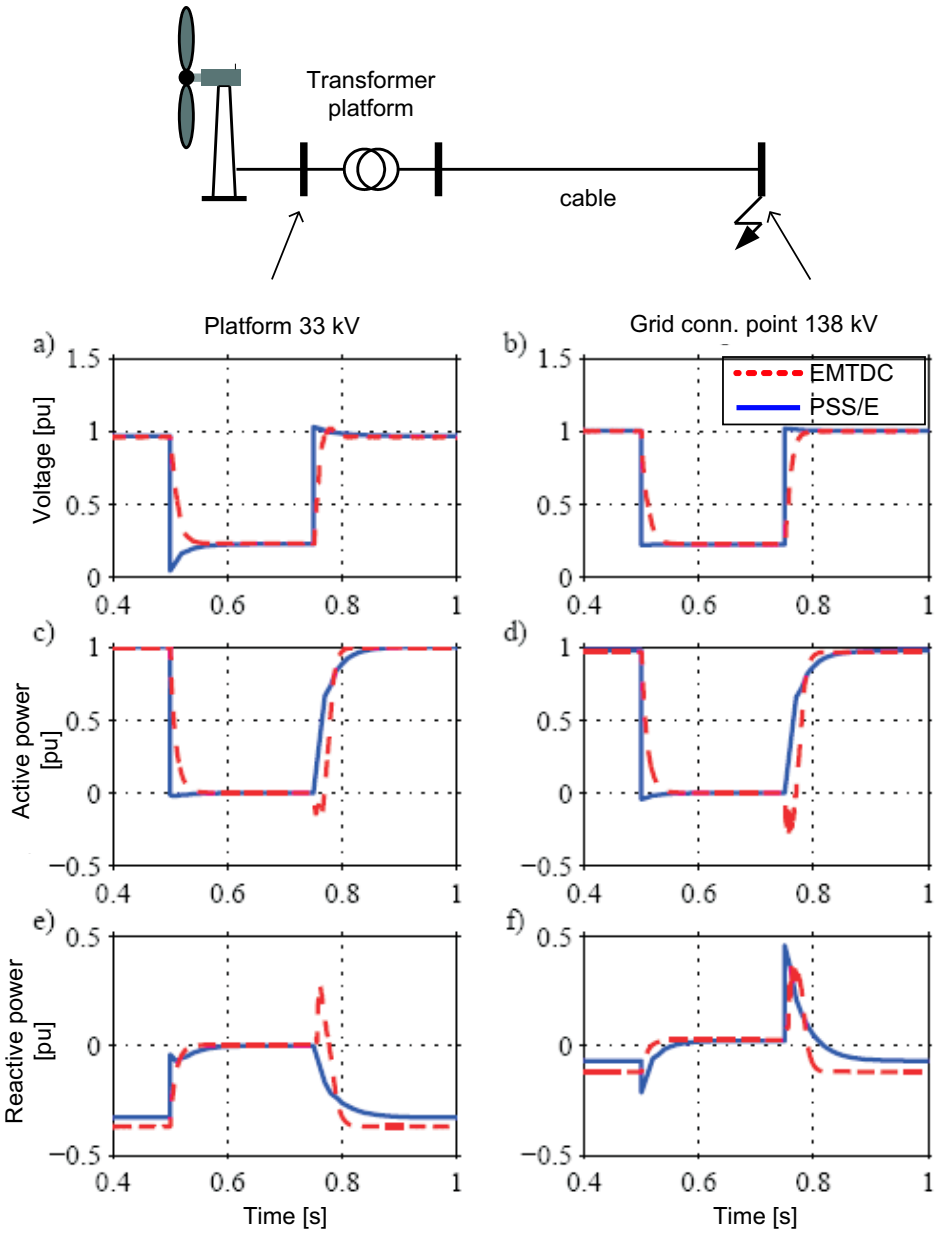


Fig. 4.7: Comparison of the simplified PSS/E model of the WECS shown in section 4.4 (Fig. 4.5) with that of the detail EMTDC model (see Fig. 4.6).

## 4.6 Case studies

### 4.6.1 Transient stability analysis

In Chapter 6 of this thesis, the transient stability aspect of a WECS is investigated. Wind turbine systems B, C, D and E (see Chapter 3 for the description of different systems) are considered in the simulation. In this study, the active and reactive power controllability of wind turbine systems C, D and E are tested to increase the transient stability of a nearby conventional generator and to increase the damping of a line power oscillation and the results are compared with a case considering system B.

### 4.6.2 Voltage stability analysis

In Chapters 7 and 8, voltage stability aspects of systems A, B, C and D are investigated. In Chapter 7, the steady state and long term voltage stability aspects are investigated. Wind turbine systems A, B, C and D are considered here. In Chapter 8, the short term aspect is covered. Wind turbine systems B, C and D are assumed in this case.

### 4.6.3 Large scale wind power integration into the Nordic grid

In Chapter 9, the effect of a large scale wind power integration into the Swedish grid is investigated. As mentioned earlier, the Cigré Nordic32A test system [31] is considered as a representation of the Swedish transmission network for this study. Wind turbine systems B and C are used in this study.

# Chapter 5

# Power system stability aspects of wind turbine installations

This chapter starts with a brief overview of the power system stability. Later, power system stability aspects of different WECSs are presented. Finally, the operation of WECSs are described.

## 5.1 Overview of the power system stability

### 5.1.1 Transient stability

Transient stability is the ability of the power system to maintain synchronism after a severe transient disturbance like a fault, loss of generation or loss of a large load. During a disturbance, the generators gain kinetic energy due to the large imbalance between the prime mover power and the output power of the electric generator, and this leads to a large angular separation among the machines of the system. When this angular separation exceeds a certain limit, the system looses synchronism [19].

Reduction of the accelerating torque of the machines by applying artificial load, application of regulated shunt compensation to increase the flow of synchronizing power among the interconnected machines are examples of some methods to improve the transient stability of the power system [19].

### 5.1.2 Voltage stability

Voltage stability is related to the ability of a power system to maintain acceptable voltage profile throughout the system [18], [19]. Reactive power consumption of the loads is the driving force of voltage instability. For this reason this phenomenon is also called ‘load instability’ [18], [20]. Other factors influencing this phenomenon are the capacity of the transmission system, generator reactive power - voltage control limits, characteristics of reactive compensating devices and the action of the under-load tap changer (ULTC) under low voltage conditions [18], [20], [19].

Preventive measures to avoid voltage instability are the application of reactive power compensating devices, control of generator reactive power output, control of transformer tap changers, under-voltage load shedding, etc.

## 5.2 Transient stability aspects of systems C, D and E

The power system setup shown in Fig. 4.1 can be simplified to the one shown in Fig. 5.1, where $X_{GF}$ is the inductive reactance and $R_{GF}$ is the resistance seen by the generator when a fault occurs at a position F without the presence of a wind farm. This network resistance $R_{GF}$ is the only resistance seen by the generator during a fault. The active loss associated with this resistance during a fault is supplied by the generator and this is the only way of transporting active power from a generator during a fault. The higher this active power transfer is during a fault, the less the accelerating energy gained by the generator during this faulted time is. But in presence of a wind farm, by injecting active current during a fault, the equivalent impedance seen by a generator can be changed.

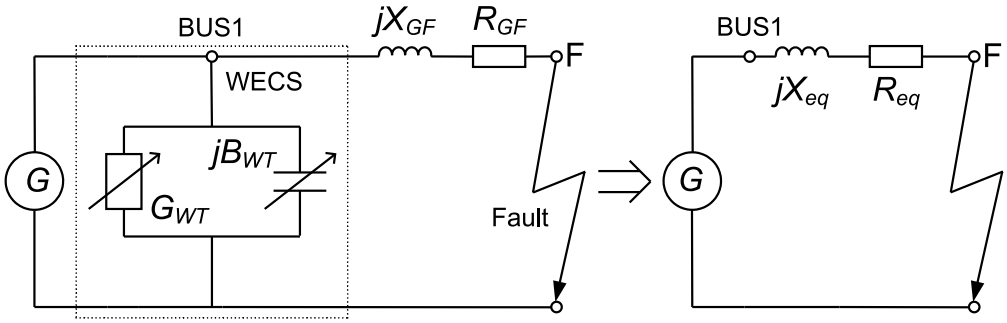


Fig. 5.1: Equivalent sketch of the power system setup shown in Fig. 4.1 including the WECS model.

Let us examine the equivalent impedance seen by the generator in the presence of a wind farm. The equivalent impedance $Z_{eq}$ is given by the following equation

$$Z_{eq} = R_{eq} + jX_{eq} = \frac{(G_{GF} - G_{WT})}{(G_{GF} - G_{WT})^2 + (B_{GF} - B_{WT})^2} + j\frac{(B_{GF} - B_{WT})}{(G_{GF} - G_{WT})^2 + (B_{GF} - B_{WT})^2} \tag{5.1}$$

where $G_{GF}$=$R_{GF}/(R_{GF}^2 + X_{GF}^2)$ and $B_{GF}$=$X_{GF}/(R_{GF}^2 + X_{GF}^2)$. Values of $G_{WT}$ and $B_{WT}$ are given by (4.3).

A WECS situated near a conventional generator, injecting active current at unity $pf$ (system B, $B_{WT}$=0) during a network fault, will reduce the resistance seen by the generator (see Fig. 5.2) and can thus reduce the transient stability of the machine. On the other hand, systems C, D and E have the possibility to control the active and reactive current injection during a grid fault. So, in principle, these systems can change the active current injection to zero ($G_{WT}$=0) and in this way keep the resistance seen by the generator to its initial value. They also have the possibility to inject reactive current during a fault (making the value of $(B_{GF} - B_{WT})$ lower, i.e. reduce the reactive impedance seen by the generator).

Combining these two possible operations during a grid fault, the combined effect of which is a reduced $X_{eq}/R_{eq}$ ratio seen by the generator (see Fig. 5.2), a nearby WECS can increase the active power transfer from a conventional generator and can thus increase the transient stability of the machine. After the fault clearing, by reducing the active current injection from a WECS to zero, the effective load seen by the generator is increased and vice versa. So, a sustained operation of a WECS in the mode, suggested in this section, during and after a fault, until a nearby disturbed machine restores its predefined stable operation,

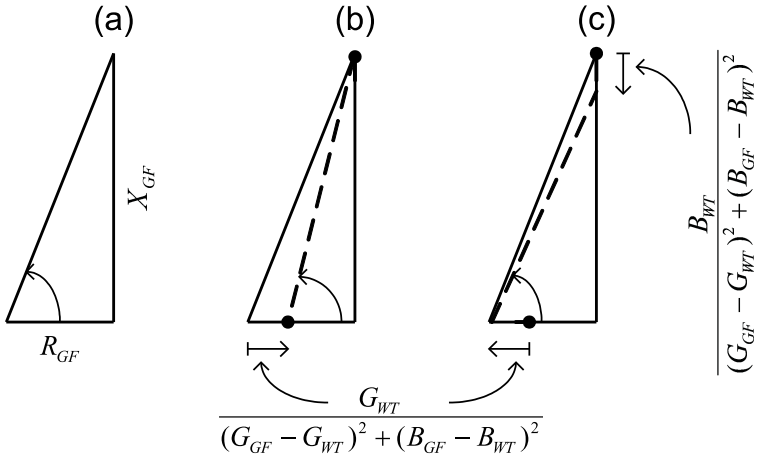


Fig. 5.2: The impedance seen by a generator during a fault at F, (a) no nearby WECS, (b) a system B type WECS and (c) WECS of type C, D or E.

can increase the transient stability of the machine as well as enhance the damping of a power oscillation.

## 5.3 Steady state voltage stability aspects of systems C and D

The reactive power injection capability of the wind turbine systems C and D can be seen as a shunt compensation for the power grid. The power system shown in Fig. 4.2 can be simplified to the one shown in Fig. 5.3, where $B_l$ is the line charging susceptance and $X_l$ is the inductance of the line. The Thevenin equivalent seen by the load has the following emf and impedance

$$E_{th} = \frac{1}{1-a-jb}E \tag{5.2}$$

$$Z_{th} = R_{th} + jX_{th} = \frac{j}{1-a-jb}X_l \tag{5.3}$$

where $a = X_l(B_l + B_{WT})$ and $b = X_l G_{WT}$. The maximum deliverable power to the load for a given power factor $\cos\phi$ is

$$P_{max} = \frac{\cos\phi}{|Z_{th}| + Re\{Z_{th}\}\cos\phi + Im\{Z_{th}\}\sin\phi}\frac{{E_{th}}^2}{2}. \tag{5.4}$$

Replacing $E_{th}$ and $Z_{th}$ into equation 5.4 gives

$$P_{max} = \frac{\cos\phi}{\sqrt{(1-a)^2+b^2} - b\cos\phi + (1-a)\sin\phi}\frac{E^2}{2X_l} \tag{5.5}$$

and the corresponding voltage at this maximum load is

$$V_{maxP} = \frac{1}{1-a-jb}\frac{E}{\sqrt{2}\sqrt{1+\frac{(1-a)\sin\phi - b\cos\phi}{\sqrt{(1-a)^2+b^2)}}}}. \tag{5.6}$$

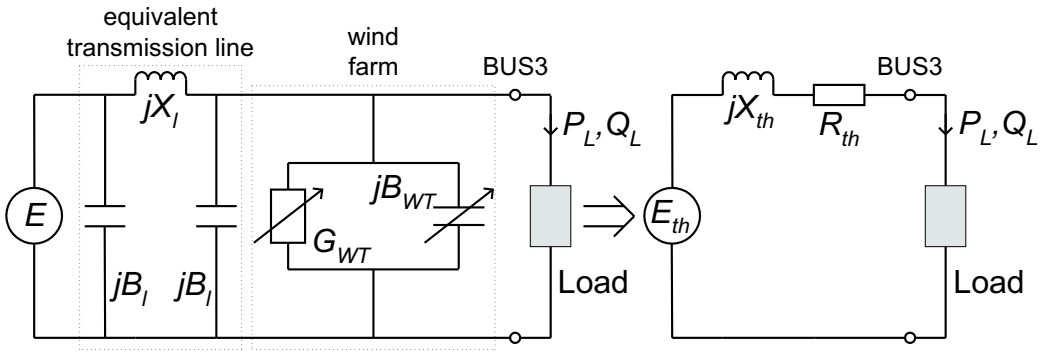


Fig. 5.3: Shunt compensation by wind turbine systems C and D.

(5.5) shows that with increasing reactive power injection from the wind turbine, which means increasing $a$, the maximum deliverable power to the load increases. The load voltage at this maximum load also increases with increasing reactive power injection. The maximum deliverable load also depends on the active production of the wind turbine, which corresponds to $G_{WT}$. Similar calculations are shown in [20] for a pure capacitive shunt compensation.

## 5.4 Optimal operation of systems C and D for maximum voltage support

Let us consider a situation when a WECS is connected near a load. Such a setup is shown in Fig. 4.3. The equivalent seen by a WECS is shown in Fig. 5.4 where $X$ and $R$ are the equivalent system inductance and resistance, respectively. The voltage drop over the network impedance due to the load ($I_L\angle\phi_L$) and in presence of a WECS ($I_{WT}\angle\phi_{WT}$) is given by (note the vector diagram in Fig 5.4)

$$\Delta V = E - V = (I_L \cos\phi_L - I_{WT}\cos\phi_{WT})R + (I_L \sin\phi_L - I_{WT}\sin\phi_{WT})X. \quad (5.7)$$

In case of a severe voltage dip, a WECS will hit its converter current limit and will inject the maximum current $I_{max}\angle\phi_{WT}$. The power factor angle $\phi_{WT}$ is $0^o$ for a system B type WECS. Let us find the optimal $\phi_{WT}$ for systems C and D which will make the value of $\Delta V$ a minimum for a given load. The derivative of $\Delta V$ w.r.t. $\phi_{WT}$ is

$$\frac{d\Delta V}{d\phi_{WT}} = RI_{max}\sin\phi_{WT} - XI_{max}\cos\phi_{WT}. \quad (5.8)$$

Equating $\frac{d\Delta V}{d\phi_{WT}}$ to 0 gives the optimal value of the power factor angle of a WECS for the short term voltage stability improvement, which is

$$\phi_{WT} = \arctan\frac{X}{R}. \quad (5.9)$$

So, during a severe voltage dip, the voltage support provided by a WECS is maximum when it changes its power factor angle to $\arctan\frac{X}{R}$ from the nominal value of $0^o$.

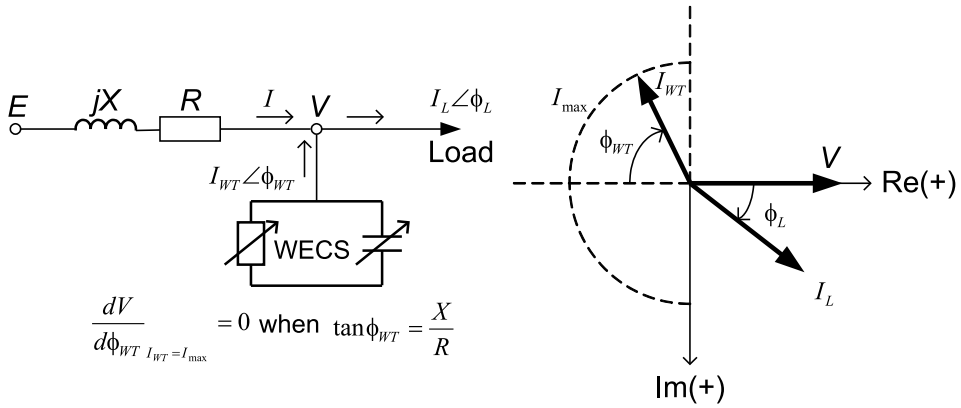


Fig. 5.4: Optimal short-term voltage support by wind turbine systems C and D.

## 5.5 Voltage boosting capacity of systems C and D

(5.7) could be re-written as

$$V = E - (I_L \cos\phi_L - I_{WT}\cos\phi_{WT})R - (I_L \sin\phi_L - I_{WT}\sin\phi_{WT})X. \tag{5.10}$$

During normal operation i.e. when $\phi_{WT}$=$0^o$, the voltage at the WECS terminal, $V_o$, is given by (from (5.10))

$$V_o = E - (I_L \cos\phi_L - I_{WT})R - (I_L \sin\phi_L)X. \tag{5.11}$$

As mentioned in Section 5.4, the voltage at the WECS terminal is maximum when $\phi_{WT}$ = $\arctan\frac{X}{R}$ and $I_{WT}$=$I_{max}$. The maximum voltage, $V_{max}$, is given by

$$V_{max} = E - (I_L \cos\phi_L - I_{max}\frac{R}{\sqrt{R^2+X^2}})R - (I_L \sin\phi_L - I_{max}\frac{X}{\sqrt{R^2+X^2}})X. \tag{5.12}$$

The boost in the terminal voltage provided by this altered operation of a WECS could be found by subtracting (5.11) from (5.12), which gives

$$V_{boost} = V_{max} - V_o = I_{max}\sqrt{R^2+X^2} - I_{WT}R. \tag{5.13}$$

In per unit quantities, the voltage boost can be expressed as:

$$V_{boost,pu} = \frac{S_{WT}}{S_k} - I_{WT,pu}R_{pu} \tag{5.14}$$

where $S_{WT}$ is the capacity of the wind turbine, $S_k$ is the grid short circuit capacity at the wind turbine connection point, $R_{pu}$ is the grid resistance. For a large grid impedance angle the voltage boost can be approximated as

$$V_{boost,pu} \simeq \frac{S_{WT}}{S_k} \tag{5.15}$$

So, in principle, a reduction in the bus voltage at the WECS connection point from the nominal value, no more than $V_{boost}$, could be mitigated by systems C and D by utilizing the reactive power injection capability of their grid side converters.

## 5.6 Short term voltage stability aspects of systems C and D

As mentioned earlier, the driving force of the short term voltage instability is the tendency of dynamic loads to restore their consumed power in the time frame of a second. A typical load of this type is the induction motor.

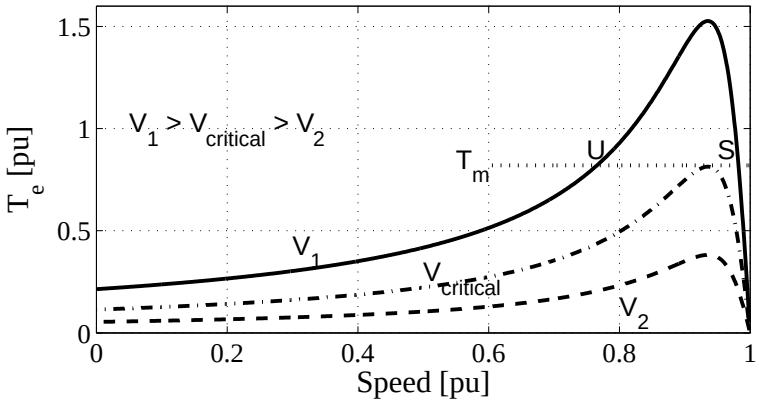


Fig. 5.5: Speed-torque curve of an induction motor. S- stable equilibrium point, U- unstable equilibrium point, $T_m$- load torque.

The speed-torque curve of an induction motor is shown in Fig. 5.5. In the figure, S denotes the stable operating point of the motor at rated voltage $V_1$ i.e. the intersection point of the motor electrical torque and the load torque. The other intersection point U denotes an unstable operating point of the motor. Following a disturbance, if there exists no intersection point between the electrical and the mechanical torque curve due to an increase in transmission impedance (a reduction in grid voltage, note the speed-torque presented in a broken line in Fig. 5.5), the equilibrium disappears and the motor stalls. Let us define the critical voltage when the motor speed-torque curve touches the load torque curve as $V_{critical}$ i.e. if the grid voltage goes below $V_{critical}$ following a grid disturbance, the motor would stall. As calculated in Section 5.5, a WECS of type C or D can boost the voltage at its connection point to an amount $V_{boost}$. So the critical value of the grid voltage which will cause an induction motor to stall can be reduced to $V_{critical}$-$V_{boost}$ in presence of a WECS and a motor stalling due to a reduction in the grid voltage could be avoided.

The differential equation of the rotor motion of an induction motor can be written in terms of slip as

$$2H\dot{s} = T_m - T_e \tag{5.16}$$

where H is the inertia constant of the rotating mass, $T_m$ is the per unit load torque and $T_e$ is the per unit electrical torque developed by the motor. The electrical torque is a function of terminal voltage and slip [20] i.e.

$$T_e = V^2 f(s). \tag{5.17}$$

During a fault, the motor bus voltage is reduced drastically and accordingly also, the electrodynamic torque of the motor, $T_e$. The motor decelerates quickly due to the imbalance in the load and the electrical torque which is governed by (5.16). For a slowly cleared fault and/or a highly loaded motor, the motor slip at fault clearing may exceed the unstable equilibrium point U (in Fig. 5.5). Although the motor's electrical and mechanical torque

curves intersects in this case, the motor cannot re-accelerate after the fault is cleared as the speed reduced beyond the unstable equilibrium point U and the motor stalls. The result is an unacceptably low voltage at the network near the motor bus. By fully utilizing the voltage boosting capacity of a WECS during this situation, the motor bus voltage during a fault could be increased by an amount $V_{boost}$ which corresponds to an increase in the $T_e$ by an amount

$$\Delta T_e = (2V + V_{boost})V_{boost}f(s). \tag{5.18}$$

This corresponds to a less reduction in motor speed for a given fault duration i.e. increased critical fault clearing time which is an indication of the voltage stability improvement.

## 5.7 Operation of the WECS

### 5.7.1 Transient stability and power oscillation damping enhancement

The main idea of improving transient stability of a generating unit is to reduce the net available energy for acceleration of the generating unit during a major grid disturbance (fault). As discussed in Section 5.2, a WECS operating as it is during a grid fault (system B), can reduce the transient stability of a nearby conventional generator by reducing the active power transfer from the generator during a fault. Wind turbine systems C, D and E have the possibility to modify their normal operation during a major disturbance (fault) and can thus improve the transient stability of a nearby generator. As discussed in Section 5.2, by setting the active current injection from a WECS to zero and injecting reactive current during a grid disturbance, the active power transfer from a nearby generator could be increased which would reduce the available accelerating energy for the generator during and immediately after a grid fault (when the generator rotor angle accelerates). This would help increasing the transient stability of the machine. On the other hand, when the generator rotor angle decelerates, it is beneficial to reduce the load seen by the generator either by injecting active power from an alternate energy source (systems C and D can restore their normal active power production and system E can inject extra active power on top of its normal production by discharging the energy stored in its storage device) or by absorbing reactive power (system D has the possibility of exchanging reactive power during a rated power operation). This contingency operation of a WECS will increase the transient stability of a nearby conventional generator and also improve the damping of power oscillations.

The contingency operation of different WECSs to improve transient stability and power oscillation damping are summarized in Fig 5.6, where $n$ stands for normal operation of a WECS, $a$ stands for contingency operation of a WECS when the rotor angle of a nearby generator is accelerating i.e. the rotor speed deviation is beyond a certain positive value, and $d$ stands for contingency operation of a WECS when the rotor angle of the generator is decelerating i.e. the rotor speed deviation is beyond a certain negative value. Wind turbine system B always operates at unity $pf$. System C reduces the active current injection to zero and injects reactive current to its limit when the generator rotor angle accelerates (observe $a$ in Fig 5.6). System C has the facility to dissipate/dump the input wind energy that it fails to deliver to the grid during this contingency operation. When the rotor starts to decelerate, system C restores its normal operation (see $d$ in Fig 5.6). Wind turbine system D is the one with a larger grid side converter. During the accelerating period of the rotor of a nearby generator, system D reduces the active current injection to zero and injects reactive current to

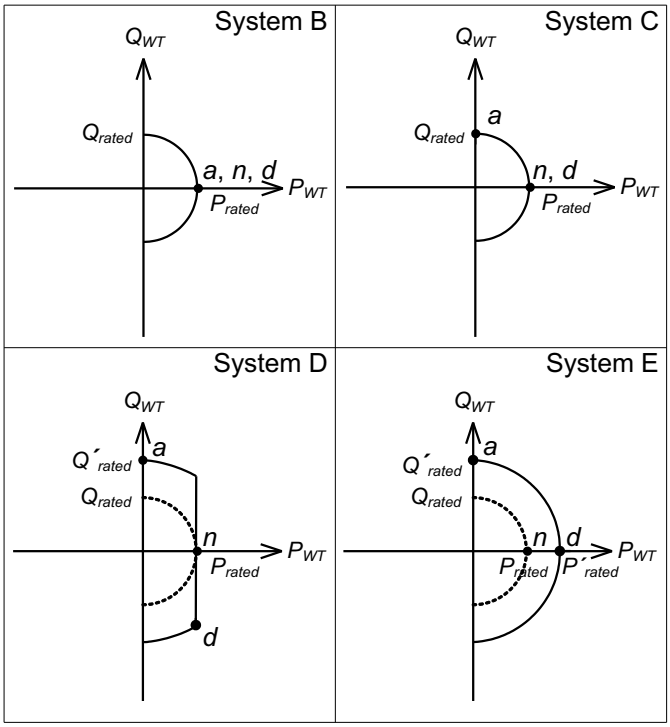


Fig. 5.6: Operation of wind turbine systems B, C, D and E for transient stability enhancement and power oscillation damping. $n$- normal operation, $a$- contingency operation when the rotor angle of a nearby generator accelerates and $d$- contingency operation when the rotor angle of a nearby generator decelerates.

its limit ($a$). When the rotor decelerates, system D restores the active power production and absorbs reactive power from the grid (see $d$ in Fig 5.6). The operation of system E during the accelerating period of the rotor of a nearby generator is similar to that of systems C and D, i.e. to reduce the active current injection to zero and to inject reactive current to its limit. The input wind power that it fails to deliver to the grid during this contingency period is utilized to charge the energy storage device. But during the decelerating period of the rotor, system E restores its normal operation and discharges the stored energy on top of it (see $d$ in Fig 5.6).

### 5.7.2 Voltage stability enhancement

The main idea of improving the voltage stability of the power system is to provide the reactive power compensation near load centers. As mentioned earlier, by incorporating the SVC/STATCOM function into the control of a modern WECS, it could also be seen as a controllable reactive power source.

By utilizing the reactive power injection capability of systems C and D, the maximum deliverable load and hence the steady state voltage stability of the system increases, as discussed in Section 5.3. In Chapter 7, wind turbine systems C and D are operated in a voltage control mode in order to study the voltage stability aspects of these systems. In this mode, a WECS tries to control the voltage of the point of common coupling (pcc) bus (for example, BUS3 in Fig 4.2) or a remote bus (BUS4 in Fig 4.2) by utilizing its reactive power injection capability. The operation of systems C and D for this purpose is demonstrated using the capability curve as shown in Fig. 5.7a. Wind turbine system C reduces the active power

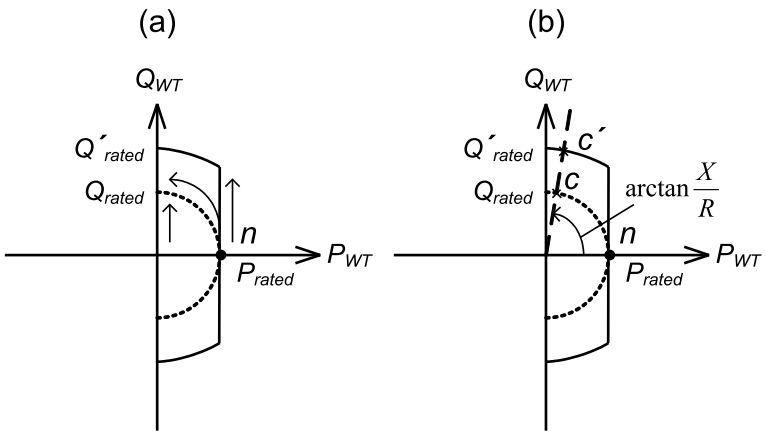


Fig. 5.7: Operation of wind turbine systems C and D for voltage stability enhancement, (a) steady state and long term voltage stability enhancement and (b) short term voltage stability enhancement.

production to make room for the required reactive power to control the voltage during a high wind speed situation (observe the curved arrow in Fig. 5.7a) or during a low wind speed operation, utilize the remaining current injection capacity to provide the necessary reactive power (observe the smaller arrow in Fig. 5.7a). System D, on the other hand, utilizes its over rated grid side converter to provide the necessary reactive power support during a high wind speed operation, without reducing the active power production (observe the larger arrow in Fig. 5.7a).

By utilizing the fast controllability of the grid side converter of systems C and D, short term voltage instability due to induction motor stalling could be prevented, as mentioned earlier. During a severe voltage dip, the grid side converter of a WECS reaches its current limit and the maximum possible voltage support is provided by a WECS when it operates according to the optimal condition discussed in Section 5.4. In the short term voltage stability study, presented in Chapter 8, the contingency operation of systems C and D is based on this optimal condition. The contingency operation of systems C and D for short term voltage stability enhancement is indicated by $c$ and $c'$, respectively, in Fig 5.7b. When the voltage of the pcc bus is above a certain minimum value, the WECS operates $normally$ i.e. unity power factor operation (observe $n$ in Fig 5.7b). When the pcc voltage goes below the minimum threshold value, the WECS enters into the contingency mode (observe $c$ and $c'$ in Fig 5.7b).

# Chapter 6

# Analysis of the transient stability aspect of the WECS

The impact of a WECS during and after a transient disturbance has been studied in this chapter. Wind turbine systems B, C, D and E are investigated here. This chapter starts with a short overview of the investigated power system and WECSs considered in this study. Later the impacts of different types of WECSs on the transient stability of a nearby generator and on the grid power oscillation are quantified.

## 6.1 Over view of the investigated system

Power system setup-1, presented in Chapter 4, Section 4.2, is employed in this study. The layout of the investigated power system is again shown here in Fig. 6.1 for convenience. A three-phase to ground fault (200 ms duration) is applied at the middle of the line and the generator rotor angle and the grid power ($P_{grid}$) are studied in the presence of different types of WECS. It is assumed that the energy storage device associated with system E is capable of injecting active power equal to the rated power of the turbine at the rated voltage for a time duration sufficient for counteracting a power oscillation in the range of 0.1 to 2 Hz. This means that system E should be able to feed out a power increase of 1 pu when it is already operating at the rated power. In this case the grid side converter needs to be over dimensioned by a factor of two. System D is assumed to have a 50% over-rated grid side converter.

## 6.2 Impact on Transient stability

The definition of the transient stability margin used in this chapter is shown in Fig. 6.2. It is adopted from [21]. The area under the power-angle curve indicated by ‘A2+A3’ is the area available for the generator to dissipate the accelerating energy that has been gained during the transient period. The area indicated by ‘A3’ is the margin available for the generator depending on the present operating point and the severity of the fault. The ratio between area ‘A3’ and ‘A1+A2+A3’ is defined as the transient stability margin (TSM).

Fig. 6.3 shows the generator rotor angle swing, when a three phase to ground fault is applied at the location F for 200 ms, in presence of different types of WECSs, namely,

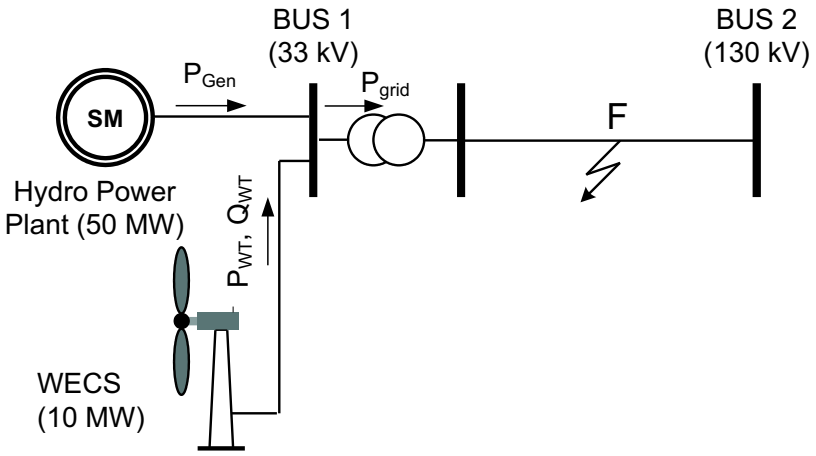


Fig. 6.1: Layout of the investigated power system with a WECS.

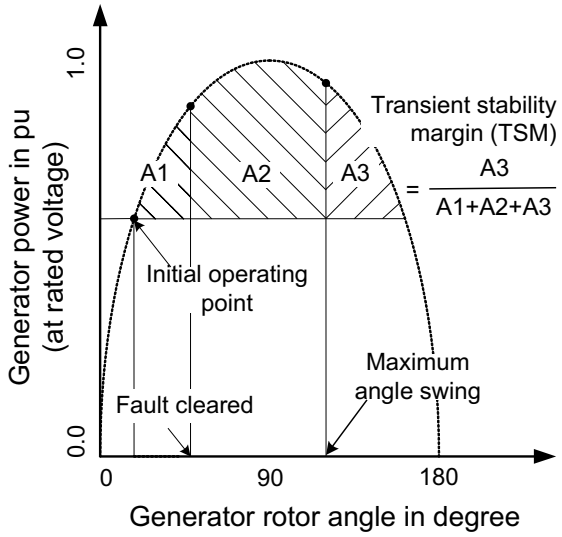


Fig. 6.2: Transient stability margin (TSM).

systems B, C, D and E. The generator maximum rotor angle swing is $109^o$ when a nearby connected WECS is a system B type WECS. The transient stability margin is 20% in this case. The maximum rotor angle swing is reduced to $96^o$ when the connected WECS is a system C type installation which corresponds to a 40% transient stability margin. The reduced maximum rotor angle swing of a hydro generator, when subject to a grid fault, in presence of a nearby system C type WECS shows the system C's transient enhancing property. In presence of systems D and E, the maximum rotor angle swing of the generator is even lower ($95^o$), although the improvement is not so significant. The response of different types of WECS is shown in Fig. 6.4. In Fig. 6.4, $a$, $n$ and $d$ correspond to operation of a WECS in different operational modes as presented in Chapter 5, Section 5.7.1.

The critical clearing time of a fault ($t_{critical}$), when it is applied at F, is calculated in the presence of different WECSs. The critical fault clearing time is 252 ms when a system B type WECS is connected near the generator. It means that if a solid three phase to ground fault at F exists longer than 252 ms, the generator will loose synchronism. When the nearby WECS is a system C type WECS, the critical fault clearing time, $t_{critical}$, increases to 292

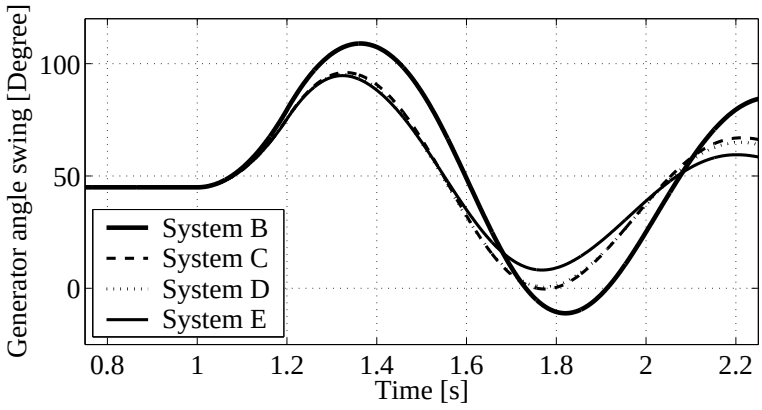


Fig. 6.3: Generator's rotor angle swing in presence of different types of WECS.

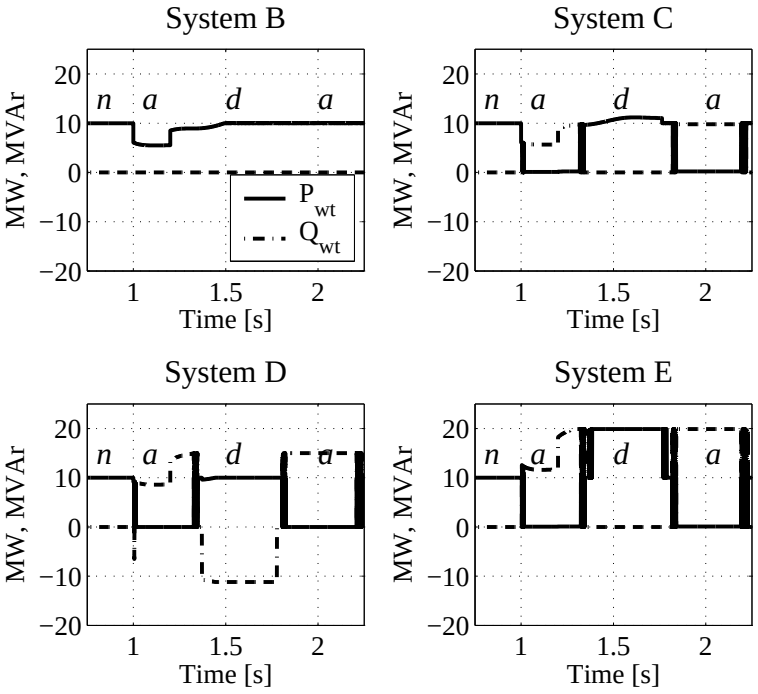


Fig. 6.4: Response of different types of WECS to a grid fault. $a$, $n$ and $d$ are different contingency operational modes of a WECS (presented in Chapter 5, Section 5.7.1).

ms. In presence of systems D and E, $t_{critical}$ is further increased to 295 ms.

The maximum rotor angle swing, the transient stability margin (TSM) and the critical fault clearing time in presence of different types of WECS are listed in Table 6.1.

## 6.3 Impact on power oscillation damping

Besides influencing the transient stability of a nearby generator, a WECS could also improve the damping of a power oscillation. In Fig. 6.5, the transmitted power into the grid, $P_{grid}$ is shown in presence of different investigated WECS when the system is disturbed by a solid three phase to ground fault at F. As could be noted from the figure, the damping of

Table 6.1: List of maximum angle swing, TSM and critical fault clearing time ($t_{critical}$) in presence of different investigated WECS.

| | Maximum rotor swing | TSM | $t_{critical}$ |
|---|---|---|---|
| System B | $109^o$ | 20% | 252 ms |
| System C | $96^o$ | 40% | 292 ms |
| System D | $95^o$ | 42% | 295 ms |
| System E | $95^o$ | 42% | 295 ms |

the grid power oscillation is improved when systems C, D or E is connected rather than system B. The damping constant (DC) of the grid power oscillation is 0.6 when the WECS is a system B type turbine. The damping constant is increased to 1.1 when a system C type WECS is connected near the generator. System D improves the DC to 1.4 which is accomplished by utilizing the larger grid side converter. The improvement in DC is the largest for this particular case, when system E is connected near the generator. The significant improvement in DC with system E is due to the fact that it includes an energy storage device in its design and by subsequent charging and discharging of this device, it counteracts the power oscillation in a more effective way than system D.

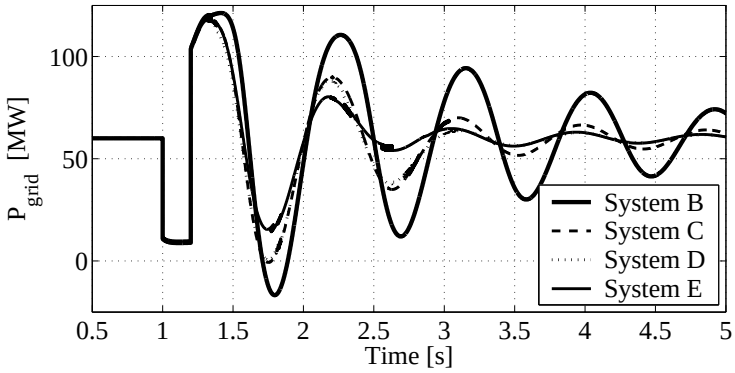


Fig. 6.5: Injected active power into the grid in presence of different types of WECS.

## 6.4 Discussion

The main results from the above calculations are listed in Table 6.2, where the critical fault clearing time and the damping constant are summarized. System C provides a significant improvement in the transient stability of a nearby generator and the damping of the grid power oscillation compared to system B. Important to note is that, the hardware setup of systems B and C is quite similar but in system C the grid reinforcing algorithm is incorporated in the control of the grid side converter. Although the enhancement in transient stability is slightly larger with systems D and E compared to system C, but the improvement made in the damping of the grid power oscillation is quite significant. Note that, although the hardware setup

of system D is quite similar to that of system C except the over-dimensioned grid side converter, the hardware setup of system E is different. It includes an extra energy storage device in its design. A larger grid side converter and an extra energy storage device associated with system E are drawbacks of this system. But it is obvious that with a negligible or a little extra effort, the existing wind turbine system B could be modified to a grid reinforcing type wind turbine system (system C or D).

Table 6.2: List of critical fault clearing time ($t_{critical}$) and damping constant (DC) of the grid power oscillation.

| | $t_{critical}$ | DC |
|---|---|---|
| System B | 252 ms | 0.6 |
| System C | 292 ms | 1.1 |
| System D | 295 ms | 1.4 |
| System E | 295 ms | 1.9 |

# Chapter 7

# Analysis of the steady state and the long term voltage stability aspects of the WECS

Variable speed wind turbines have a converter based reactive power injection facility already included in their design, as mentioned earlier. An interesting possibility, accordingly, is to utilize the reactive power injection capability of the variable speed wind turbine for improving the voltage stability of the power grid. The purpose of this chapter is to investigate the effect that wind generators have on the voltage stability. In particular, to study the possibilities of different wind turbine systems (systems A, B, C and D) with various reactive power control algorithms, and to study the impact of reactive power injection by the wind turbine systems on the steady-state power transfer limit. Moreover, of interest is to determine which load/wind generation situations that are the most critical. At the end of this chapter, the findings are quantified using case studies.

## 7.1 Overview of the investigated system

the power system set-up-2 as presented in Chapter 4, Section 4.2, is utilized in this study. The system is again presented here in Fig. 7.1 for convenience. Wind turbine systems A, B, C and D are investigated here. The description of these wind turbine systems are given in Chapter 3. In the calculation, two different wind speed situations are considered: high and low. At high wind speed, the turbine operates at rated power and at low wind speed it operates at 30% of its rated production. The load connected at BUS4 is a 0.85 lagging *pf* static ZIP load consisting of 50%Z load, 25%I load and 25%P load. The active ($P_L$) and reactive power ($Q_L$) at any voltage $V$ are accordingly given by

$$P_L = zP_o\{0.5(\frac{V}{V_o})^2 + 0.25(\frac{V}{V_o}) + 0.25\} \tag{7.1}$$

$$Q_L = zQ_o\{0.5(\frac{V}{V_o})^2 + 0.25(\frac{V}{V_o}) + 0.25\} \tag{7.2}$$

where z is a demand variable which represents the total amount of equipment connected at the bus, $V_o$ is the nominal voltage of the load bus, $P_o$ and $Q_o$ are load active and reactive power demand at nominal voltage, respectively, when $z$=1.

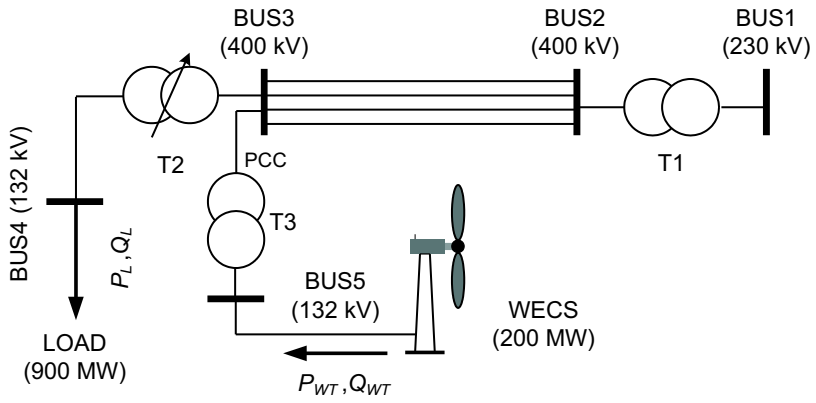


Fig. 7.1: Single line diagram of the investigated power system.

## 7.2 $PV$ diagram

Fig. 7.2 illustrates the definitions of the quantities $P_{allow}$, $P_{max}$ and $V_{maxP}$ using a *PV* diagram. $P_{allow}$ defines the allowed active load that can be drawn keeping the bus voltage at 0.95pu and $P_{max}$ is the maximum deliverable load. The voltage is defined as $V_{maxP}$ when the active load consumption is $P_{max}$. In the following sections, the results from the analysis will be presented in *PV* diagrams for BUS4, see Fig. 7.1.

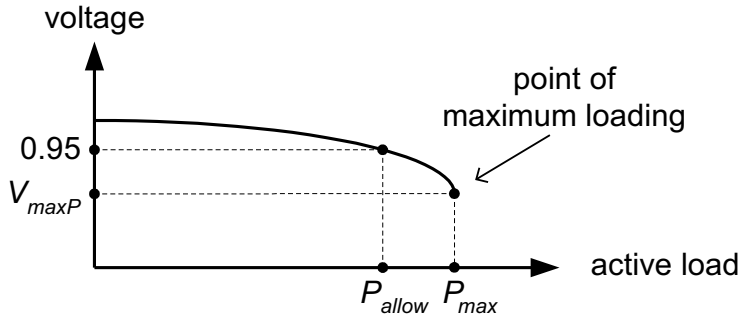


Fig. 7.2: $PV$ diagram showing $P_{allow}$, $P_{max}$ and $V_{maxP}$.

## 7.3 Voltage stability enhancement under different wind conditions

### 7.3.1 Low wind speed situation

The operating point of the wind turbine system *C* during a low wind speed situation is shown in point $LW_1$ in Fig. 7.3, where the power factor is kept at unity. At this operating point, the wind turbine does not utilize the full capacity of its power electronic converter. Keeping the active power production at the same level, the wind turbine system can inject a substantial amount of reactive power into the grid until it reaches the operating point $LW_2$, shown in Fig. 7.3. The reactive power injection capability of this type of wind turbine system can be seen as a shunt compensation for the power system but with negligible additional cost.

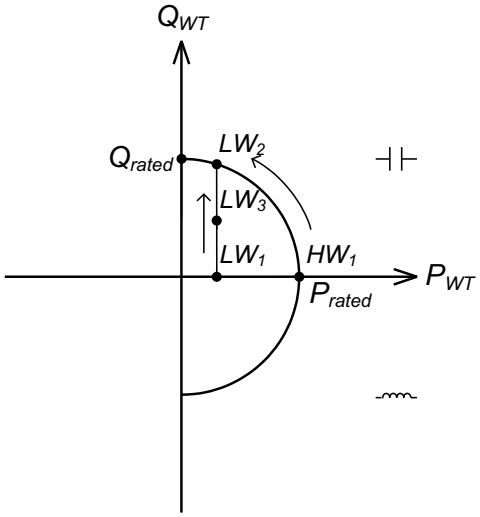


Fig. 7.3: Variable speed wind turbine's capability curve at nominal voltage (system *B* and *C*).

Fig. 7.4 shows the *PV* curves at the load bus (BUS4) in the presence of the different wind turbine systems. It is clear from Fig. 7.4 that the maximum deliverable power ($P_{max}$) is increased by using the reactive power injection facility of the variable speed system *C*. In other words, the voltage stability margin can be increased by reactive power injection from system *C*. Fig. 7.4 shows one particular case where system *C* uses 50% of its available reactive power resource (operating point $LW_3$ in Fig. 7.3). In this case, $P_{allow}$ increases from 885MW to 960MW and $P_{max}$ increases from 916MW to 985MW. By using system *D* during low wind speed situations these quantities can be increased even more.

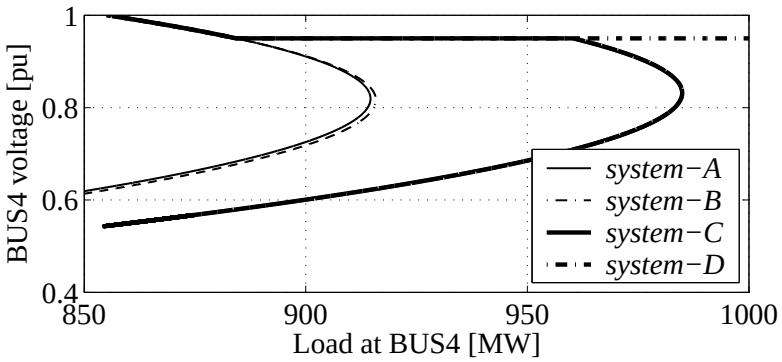


Fig. 7.4: BUS4 $PV$ diagram considering the four types of wind turbine systems at BUS6. Low wind speed situation.

Fig. 7.5 shows the allowed and maximum steady-state power obtained using different levels of reactive power injection from the wind farm. Both $P_{max}$ and $P_{allow}$ at the load bus (BUS4) increase with increasing reactive power injection by the wind farm at BUS6, which is as expected. It can be noted that at a higher reactive power injection level of the wind farm, the normal operating point progressively approaches the nose point of the $PV$ curve (Fig. 7.5).

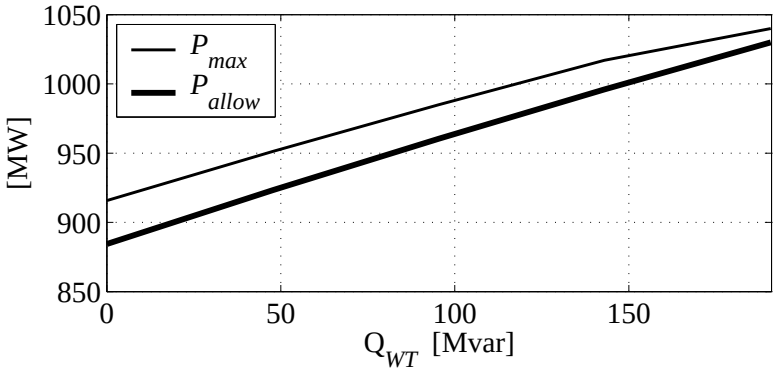


Fig. 7.5: $P_{max}$ and $P_{allow}$ at BUS4 with different reactive injection levels of the wind turbine systems. Low wind speed situation.

Fig. 7.6 shows the percentage improvement in $P_{max}$ and $P_{allow}$. These quantities increase up to 14% and 17%, respectively, when the reactive power injection capacity of the wind farm is fully used.

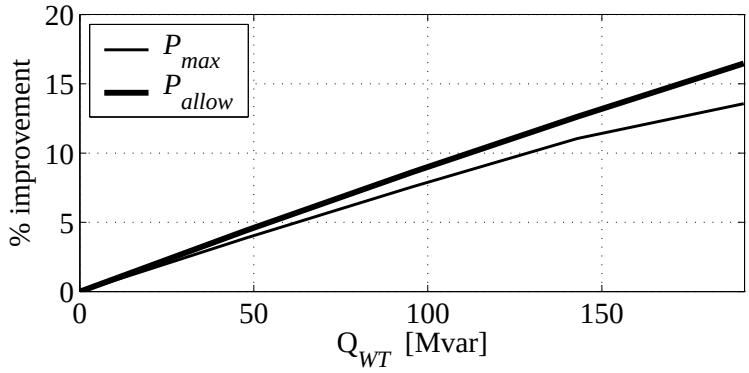


Fig. 7.6: Percentage improvement in $P_{max}$ and $P_{allow}$. Low wind speed situation.

The above simulations show a grid stabilizing property of a wind farm based on system *C*. It is clear from the calculations that, at low wind speed the power electronic converter of the turbine can be utilized to increase the voltage stability limit of the nearby load bus. As mentioned above, this can be done with negligible extra cost.

### 7.3.2 High wind speed situation

The power production from the turbine reaches the rated value during a high wind speed situations. The operating point shifts to $HW_1$, as shown in Fig. 7.3. The reactive power injection capability of the wind turbine system *C* is zero at this point. One way to provide emergency reactive power support to the grid during high wind speed situations is to reduce active power production from the wind farm system (*C*), and to utilize the relieved capacity of the existing power electronic converter to produce reactive power. Instead of operating at $HW_1$, the wind farm then will operate at any point in the first quadrant of the capability diagram, depending on the grid's need, observe the curved arrow in Fig. 7.3.

A method for avoiding a voltage collapse event, due to the generator's armature current protection, by rescheduling the conventional generator, is illustrated in [33]. The possibility of such rescheduling of a modern wind farm is investigated here.

Fig. 7.7 shows the effect of shifting the operating point of the turbine, from the normal operation ($HW_1$), at $P_{max}$ and $P_{allow}$. As shown in the figure, both $P_{max}$ and $P_{allow}$ can be increased from their initial values (when, $P_{WT}$ = $P_{rated}$ and $Q_{WT}$ = 0) by reducing active power production from the turbine and utilizing the remaining capacity of the grid side converter to inject emergency reactive power into the grid. By employing this active power reduction mode of operation, both $P_{max}$ and $P_{allow}$ can be improved up to 12% and 15%, respectively, from their initial values.

The curves show that wind turbine system *C* can assist the grid even during high wind speed operation by reducing its active power production level and using the remaining capacity of the power electronic converter to inject reactive power. Operation of the investigated system *C* in this active power reduction mode can be seen as a grid stabilizing property of the wind turbine. If the wind farm owner can be compensated for this *non-supplied production* as a form of *lost opportunity payment*, operation in this mode can be economically viable.

This active power reduction mode can also be employed during low wind speed operation if the reactive power needed by the grid is higher than the available reactive power injection capacity of the wind farm at this wind speed. Of course, operation of the wind farm in this *untraditional* mode depends on grid regulations and the level of compensation from the system operator.

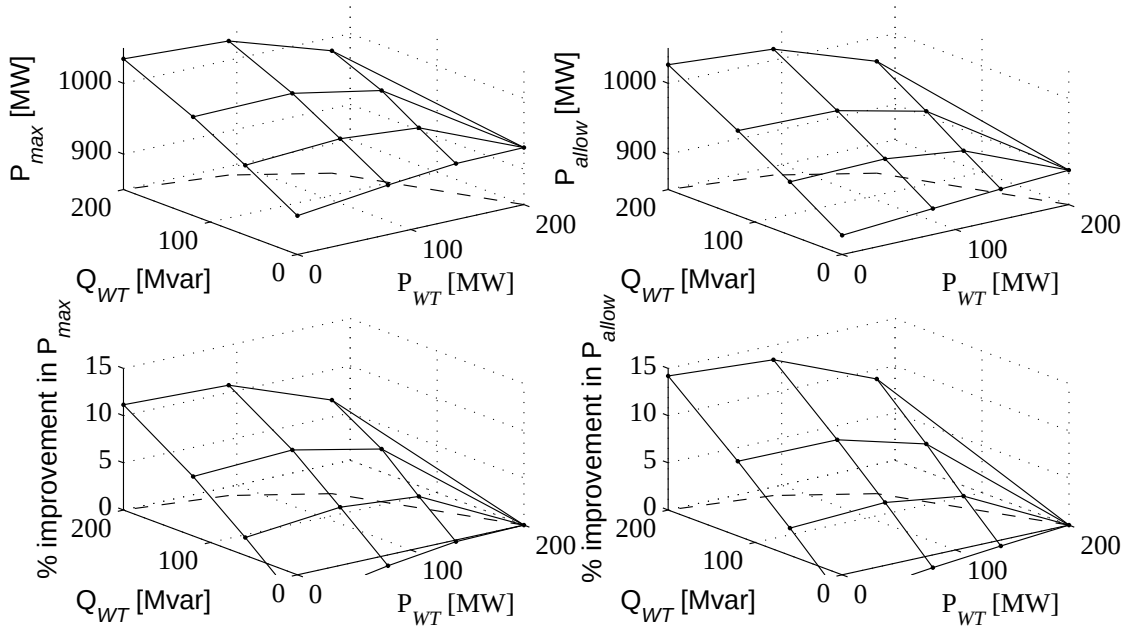


Fig. 7.7: $P_{max}$, $P_{allow}$ and percentage improvement in $P_{max}$ & $P_{allow}$ at BUS4 during active power reduction mode of operation.

## 7.4 Over-dimensioning of the grid side converter

### 7.4.1 New operating region

Another way of providing reactive power support to the grid during high wind speed operation is to increase the size of the grid side converter (over-dimensioning). In this study, a 50% larger grid side converter is considered. The active and reactive power production range of this type of wind turbine, system-*D*, is presented in Fig. 7.8. If a disturbance occurs in the grid, system *D* can maintain the active power production at high wind speed and still feed reactive power into the grid, reaching the point $HW_2$ (Fig. 7.8).

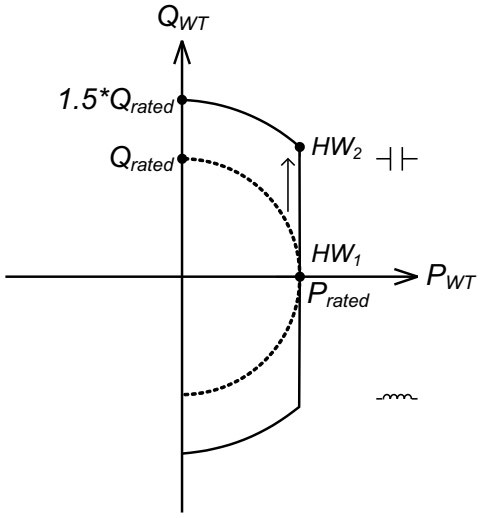


Fig. 7.8: Capability curve of a modern variable speed wind turbine with an over dimensioned grid side converter (system-*D*).

### 7.4.2 Voltage stability enhancement during high wind condition

Fig. 7.9 presents the *PV* diagram of BUS4 considering a high wind speed situation. From this figure, it is clear that the maximum deliverable power to the load is increased when system *D* is used during a high wind speed situation without reducing the active power production. One particular case is shown where system *D* fully utilizes its reactive power injection capability ($HW_2$ in Fig. 7.8). System *C* can also increase this quantity during high wind speed operation by reducing its active power production and utilizing the remaining capacity of the converter to inject reactive power. Fig. 7.9 shows one case where system *C* reduces its active production by 30% to allow for injecting reactive power and by doing so, increases $P_{allow}$ and $P_{max}$. It is interesting to note that, the standard variable speed system *B* does not provide much improvement in $P_{allow}$ and $P_{max}$ compared to the traditional fixed speed system *A*, while the use of systems *C* and *D* provides substantial improvement.

Fig. 7.10 presents $P_{max}$ and $P_{allow}$ for different reactive power injection levels of the wind farm. At higher reactive injection levels (near $HW_2$), the normal steady-state operating point ($P_{allow}$) is close to the maximum power transfer limit (nose point), which represents a highly compensated situation. But the high reactive power injection capacity of this type

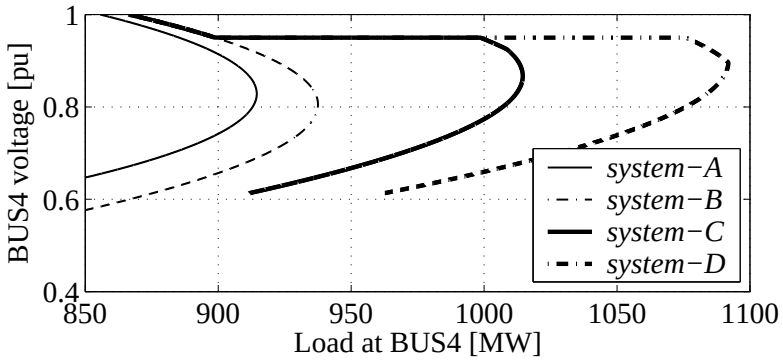


Fig. 7.9: BUS4 $PV$ diagram considering the four types of wind turbine systems at BUS6. High wind speed situation.

of wind turbine system can be valuable for maintaining the transient voltage stability of the system, as well as increasing the steady-state power transfer level.

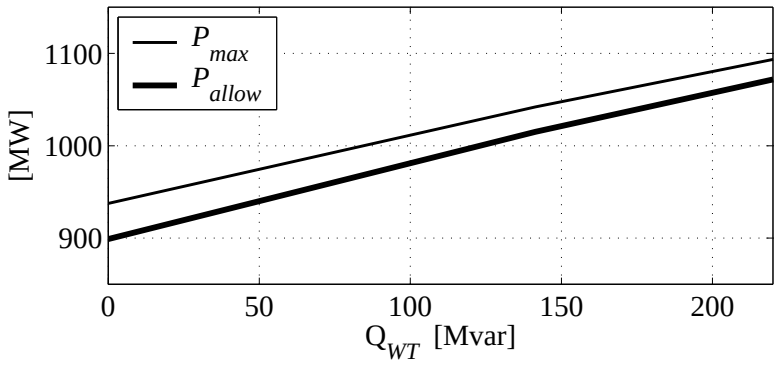


Fig. 7.10: $P_{max}$ and $P_{allow}$ at BUS4 with different reactive power injection levels of the wind turbine systems. High wind speed situation.

Fig. 7.11 shows the percentage improvement in maximum and allowed power. By utilizing the full reactive power injection capacity, the maximum and allowable power increases up to 17% and 20%, respectively.

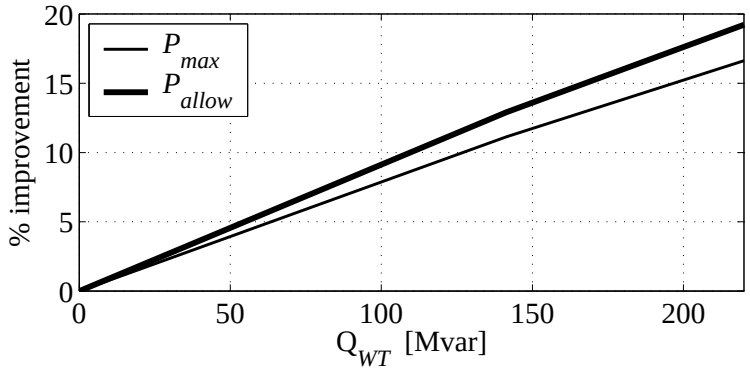


Fig. 7.11: Percentage improvement in $P_{max}$ and $P_{allow}$. High wind speed situation.

Based on the results presented above, it can be said that the reactive power injection capability of system D increases the voltage stability limit of the load bus during high wind speed operation without reducing active power production from the farm, while a minor improvement is obtained if the converter rating is kept constant.

## 7.5 Transformer's tap changing action and the WECS

So far, results have been presented without considering the tap changing action, in order to purely see the effect of the reactive power injection from the wind turbine. However, tap changer action is an important issue, in fact, one of the driving forces of voltage instability [20], [19]. By trying to restore the load side voltage to a predefined voltage range, the ULTC progressively degrades the transmission level voltage which can lead to a possible voltage collapse event. One possibility lies in utilizing the reactive power injection capability of wind turbine systems C and D to avoid such destabilizing situations.

For this purpose, systems C and D try to maintain the steady-state voltage at the transmission level (BUS3), where they are integrated into the grid, within a predefined limit. This voltage regulation limit of the grid can be the same or may differ from the dead band of the tap changing transformer. Here, both limits are assumed to be the same ($\pm$5% deviation). Simulations are performed here using the tap changing action of transformer $T_2$. Two cases are studied here, a high load - low wind situation (case 1) and a high load - high wind situation (case 2).

In Case 1, a low wind speed situation is considered at the wind turbine installation which implies 60 MW of wind power generation. The total load at the load bus (BUS4) is (910 MW, 560 Mvar). The grid disturbance is applied by disconnecting one of the high voltage transmission lines. The results are presented in Fig. 7.12. After the line disconnection, the BUS3 voltage drops due to the increasing reactive losses in the line and also due to the reduced line charging. With wind turbine system A or B integrated into the power system, the transmission level voltage (BUS3) drops further due to the tap changing action of the transformer. The tap changing action restores the load side voltage (BUS4), but one drawback is that it has a negative impact on the grid side voltage and can initiate a voltage collapse event (Fig. 7.12). However, when considering system *C* or D, the possible voltage collapse event is avoided. In this case, the wind turbine system utilizes its reactive power injection capability to maintain the voltage on the transmission level (BUS3) within the allowed limit ($\pm$5% deviation) after the grid disturbance. Most of the load side voltage (BUS4) is also restored by this action taken by the wind farm and part of the load side voltage is restored, in this case, by a few tap movements of the transformer. The voltage reduction at the transmission level due to this tap movement is counteracted by subsequent reactive power injection by the wind farm.

A high wind generation and high load scenario is considered in Case 2. The results are shown in Fig. 7.13. Using wind turbine systems *A* and *B*, the power system approaches a voltage collapse event after the disconnection of one of the transmission lines. But with system *C*, employing the active power reduction mode during a high wind speed situation, by reducing the active power production from the turbine to allow for reactive power injection, the voltage collapse event is avoided. In this particular situation, a 50% reduction in the active power generation is needed. The voltage collapse event can also be avoided, as expected, by using system *D*. By employing system *D*, no reduction in active power production

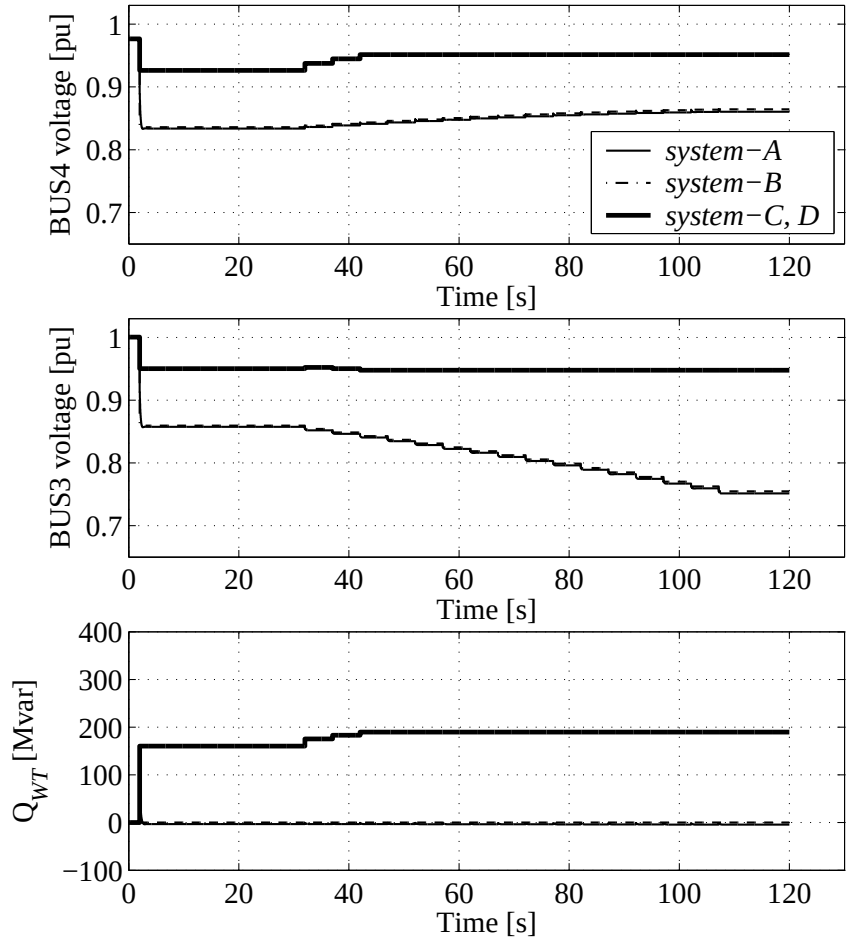


Fig. 7.12: Case 1 (high load, low wind): BUS3 and BUS4 voltage after the disconnection of one of the transmission lines and the response of different types of wind farms to this disturbance.

is required. In this case, a 25% over-dimensioning of the grid side converter is enough to avoid an emerging voltage collapse event.

## 7.6 Discussion

The economic aspects associated with the active power reduction mode and the over-dimensioning of the grid side converter are beyond the scope of this study. Large hydro generators that have an agreement with the system operator trade their reactive power effort as an ancillary service, which the system operator uses to secure voltage stability of the system [34]. With increasing wind power penetration level, if the wind farm can trade its reactive power injection capability like large hydro generators, then over-dimensioning of the grid side converter can be economically viable. Also, if a wind farm owner could obtain compensation for *non-supplied production*, as a form of *lost opportunity payment*, the active power reduction mode of operation would be possible to implement.

The case studies considering the tap changing action of the transformer, presented in the paper, show that by incorporating a suitable voltage control algorithm into the control of a

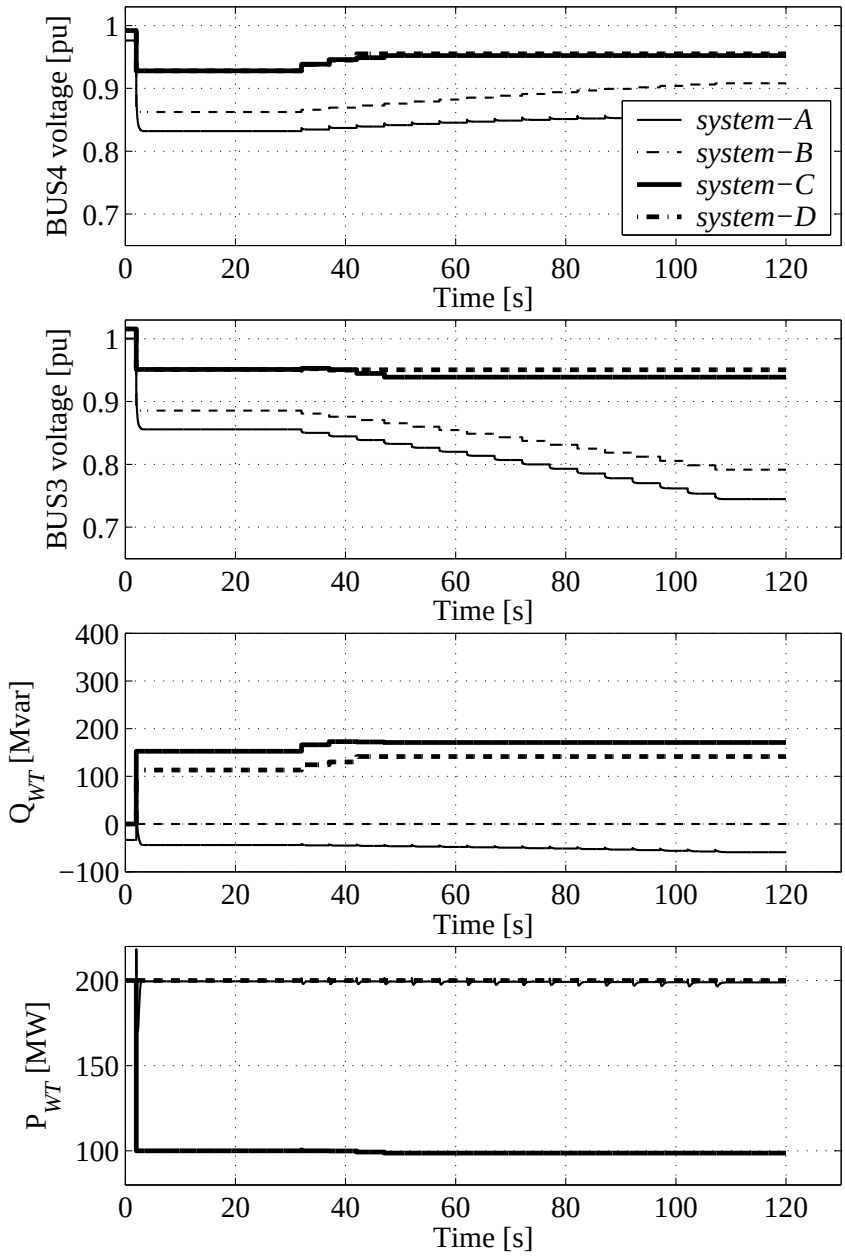


Fig. 7.13: Case 2 (high load, high wind): BUS3 and BUS4 voltage after the disconnection of one of the transmission lines and the response of different types of wind farms to this disturbance. Active power production ($P_{WT}$) from system *A*, *B* and *D* remains at 200 MW.

modern WECS (system C or D), a possible voltage collapse event due to tap movement could be avoided. This can be seen as a global voltage stabilizing property of wind turbine systems (*C* and *D*).

# Chapter 8

# Analysis of the short term voltage stability aspects of a WECS

The main purpose of this chapter is to investigate the short term voltage stability aspects of the distributed variable speed wind generation mixed with voltage sensitive loads, such as induction motors, power electronic supplied equipments, at weaker parts of the network as well as to investigate the possibility of mitigating voltage dips by utilizing the turbine. This chapter starts with an overview of the investigated system followed by the description of different cases investigated here. Later, results and discussions will be presented.

## 8.1 Overview of the investigated system

The power system set-up-3 as presented in Chapter 4, Section 4.2, is utilized in this study. The system is again presented here in Fig. 8.1 for convenience. Wind turbine systems B, C and D are considered in this investigation. It is assumed that the load of feeder-1 is of constant current type load, the load of feeder-2 is of induction motor type load and the load of feeder-3 is of constant impedance type load. The parameters for the induction motor are chosen based on a typical value from [20]. The load $pf$ of all feeders are assumed to be 0.98 lagging.

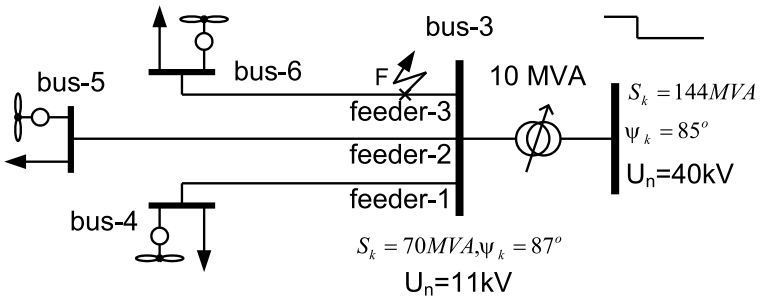


Fig. 8.1: Single line diagram of the investigated power system.

## 8.2 Different cases

In the calculation, a high wind speed - high load demand situation is considered. Depending on the wind turbine technology utilized, five different cases are investigated. They are:

case-1: In this case, it is assumed that all the wind turbines connected at the sub-station are of system B type, i.e. producing active power at unity $pf$.

case-2: A combination of systems B and C type of WECS is assumed in this case. The WECS connected at bus-5 is a system B type wind turbine while the other two buses are assumed to have system C type WECS which means, in this case 40% of the total integrated WECS are system B type and the remaining 60% are of system C type.

case-3: In this case 60% of the total integrated WECS are of system B type (integrated at bus-4 and bus-6) and the remaining 40% are of system C type (integrated at bus-5).

case-4: In this case, it is assumed that all the wind turbines connected at the sub-station are of system C type.

case-5: In this case, all feeders are assumed to be integrated with system D type WECSs.

## 8.3 Short term voltage stability improvement

As mentioned earlier, to avoid short term voltage instability due to the tendency of dynamic loads, such as induction motors, to restore consumed power in the time frame of a second, fast reactive support near the load center is essential. The reactive support should be able to restore a stable equilibrium point under the worst contingency considered and should be fast enough to act before the motor slip exceeds the stall point. Two short term voltage instability mechanisms are investigated here. One is due to a short circuit and the another one is due to an increase is the transmission impedance. The second mechanism corresponds to the disconnection of a parallel line in the network.

### 8.3.1 Instability due to a short-circuit

A three phase short-circuit fault (354 ms duration) is applied in feeder-3 at location F as shown in Fig. 8.1. When all wind turbines are of system B type (case-1), after the fault clearing (by removing the faulted feeder), the motor slip exceeds the post disturbance unstable equilibrium value and it cannot re-accelerates even after the fault is cleared (see Fig. 8.2). The voltage at Bus-5 is also shown in the figure. The Bus-5 voltage is reduced to around 0.2 pu during the fault. The response of different wind turbines to this disturbance is shown in Fig. 8.3 where it can be seen that the active power production from all turbines is reduced which is due to the reduction of their corresponding bus voltages.

In cases where both systems B and C types of WECS are integrated in the system (case-2 and 3), motor stalling is avoided, as shown is Fig. 8.2. During the disturbance, system C type WECS operates in such a way that it increases its connection point voltage to a highest possible value and in this way it can help reducing the deceleration of the motor. The optimal operation for this purpose has been described in Chapter 5, Section 5.4. In Fig. 8.2, observe the higher remaining voltage at bus-5 for cases 2 and 3. Interesting to note is that, although in case-2 60% of the integrated WECSs are system C type (which are assumed to be connected at bus-4 and at bus-6), the remaining voltage at bus-5 is higher in case-3 where only 40% of the integrated WECSs are system C type (which is assumed to be connected at bus-5 i.e.

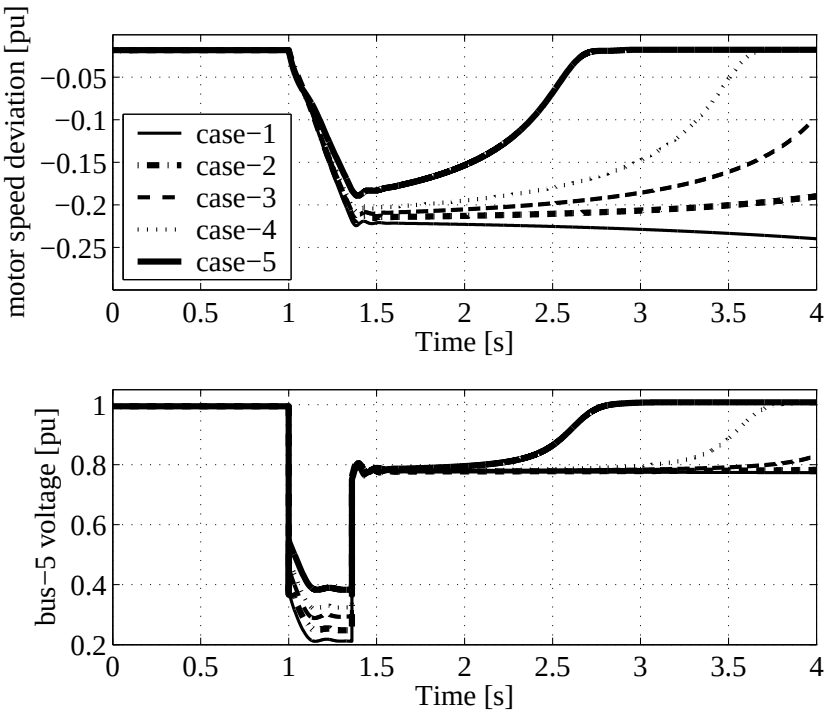


Fig. 8.2: Motor speed deviation and bus-5 voltage for different cases.

near the motor load). The response of turbines in these cases (case-2 and 3) connected at different buses, to this disturbance, is shown in Fig. 8.3.

In the fourth case, where all WECSs are assumed to be system C type, the motor deceleration is reduced further and after the fault clearing, the motor starts accelerating and reaches its post disturbance equilibrium point in 2.5s. When all WECSs are of system D type (case-5), the remaining voltage at bus-5 during the disturbance increases up to 0.4 pu and the motor reaches its post disturbance equilibrium operation in less than 1.5 s after the fault clearing.

Finally, in Table 8.1, the critical fault clearing time ($t_{critical}$) is shown for different investigated cases when a three phase short-circuit fault is applied at a location F in feeder-3. As expected, in the presence of system C or D type wind turbines, the value of $t_{critical}$ increases compared to the case when only system B type WECSs are employed.

Table 8.1: Critical fault clearing time ($t_{critical}$) for a three-phase short-circuit fault at location F (in Fig. 8.1) for five different investigated cases.

| Case | $t_{critical}$ |
|---|---|
| Case-1 | 354 ms |
| Case-2 | 368 ms |
| Case-3 | 377 ms |
| Case-4 | 390 ms |
| Case-5 | 438 ms |

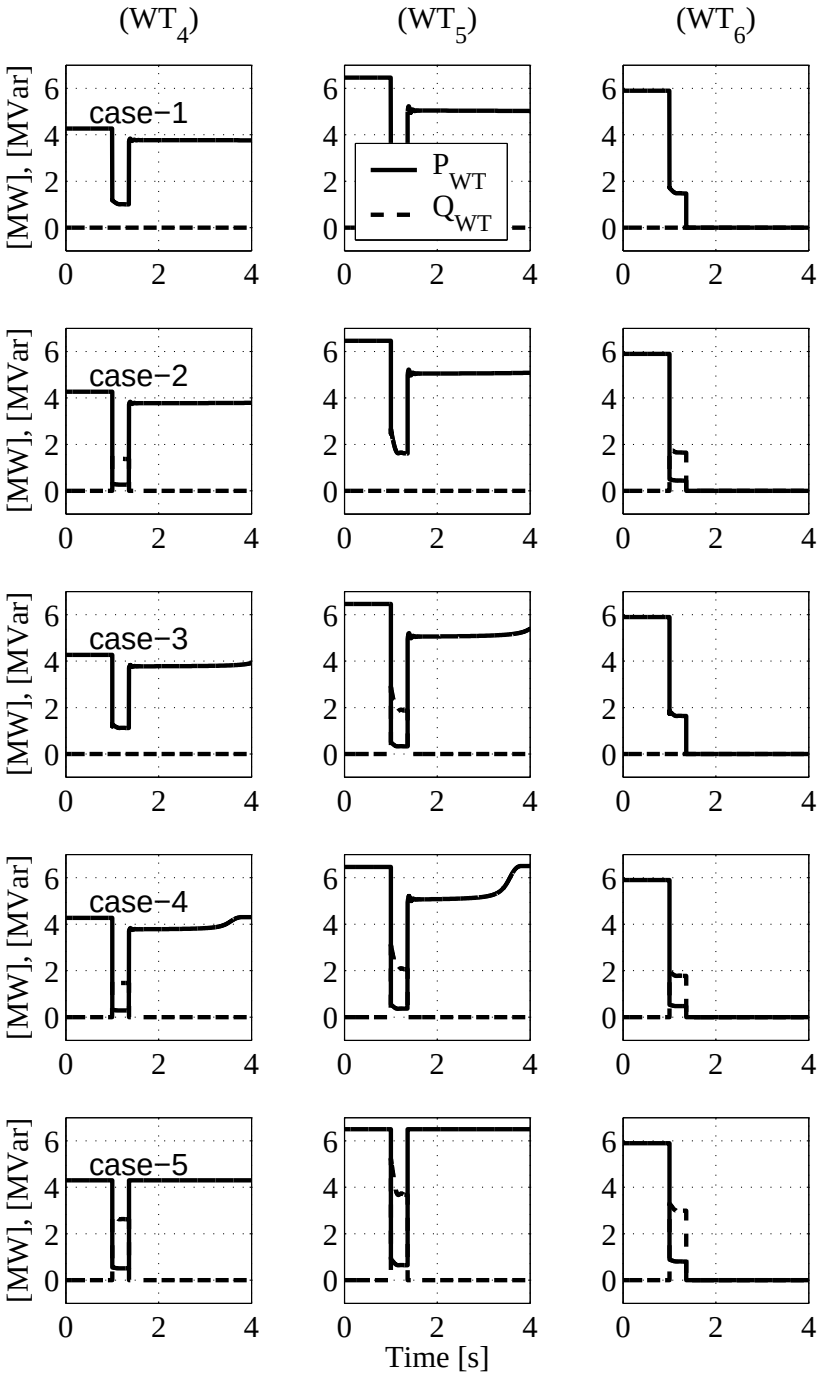


Fig. 8.3: Active and reactive power of different wind turbines for different investigated cases.

### 8.3.2 Instability due to an increase in the transmission impedance

After a disturbance that results in the disconnection of transmission lines, the transmission impedance will increase and hence a reduction in voltage will be experienced in the distribution network until the tap changing transformer in a sub-station restores the voltage to its nominal value. Due to the fact that this tap changing action is a slow phenomena, this reduction in voltage due to the increase in transmission impedance can lead an induction motor to stall as the motor mechanical and electrical torque curves may not intersect after the dis-

turbance and the network voltage may collapse (note the speed-torque curve of an induction motor at a reduced voltage $V_2$ as shown in Fig. 5.5 in Chapter 5).

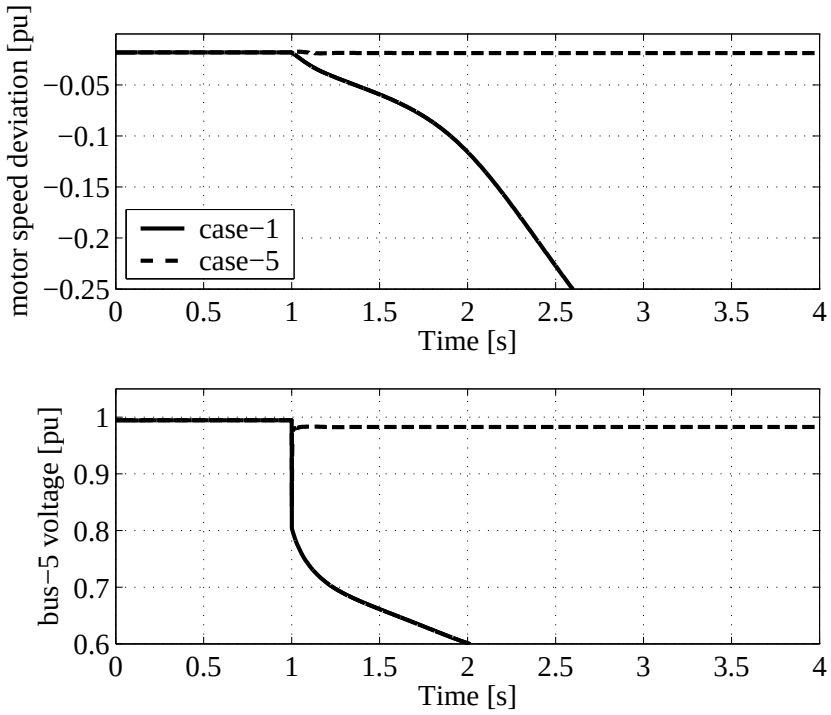


Fig. 8.4: Motor speed deviation and bus-5 voltage for different cases.

Due to an increase in the transmission impedance, a 75% voltage dip (remaining voltage 75%) is experienced at the grid (see Fig 8.1). The motor electrical and mechanical torque curves do not intersect at this reduced voltage. As a result the motor stalls and the voltage collapses when the WECSs are assumed to be of system B type. The motor pu speed deviation and the bus-5 voltage is shown in Fig 8.4 where it is shown that after the disturbance the motor decelerates rapidly resulting in a rapid reduction in the voltage as well. When case-5 is considered i.e. when all WECSs are assumed to be system D type, instability is avoided. With the help of a larger grid side converter, system D managed to maintain the active power production at the pre-disturbance value and utilize the remaining capacity of the converter to provide reactive power support to maintain the connection point voltage (see Fig 8.5). Instability could also be avoided in case-4 where all WECSs are assumed to be of system C type. In that case, due to the need of a longer duration reactive power support, the rotor blades of the turbine have to be pitched out of the wind to reduce the energy capture from the wind and instantaneous power restoration could not be possible in that situation.

## 8.4 Mitigation of voltage dips

### 8.4.1 Voltage dip

Voltage dips are short duration reductions in rms voltage caused by short circuits, overloads and starting of large motors [35]. The interest in voltage sags is mainly due to the fact that they cause problems on several types of equipments such as adjustable-speed drives, process

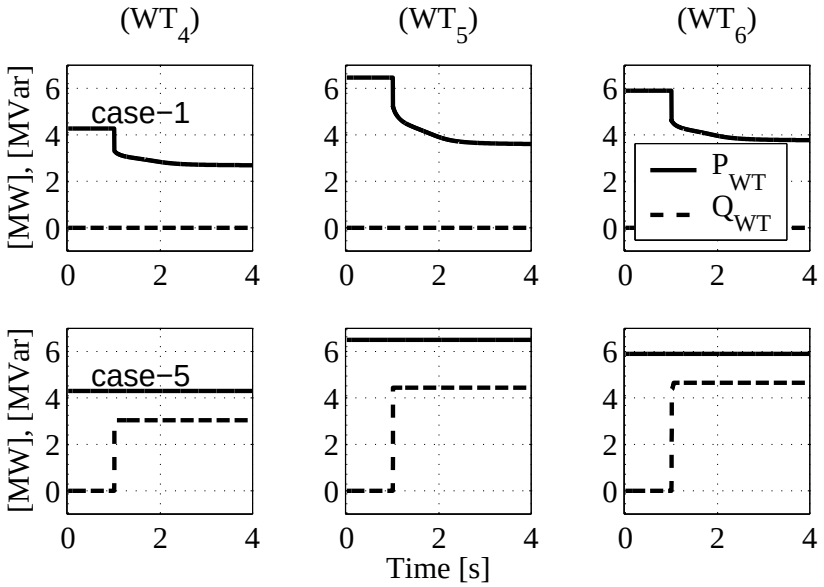


Fig. 8.5: Active and reactive power of different wind turbines for different investigated cases.

control equipment and computers. Most of the current interest in voltage dips is directed to voltage dips due to short circuit faults [35].

### 8.4.2 Consequences of a voltage dip

As mentioned earlier, loads like adjustable speed drives, process control equipment and computers are notorious for their sensitivity. Some types of equipment trip when the rms voltage drops below 90% for longer than one or two cycles [35]. If this equipment is a process control equipment of a paper mill, the damage due to voltage dips is enormous. A voltage dip is not as damaging to industry as an interruption, but there are far more voltage sags than interruptions, so the damage due to voltage sags can still be larger [35].

### 8.4.3 Mitigation methods

As mentioned earlier, tripping of sensitive equipments due to voltage dips is the main problem associated with this event. If there were no equipment tripping, there would not be any voltage quality problem. Five types of mitigation methods are addressed in [35] of which three methods involve improvement in power system such as, reducing the number of short circuits faults, reducing the fault clearing time and changing the system design. As can be understood, modification of an existing power system to mitigate voltage dips will be fairly expensive to realize. The two other mitigation methods as mentioned in [35] are namely, utilization of mitigation equipments between the sensitive equipment and the supply and improving the immunity of the equipment. As mentioned in [35], improvement in equipment immunity is the most effective solution against equipment tripping due to voltage sags. For consumer electronics and most adjustable speed drives, these are off-the-shelf equipments and customers have no direct influence on the immunity level of the equipment. Only large industrial equipment is custom made where the customer has the possibility to define the immunity level. Installation of mitigation devices near the system-equipment interface is

the most commonly applied method of voltage dip mitigation. Some examples of mitigation devices are:

- Uninterruptible power supplies (UPS) are very much used for computers, servers and process control equipment.

- Motor-generator set with a flywheel. The sensitive equipment is connected to the grid through the motor-generator set. During a voltage dip event, the system is disconnected from the grid and the generator feed the sensitive load by utilizing the stored rotational energy in the flywheel.

- Shunt or series connected voltage source converter (VSC) to inject a required amount of current or voltage into the grid.

### 8.4.4 Mitigation of voltage dips by a WECS

As mentioned earlier, a variable speed wind turbine with a full scale power electronic converter (system B) has the possibility to provide a fast reactive power compensation by utilizing its grid side converter. Such variants of a variable speed wind turbine is defined as systems C and D in this thesis. The voltage boosting capacity of systems C and D has been calculated in Section 5.5 of Chapter 5. In per unit, the voltage boosting capacity is

$$V_{boost,pu} = \frac{S_{WT}}{S_k} - I_{WT,pu}R_{pu} \tag{8.1}$$

where $S_{WT}$ is the capacity of the wind turbine, $S_k$ is the grid short circuit capacity at the wind turbine connection point. For a large grid impedance angle it could be approximated as

$$V_{boost,pu} \simeq \frac{S_{WT}}{S_k}. \tag{8.2}$$

So, in principle, a reduction in the WECS terminal voltage from the nominal value no more than $V_{boost,pu}$ could be mitigated by a WECS of type C or D.

To illustrate the voltage mitigation capability of a WECS, an example is presented here. A short circuit fault is applied at location F of the feeder-3 with a certain fault impedance. After 300ms the fault is removed by the associated protection by disconnecting the faulted feeder. Cases 1, 4 and 5 are considered here. When all WECSs are assumed to be of type B (case-1), the voltages at different load buses (note the voltage at different load buses as shown in Fig. 8.6) are reduced to a value below 0.8 pu which could lead to tripping of sensitive loads. WECSs of type C could mitigate this voltage dip event as can be seen in Fig. 8.6 (case-4). In this case, the WECSs are operated according to the principal described in Section 5.4 of Chapter 5. When WECSs of type D are used, the voltage dip event is also mitigated, but in this case active power production from different WECSs can be maintained at the post disturbance value while providing reactive power support with the help of a larger grid side converters. The active and reactive power of different WECSs are presented in Fig 8.7.

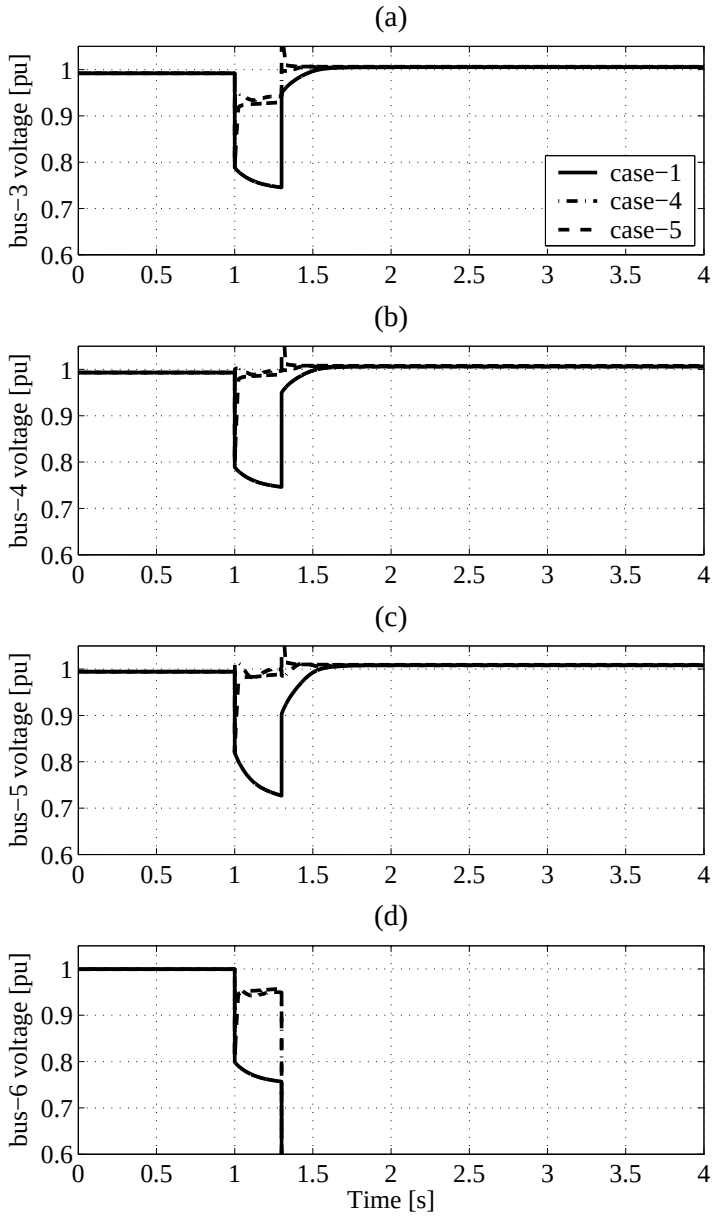


Fig. 8.6: Voltage at the sub-station bus (bus-3) and at other load buses.

## 8.5 Discussion

A small scale wind energy installation (<10 MW) integrated into the weaker part of a distribution network has the potential to improve the short term voltage stability of the network and also to mitigate voltage dips provided that the grid side converter control has been modified. As mentioned earlier, systems C and D are such modified versions of one commonly used WECS which is defined in this thesis as system B (variable speed wind turbine with full scale power electronic converter capable of producing active power at unity $pf$). As presented in this chapter, by utilizing the fast controllability of the power electronic converter of a WECS, short term voltage instability is avoided. Of course the improvement depends on the boosting capacity of the WECS at the connection point to the grid which is determined by the ratio between the capacity of the grid side converter and the short-circuit capacity of

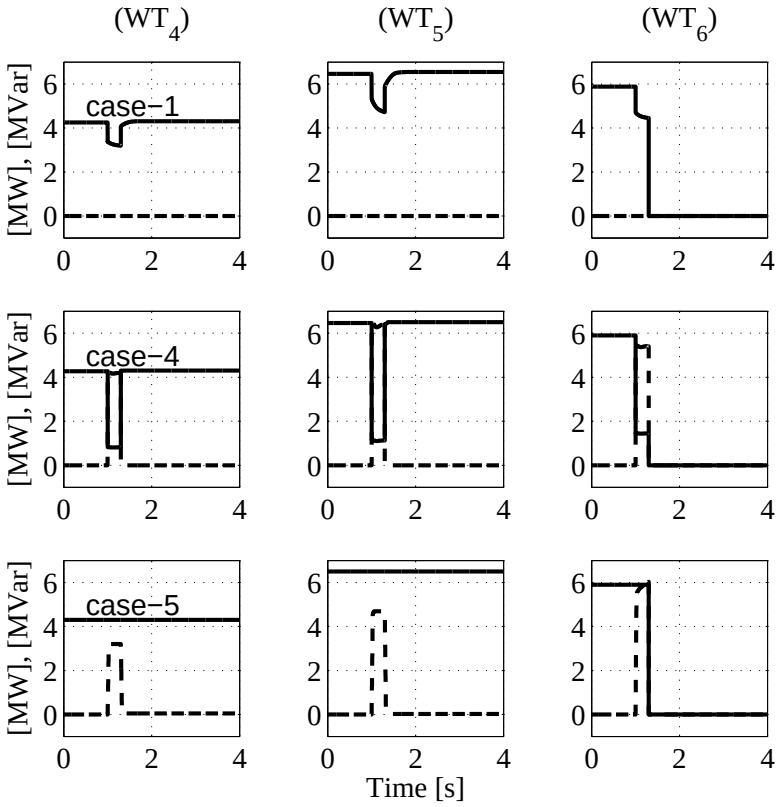


Fig. 8.7: Wind turbines active and reactive power during a voltage dip event. Legend same as Fig. 8.5.

the grid at the connection point. Depending on this boosting capacity of a WECS, voltage dips up to a certain amount can also be mitigated with systems C and D and thus tripping of sensitive loads can be avoided due to a voltage dip event.

# Chapter 9

# Large scale wind power integration into the Nordic grid

As mentioned earlier, in Sweden several large wind farm projects are under planning stage which could be realized in next few years. The main purpose of this chapter is to investigate the effect of these planned large wind farms on the transient stability of nearby located conventional synchronous generators. In addition, power oscillations in the transmission lines near the wind farm locations are also studied. This chapter starts with the description of the modified Nordic32 grid. Results from the investigations are then presented. Discussions are presented at the end of the chapter.

## 9.1 Modified Nordic32 grid

As mentioned earlier, the CIGRE Nordic32 test system is used as a representation of the Swedish transmission grid in this investigation. The total installed capacity of this test system is 16.5 GW and the load is 10.9 GW. Accordingly, it is assumed that this test system is a 50% scaled down version of the Swedish system (33.5 GW installed capacity). The original Nordic32 grid has been modified in this work to incorporate the current network situation. Two thermal generating units at bus 4063 (530 MW each) have been taken out of operation and two new generating units (530 MW each) have been added at bus 4062 (Fig. 9.1). The reason for this modification is due to the fact that, two units of the nuclear power plant Barsebäck, situated near Malmö, are no longer in operation now [36].

A 320 MW wind farm is connected at the southwest region as shown in Fig. 9.2. This corresponds to a 3% wind energy penetration level (the ratio between the wind power and the total load). This wind farm resembles the planned 640 MW Kriegers Flak wind farm in the south of Sweden.

To simulate a high wind energy penetration scenario, another large wind farm (1 GW) is connected in the south part of the central region as shown in Fig. 9.2. This wind farm represents the planned wind farm Södra Midsjöbanken. Two thermal units connected at bus 4062 are in this case taken out of operation from the southwestern region (530 MW each) to accommodate the new wind power. This situation corresponds to a 12% penetration level of wind power. To provide voltage support in the southwestern region, 2 synchronous condensers are connected in place of the two generators at bus 4062.

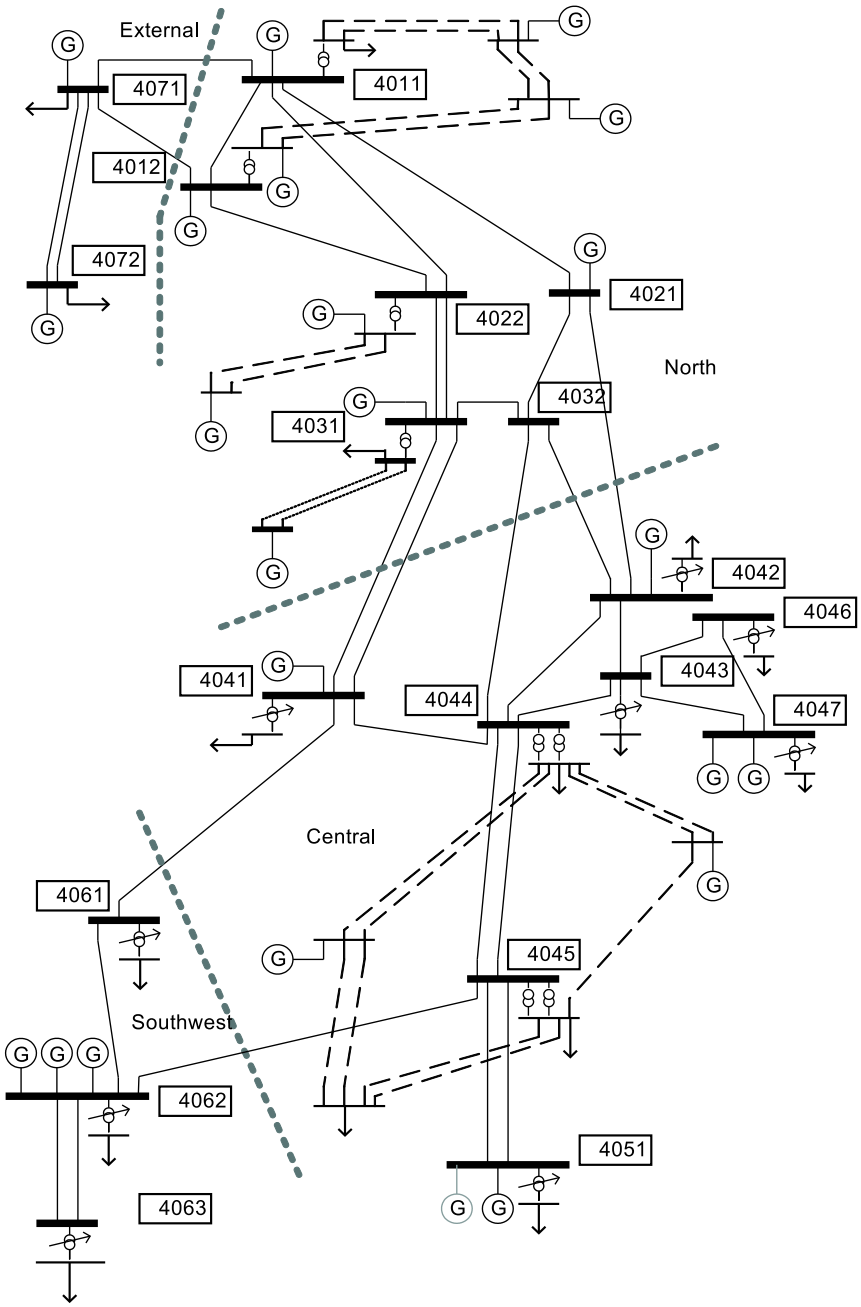


Fig. 9.1: Modified Nordic32 grid.

## 9.2 3% wind energy penetration scenario

As mentioned earlier, wind park-1 with a rating of 320 MW connected at the southwestern region corresponds to a 3% penetration scenario. The load and generation balance of the system is maintained by increasing the system load by 320 MW. As the wind farm is connected to the grid by a long cable, the wind farm has to be operated at a lagging power factor to assure a zero reactive power exchange with the grid. Wind park-1 operates at a lagging power factor of 0.98 which corresponds to 65 MVAr of reactive power absorbtion at the wind farm. The operating voltage at the wind turbine terminal is 0.95 pu.

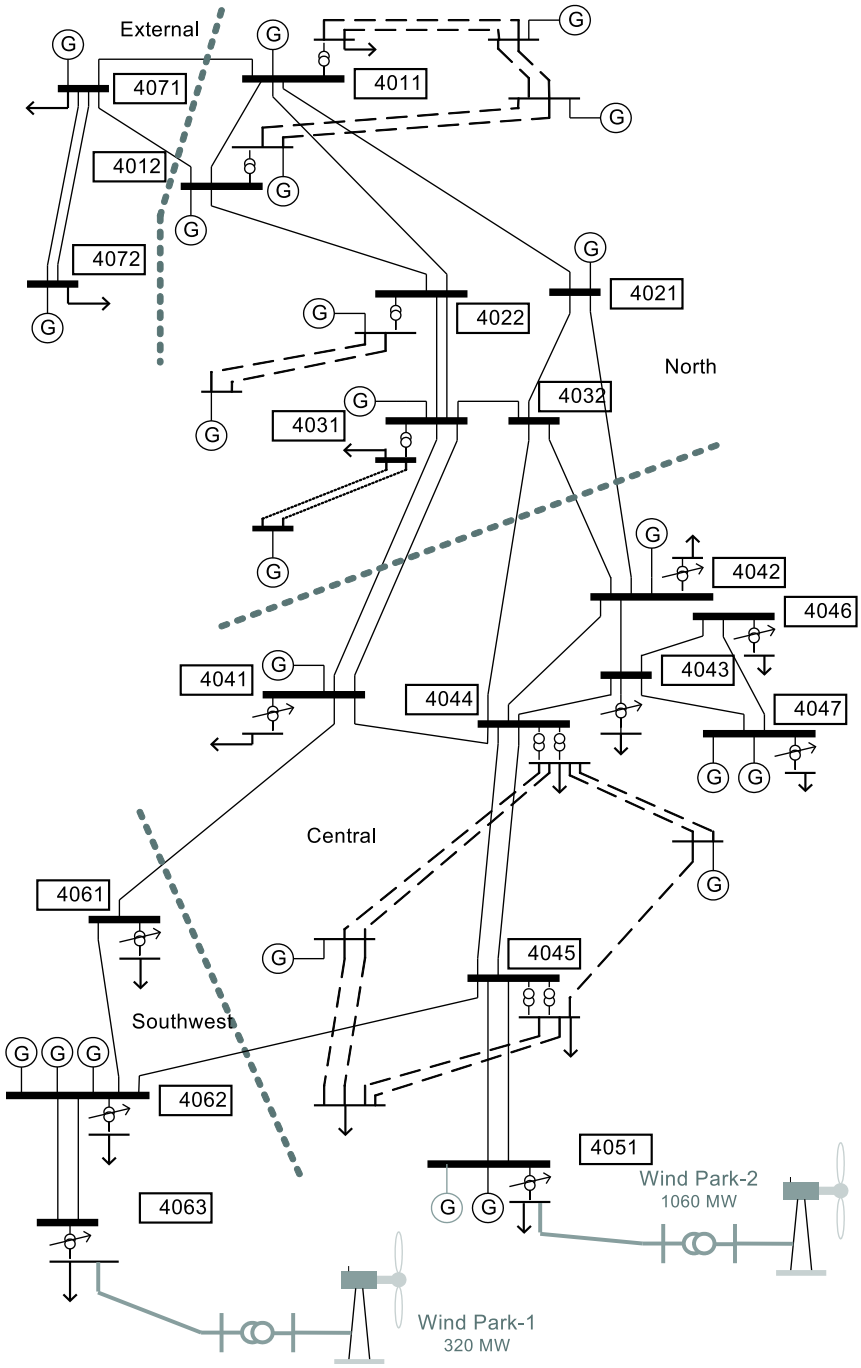


Fig. 9.2: Modified Nordic32 grid augmented with wind farms.

In following subsections the effects of different operational modes of wind park-1 on the transient stability of a nearby generator and on power oscillations are presented.

### 9.2.1 Effect on transient stability

A very common indicator of the transient stability of a synchronous generator is the critical fault clearing time ($t_{critical}$), which is defined as the maximum duration of a given fault that will not lead to the loss of synchronism of the generator [19].

To determine the transient stability limit of the system in the presence of wind park-1, a three phase to ground fault is applied at bus 4062, which is the nearest bus to the wind farm that has conventional generators connected. When the wind farm is operating in the constant power factor mode, which resembles system B, the critical fault clearing time is 263 ms. When the suggested transient stability enhancement mode is incorporated, which resembles system C, the new critical fault clearing time is 317 ms. For the purpose of comparison, the critical fault clearing time of the system without any wind farm is also calculated which is 312 ms. So a new wind farm of type B will endanger the system transient stability while wind farm of system C, which incorporated the suggested transient stability enhance mode, will increase the system transient stability.

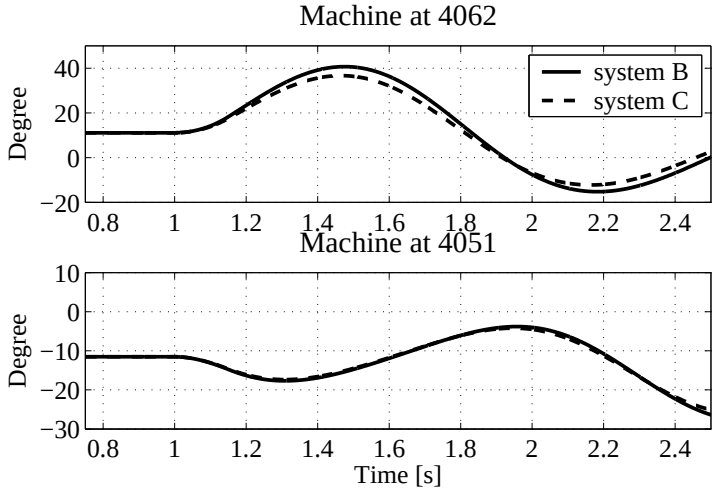


Fig. 9.3: Rotor angle swing of generators connected at bus 4062 and 4051 when a fault is applied at 4062.

Fig. 9.3 shows rotor angles of generators connected at 4062 and 4051 when a fault is applied at 4062 for 150 ms. As shown in the figure, the rotor angle swing of the generator connected at bus 4062 has been reduced when system C is utilized, compared to system B. It can be noted that the rotor angle of the generator at bus 4051 has not been affected significantly which is natural since it is electrically far away from wind park-1. So it is concluded that generators in other regions of the network, which are even further from the wind farm, will not be influenced by this modified operation of wind park-1.

### 9.2.2 Effect on power oscillations

The transmission line between bus 4062 and 4045 is disconnected which results in power oscillation in different parts of the network. The power oscillations in lines 4063-4062 and 4062-4061 are monitored. It is assumed that system C is operating in the voltage control mode. In Fig. 9.4, the power oscillations are shown. In the figure, transmission loadings are presented as a percentage of the respective SIL (serge impedance loading) of the line, which is 550 MW for all the monitored lines. An increased damping in power oscillations is observed in line 4063-4062 when the wind farm is operated in the voltage control mode. The wind farm terminal voltage and reactive power are shown in Fig. 9.5. By controlling its bus voltage by changing the reactive power, the wind farm manages to increase the damping

of power oscillations in the transmission line 4063-4062. As can be noticed from Fig. 9.4, due to the disconnection of line 4062-4045, the other transmission line 4062-4061, which connects the southwest region with the rest of the system, gets severely overloaded and the line will be tripped.

Another contingency situation is investigated where a generating unit at bus 4062 is disconnected. The resulting power oscillations in different transmission lines in the southwest region are shown in Fig. 9.6. An increased damping in power oscillations is observed in line 4063-4062 when system C is utilized instead of system B. No significant change is power oscillations are observed in the other two lines which are electrically far away from wind park-1.

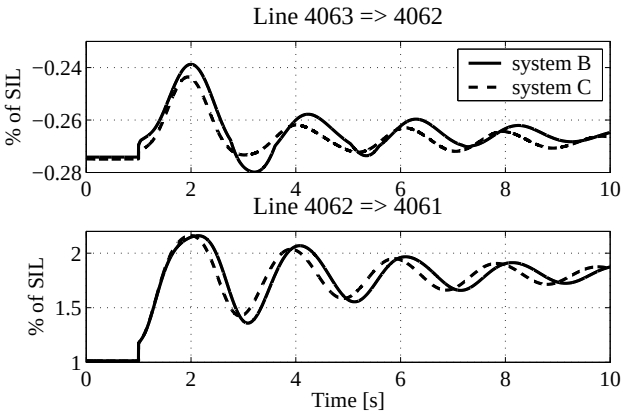


Fig. 9.4: Power oscillations in lines 4063-4062 and 4062-4061 when the line 4062-4045 is disconnected.

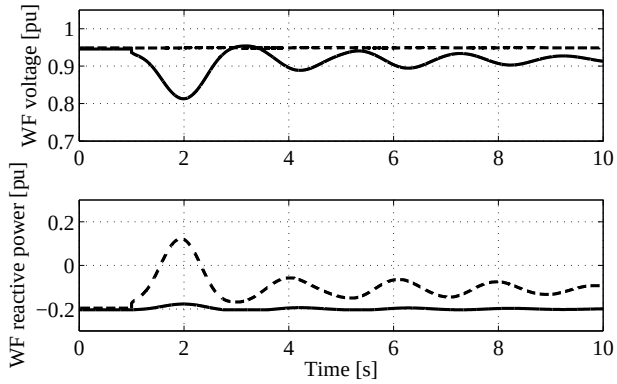


Fig. 9.5: Voltage at the wind farm terminal and the wind farm reactive power when line 4062-4045 is disconnected.

So it is concluded from this low penetration scenario analysis that by incorporating the transient stability enhancement mode in the operation of the planned wind farm in the south of Sweden, the transient stability of the conventional generators operating in that region can be increased. It is also found that the damping of power oscillations in transmission line 4063-4062 are increased when this wind farm is operated in the voltage control mode instead of the constant power factor mode although no significant change in power oscillations are observed in other transmission lines which are far away from the location of the wind farm.

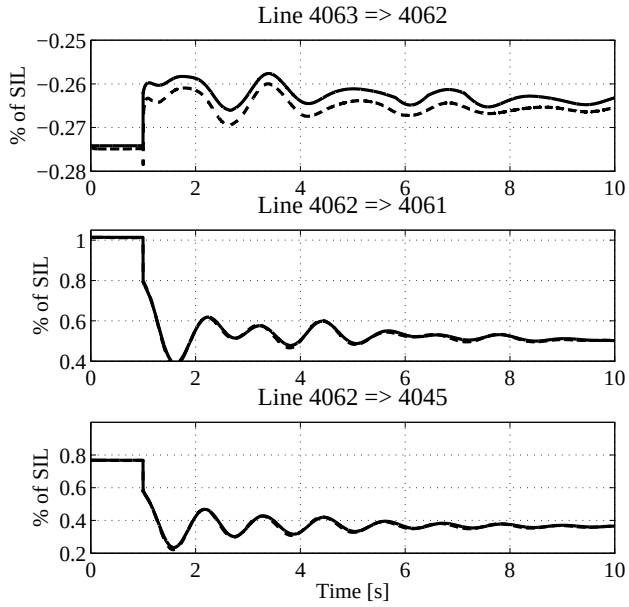


Fig. 9.6: Power oscillations in different transmission lines in the southwest region when one unit at bus 4062 is disconnected.

## 9.3 12% wind energy penetration scenario

A higher wind penetration scenario is also investigated. In this case it is assumed that another large wind farm (1 GW) is connected to the network near bus 4051. Two thermal generator units of equivalent size from the southwest region (at bus 4062) has been decommissioned in this case. To provide enough voltage support in the southwest region, two synchronous condensers are added in bus 4062. Their total capacity is 600 MVAr. This new wind farm, wind park-2, operates at a lagging power factor of 0.93 to maintain zero reactive power exchange with the grid in the pcc. The operating voltage of the wind farm is 0.97 pu.

Similar analysis of the transient stability and power oscillations are performed for this high wind penetration scenario as have already been done for the low wind penetration scenario, and the results are shown in the next subsections.

### 9.3.1 Effect on transient stability

To determine the transient stability of the system in presence of two large wind farms, a three phase to ground fault is applied at two different locations. First a fault is applied at bus 4062, which is near to wind park-1. The critical fault clearing time is 414 ms when system B is employed in wind park-1. When system C is employed, the critical fault clearing time is increased to 432 ms.

Another fault is applied at bus 4051 near wind park-2. Bus 4051 is the grid connection point of wind park-2 and a conventional generator is connected at this bus. The critical fault clearing time is 375 ms when system B is employed in wind park-2. When system C is employed, which incorporates the suggested transient stability enhancement mode, the critical fault clearing time increases to 676 ms. The critical fault clearing time of the system without any wind farm for a fault at bus 4051 is 539 ms.

### 9.3.2 Effect on power oscillations

Like the previous scenario, transmission line 4062-4045 is disconnected which results in power oscillations in different parts of the system. Power oscillations in transmission lines 4051-4045, 4063-4062, 4062-4061 and 4045-4044 are monitored. Fig. 9.7 shows the results. From the figure, it is noted that the damping of power oscillations in line 4051-4045 is reduced in the presence of a system C type wind farm which is located near bus 4051 and is operating in voltage control mode. A wind farm of system B type, which is operating at constant power factor, shows better performance in this case. It is due to the fact that two conventional synchronous generators are connected at bus 4051 which also is the connection point of the second wind farm. The interaction between the wind farm's simple voltage control mode of operation and the generator overall control may cause the reduced damping in power oscillations in line 4051-4045. Slightly reduced damping in power oscillations are also observed in line 4062-4061 and 4045-4044 when a wind farm of type C is employed compared to the case when a system B type is employed. Interesting to observe is that increased damping in power oscillations are observed in line 4063-4062. Note that wind park-1 is connected at the end of line 4063-4062 where no conventional generating unit is in operation. Therefore a simple voltage control mode operation of this wind farm increased the damping in power oscillations in line 4063-4062.

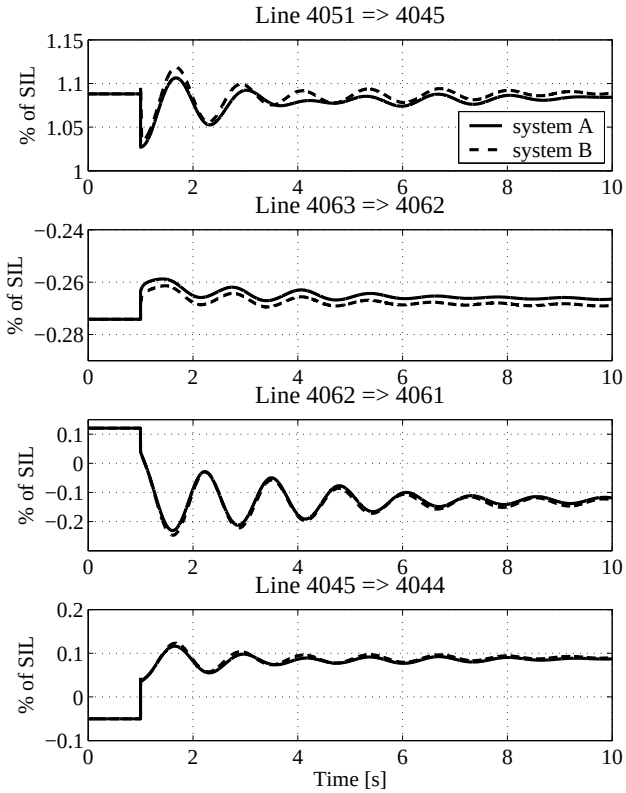


Fig. 9.7: Power oscillations in different lines when the line 4062-4045 is disconnected.

Another contingency situation is also investigated in this paper where the generating unit at bus 4062 is tripped. The resulting power oscillations in lines 4051-4045, 4063-4062, 4062-4061, 4062-4045 and 4045-4044 are shown in Fig. 9.8. A reduced damping in power oscillations are observed in line 4051-4045 when wind park-2 operates in voltage control

mode (system C) compared to the case when the wind farm operates in fixed power factor mode (system B). A reduction in the damping of power oscillations is also observed in the other lines, except for line 4063-4062. The damping in power oscillations is increased in line 4063-4062 when wind park-1 operates in the voltage control mode.

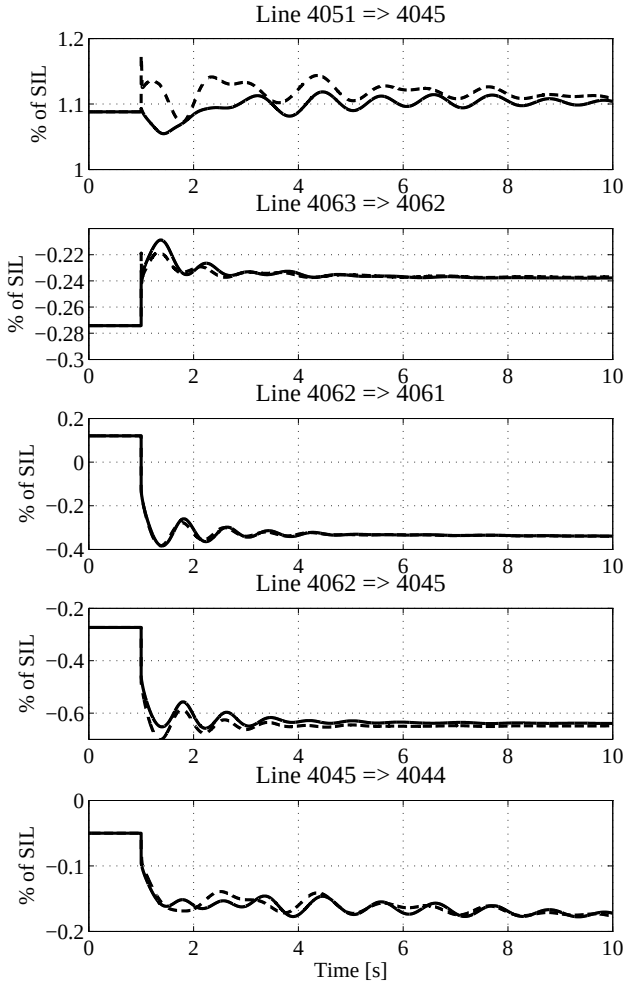


Fig. 9.8: Power oscillations in lines 4061-4062 and 4062-4061 when the line 4062-4045 is disconnected.

It is concluded from the high penetration scenario analysis that the transient stability of nearby conventional generators are increased from the base case when the proposed transient stability enhancement operation mode is incorporated into the control of the planned wind farms. It is also observed that using the simple voltage control mode of operation of wind park-2 did not increase the damping in power oscillations of the nearby transmission lines compared to the constant power factor mode operation. But the damping in power oscillations are increased in line 4063-4062 when wind park-1 operates in voltage control mode. Wind park-1 is connected at the end of line 4063-4062 where no conventional generators are in operation.

## 9.4 Discussion

In this study two different wind energy penetration scenarios are investigated. For both the scenarios it is found that by incorporating a transient stability enhancement operation mode in the control of several planned wind farms in the nordic grid, the transient stability of nearby conventional synchronous generators can be increased.

The effect of various control modes of a wind farm, namely, constant power factor operation and voltage control mode operation, on transmission line power oscillations are also investigated. In both the investigated wind penetration scenarios it is found that damping of power oscillations in line 4063-4062 are increased when wind park-1 operates in voltage control mode. While, this simple control mode employed in wind park-2 did not increase the damping of power oscillations in line 4051-4045. Interesting to note is that no conventional synchronous generator is connected at the connection point of wind park-1 while two synchronous generators are in operation at bus 4051 where wind park-2 is also connected. So care must be taken when designing the control of a large wind farm, in the situation where conventional synchronous generators are in operation near the wind farm. A voltage control mode of operation could in these situations reduce the damping of power oscillations.

# Chapter 10

# Conclusion and future work

## 10.1 Conclusion

In this thesis some grid assisting possibilities of variable speed wind turbines equipped with full-scale frequency converters have been investigated.

Results from an investigation of the transient stability influence from a wind energy installation were presented in Chapter 6. By incorporating a contingency operation mode into the control of a wind farm, it was shown that the transient stability of nearby connected conventional synchronous generators can be increased. For the investigated power system considered, the critical fault clearing time of the generator was 252 ms when a nearby connected WECS is a system B type WECS (standard variable speed operation today). When the contingency operation mode was incorporated into the control, the fault clearing time was increased to 292 ms.

In Chapter 7, results from the steady state and the long term voltage stability study were shown. It was shown that, large wind farms connected to the transmission level have the possibility to increase the steady state power transfer limit of the already existing transmission system provided that their controls have been modified properly. It was found in a case study that the steady state power transfer capacity of the transmission line could be increased by 17% during low wind speed situations when the control of the wind farm was altered without the need of larger grid side converters. In principle, wind farms with such modified control function can be seen as an active power source with a STATCOM connected in parallel with it. It was also shown that wind farms equipped with such a control function could also assist the grid to delay or even prevent a voltage collapse event.

Results from the investigation of the short term voltage stability aspects of a WECS were shown in Chapter 8. It is shown that wind farms integrated into the grid in the distribution level mixed with other loads, have the possibility to increase the short term voltage stability limit of the system. It was found that for a fault persisting more than 354 ms would cause short term voltage instability due to the stalling of motor loads in an example grid when WECSs connected to this grid did not incorporate the suggested contingency operation mode. The critical fault clearing time increased to 390 ms when their controls were modified. With the modified control, voltage dips could also be mitigated by WECSs and by doing so the tripping of sensitive loads can be avoided which would add an extra value to such WECSs. Of course, as shown in the thesis, the ability of a WECS to provide such improvement in the short term voltage stability and the voltage dip mitigation depends on the boosting capacity

of the WECS at the connection point to the grid.

Finally, the suggested grid assisting methods were incorporated into the control of two large planned wind farms in the southern part of the Swedish grid and tested in the CIGRÉ Nordic32 test grid, which is taken as a representation of the Swedish transmission network. Results were shown in Chapter 9. In one case it was found that by incorporating a contingency operation mode into the planned large wind farms, the transient stability of conventional generators located nearby the wind farms could be increased to 676 ms from the base case value of 539 ms when no wind farms were connected to the network. It was concluded that care had to be taken if voltage control mode of operation is utilized in a wind farm located close to a conventional synchronous generator. The interaction between the operational mode of a wind farm and the overall synchronous generator control may interact with each other and could lead to a reduction of damping of power oscillations in nearby transmission lines instead of increasing the damping.

## 10.2 Future work

There are several subjects worthy of further investigations. One is to investigate additional control functions that are possible to implement using wind energy installations. The possibility to and the size of the additional functions as well as their cost and use from a grid point of view are themes in need of more investigations. Examples of such additional functions are: Reactive power control in order to avoid a voltage collapse and to perform dip mitigation, damping of power system oscillations (PSS-function), primary frequency control as well as possibility to operate in island operation.

In the deregulated power market, these added features of a wind farm could add extra economic values to the wind farm owner. To realize this, ancillary services that a wind farm could provide have to be priced and it should be investigated whether this intermittent energy source can fit the existing market structure or a modified market structure has to be developed. This aspect could also be a future research directive.

A more detailed and deeper investigation is required to choose the proper control function of large wind farms located close to conventional synchronous generators. Their control functions have to be coordinated to that of nearby conventional generating units so that their mutual interaction do not lead to a reduction in the stability of the power system.

# References


[1] Gary L. Johnson, *Wind energy systems*. Englewood Cliffs, New Jersey: Prentice-Hall INC., 1985.

[2] Saifur Rahman, “Green Power: What Is It and Where Can We Find It?” IEEE Power and energy magazine, January/February 2003.

[3] (2006, Feb.) Multibrid technology website. [Online]. Available: http://www.multibrid.com/english/index.html

[4] (2006, Feb.) Vestas website. [Online]. Available: http://www.vestas.com/uk/Products/v120/v120_UK.htm

[5] (2006, Feb.) Enercon website. [Online]. Available: http://www.enercon.de/en/_home.htm

[6] (2006, Feb.) Repower systems website. [Online]. Available: http://www.repower.de/index.php?id=237&L=1

[7] J. Charles Smith, “Winds of change: issues in utility wind integration,” IEEE Power and energy magazine, November/December 2005.

[8] (2006, Feb.) German wind energy association (BWE) website. [Online]. Available: http://www.wind-energie.de/index.php?id=166

[9] (2006, Feb.) The european wind energy association website. [Online]. Available: http://www.ewea.org/

[10] (2006, Feb.) The american wind energy association website. [Online]. Available: http://www.awea.org/projects/index.html

[11] (2006, Feb.) Elåret 2005: Starket år för vattenkraft och kärnkraft gav elexport (in Swedish). [Online]. Available: http://www.svenskenergi.se/media/underlag/prm051228.pdf

[12] The Swedish National Energy Agency, Tech. Rep. no.: ER 6 2002. The Climate Report 2001. [Online]. Available: http://www.stem.se/web/biblshop.nsf/FilAtkomst/ER62002.pdf/$FILE/ER62002.pdf?OpenElement

[13] Vattenfall. (2006, Feb.). [Online]. Available: http://www.vattenfall.se/om_vattenfall/var_verksamhet/lokal/

[14] E.ON Vindprojektering Sverige AB. (2006, Feb.). [Online]. Available: http://www.eon.se/templates/InformationPage.aspx?id=42453

[15] J. Matevosyan, T. Ackermann, S. Bolik and L. Söder, "Comparision of international regulatuions for connection of wind turbines to the network," in *Proc. Nordic Wind Power Conference (NWPC'04)*, Göteborg, Sweden, March 2004.

[16] T. Ackermann, Ed., *Wind Power in Power Systems*. West Sussex: John Wiley and Sons Ltd., 2005.

[17] T. Gjengedal, "Integration of wind power and the inpact on power system operation," in *Power Engineering, 2003 Large Engineering systems Conference on*, 2003, pp. 76–83.

[18] C. W. Taylor, *Power System Voltage Stability*. New York: McGraw-Hill Inc., 1994.

[19] P. Kundur, *Power System Stability and Control*. New York: McGraw-Hill Inc., 1993.

[20] T. V. Cutsem, C. Vournas, *Voltage Stability of Electric Power Systems*. Boston: Kluwer Academic Publishers, 1998.

[21] N. G. Hingorani, L. Gyugyi, *Understanding FACTS - Concepts and Technology of Flexible AC Transmission System*. New York: IEEE Press, 2000.

[22] M. Noroozian, Å. N. Petersson, B. Thorvaldson, B. A. Nilsson and C. W. Taylor, "Benefits of SVC and STATCOM for Electric Utility Application," in *Proc. IEEE Transmission and Distribution Conference and Exposition*, Sept. 2003, pp. 1143–1150.

[23] C. A. Cañizares, and Z. T. Faur, "Analysis of SVC and TCSC controllers in voltage collapse," *IEEE Trans. Power. Syst.*, vol. 14, no. 1, pp. 158–165, Feb. 1999.

[24] A. E. Hammad, "Comparing the voltage control capabilities of present and future var compensating techniques in Transmission systems," *IEEE Trans. Power. Delivery.*, vol. 11, no. 1, pp. 475–484, Jan. 1996.

[25] E. Larsen, N. Miller, S. Nilsson, S. Lindgren, "Benefits of GTO-based compensation systems for electric utility applications," *IEEE Trans. Power. Delivery.*, vol. 7, no. 4, pp. 2056–2064, Oct. 1992.

[26] "Wind Turbines Connected to Grids with Voltages above 100 kV - Technical regulation for the properties and the regulation of wind turbines," Elkraft System and Eltra Regulation, Draft version TF 3.2.5, Dec. 2004.

[27] David M. Eggleston, Forrest S. Stoddard, *Wind turbine engineering design*, , Ed. New York, NY: Van Nostrand Reinhold Company, 1987.

[28] , *Wind turbine technology*, David A. Spera, Ed. New York, NY: ASME Press, 1994.

[29] Siegfried heier, *Grid integration of wind energy conversuion systems*, , Ed. West Sussex, England: John Wiley & Sons, 1998.

[30] N. R. Ullah, J. Groot, T. Thiringer, “The Use of a Combined Battery/Supercapacitor Storage to Provide Voltage Ride-Through Capability and Transient Stabilizing Properties by Wind Turbines,” in *Proc. 1st European Symposium on Super Capacitors and Applications ESSCAP’2004*, Belfort, France, November 2004.

[31] K. Walve, “Nordic32-A CIGRÉ Test System for Simulation of Transient Stability and Long Term Dynamics,” Svenska Kraftnat, Sweden, Tech. Rep., 1993.

[32] Å. Larsson, A. Petersson, N. R. Ullah, O. Carlsson, “Krieger’s Flak Wind Farm,” in *Nordic Wind Power Conference NWPC 2006*, Helsinki, Finland, May 2006.

[33] S. G. Johansson, “Mitigation of voltage collapse caused by armature current protection,” *IEEE Trans. Power. Syst.*, vol. 14, no. 2, pp. 591–599, May 1999.

[34] K. Bhattacharya, M. H. J. Bollen and J. E. Daalder, *Operation of Restructured Power Systems*. Boston: Kluwer Academic Publishers, 2001.

[35] Math H. J. Bollen, *Understanding Power Quality Problems*. New York: IEEE Press, 2000.

[36] Ringhals AB website. (2006, March). [Online]. Available: http://www.ringhals.se/index.asp?ItemID=1291

# Appendix A

# Parameters of investigated power systems

## A.1 Setup-1

Values of different components of set-up-2 are given in Table A.1 and A.2. System $S_{base}$ is 100 MVA. Transformer data on SBASE.

Table A.1: Transformer data

| *Parameter* | |
|---|---|
| $SBASE_{1-2}$ [MVA] | 70 |
| $V_{N1}$ [kV] | 33 |
| $V_{N2}$ [kV] | 130 |
| $R_{1-2}$ [pu] | 0.0 |
| $X_{1-2}$ [pu] | 0.1 |

Table A.2: Line data

| *Parameter* | |
|---|---|
| R, X, B [pu] | 0.06, 0.4, 0.06 |

## A.2 Setup-2

Values of different parameters of the investigated power system network, set-up-2, are given in Table A.3 and A.4. System $S_{base}$ is 1500 MVA. Transformers data are on SBASE.

## A.3 Setup-3

Values of different parameters of the investigated power system network, set-up-3, are given in Table A.5, A.6 and A.7. System $S_{base}$ is 100 MVA. Transformers data are on SBASE.

Table A.3: Transformer data

| *Parameter* | *T1* | *T2* | *T3* |
|---|---|---|---|
| $SBASE_{1-2}$ [MVA] | 1500 | 1500 | 700 |
| $V_{N1}$ [kV] | 230 | 400 | 132 |
| $V_{N2}$ [kV] | 400 | 132 | 400 |
| $R_{1-2}$ [pu] | 0.0 | 0.0 | 0.0 |
| $X_{1-2}$ [pu] | 0.07 | 0.07 | 0.07 |
| No. of steps | - | $\pm$16 | - |
| Step size | - | 15/16% | - |
| Dead band (pu bus voltage) | - | $\pm$5% | - |
| Initial time delay [s] | - | 25 | - |
| Subsequent time delay [s] | - | 5 | - |

Table A.4: Line data

| *Parameter* | *BUS2-BUS3 (four parallel lines)* |
|---|---|
| R, X, B [pu] | 0.13, 1.30, 0.18 |
| Line length [km] | 350 |

Table A.5: Transformer data

| *Parameter* | |
|---|---|
| $SBASE_{1-2}$ [MVA] | 10 |
| $V_{N1}$ [kV] | 11 |
| $V_{N2}$ [kV] | 40 |
| $R_{1-2}$ [pu] | 0.0 |
| $X_{1-2}$ [pu] | 0.08 |

Table A.6: Feeder data

| | R, X, B [pu] | $S_k \angle \psi_k$ |
|---|---|---|
| feeder-1 | 0.595, 1.785, 0 | 30MVA$\angle 78^o$ |
| feeder-2 | 0.397, 1.19, 0 | 38MVA$\angle 80^o$ |
| feeder-3 | 0.397, 0.297, 0.0004 | 56MVA$\angle 75^o$ |

Table A.7: Induction motor parameters (pu on motor base)

| $R_s$ | $X_s$ | $X_m$ | $R_r$ | $X_r$ | H | $S_{base}$ |
|---|---|---|---|---|---|---|
| 0.031 | 0.10 | 3.2 | 0.018 | 0.18 | 0.5 | 4 MVA |

# IMPROVING VOLTAGE STABILITY BY UTILIZING REACTIVE POWER INJECTION CAPABILITY OF VARIABLE SPEED WIND TURBINES

N. R. Ullah
Department of Energy and Environment
Chalmers University of Technology
Göteborg-412 96, SWEDEN
email: nayeem.ullah@chalmers.se

T. Thiringer
Department of Energy and Environment
Chalmers University of Technology
Göteborg-412 96, SWEDEN
email: torbjorn.thiringer@chalmers.se

**ABSTRACT**
The impact that wind turbines have on the voltage stability is investigated in this paper. In particular, the effect of utilizing the reactive power injection capability of modern wind energy converters is investigated. It is found that reactive power injection from the wind turbine can increase the voltage stability of the power grid substantially, as well as moderately increase the steady-state power transfer limit. For a high wind speed situation, where the wind turbine converter is fully utilized, it is found that it is worth reducing the active power production from the wind turbine in order to make room for reactive power injection, from a voltage stability point of view. An interesting observation is that a modern variable speed wind turbine constantly operating at maximum power factor does not provide much voltage stability improvement compared to a traditional fixed-speed system under its usual operating condition, i.e. at lower wind speeds. The finding is that the worst case to handle, from a voltage stability point of view, is the case where there is a high load demand, irrespective of the wind speed situation.

**KEY WORDS**
Renewable generation, variable speed wind turbine, power system stability, reactive power, ULTC.

## 1 Introduction

Voltage stability is related to the ability of a power system to maintain acceptable voltage profile throughout the system [1,3]. Reactive power consumption of the loads is the driving force of voltage instability. For this reason this phenomenon is also called 'load instability'[1,2]. Other factors influencing this phenomenon are the strength of the transmission system, generator reactive power - voltage control limits, characteristics of reactive compensating devices and the action of the under-load tap changer (ULTC) under low voltage conditions. Preventive measures to avoid voltage instability are the application of reactive power-compensating devices, control of generator reactive power output, control of transformer tap changers, under-voltage load shedding, etc.

The wind generation penetration level is increasing continuously today. The world-wide total installed capacity, by the end of 2004, was over 47 GW and the annual growth rate in 2004 was 20% [4]. The high penetration of wind energy has led to that new connection requirements (grid codes) for wind turbines are proposed. Different transmission system operators (TSO) propose their own connection rules (regarding voltage control, active and reactive power control, etc.). A comparison of some connection regulations can be found in [5].

Injecting reactive power into the load bus is a well known method to improve the steady-state power transmitted by the existing transmission line and also to improve the voltage stability limit [1-3]. Power electronic based reactive power compensators like the variable impedance type SVC (Static Var Compensator) and converter based STATCOM (Static Synchronous Compensator) can control the voltage in a continuous manner, unlike mechanically switched capacitors/reactors [6]. Several technical papers are available showing the applicability and effect of these power electronic based var compensators on the steady-state and transient voltage stability of electric power systems [7-10]. Some utility applications of these devices are listed in [6].

Variable speed wind turbines have a converter based reactive power injection facility already included in their design. An interesting possibility, accordingly, is to utilize the reactive power injection capability of the variable speed wind turbine for improving the voltage stability of the power grid.

The purpose of this paper is to investigate the effect that wind generators have on voltage stability. In particular, to study the possibilities of different wind turbine systems with various reactive power control algorithms, and to study the impact of reactive power injection by the wind turbine systems on the steady-state power transfer limit. In addition, one objective is to determine which load/wind generation situations that are the most critical. Another objective is to quantify the findings using case studies.

## 2 Analytical Procedure and Model Set-up

### 2.1 Description of the models

#### 2.1.1 Power system model

In order to study the impact that a wind farm, equipped with the control facilities proposed in this article, can have on the power system, a suitable grid is constructed. The analysis is carried out using the power system model shown in Fig. 1. The values of the network parameters are given in Appendix I. The selection of this example grid is inspired by the Swedish transmission system which is characterized by large scale power transfer through several 400 kV transmission lines from northern hydro generation sites to the load centers located mainly in the southern region. Wind generation sites primarily in the southern regions are considered.

The test system used in this paper consists of a wind farm installation connected to the 400 kV transmission grid (BUS3) and load connected at a load bus (BUS4). Part of the load is supplied by the wind farm and the rest comes from the main grid through long transmission lines. The wind farm rating is 200 MW. For a given wind speed situation, the maximum amount of load that can be supplied by the transmission line depends on line properties. The transformers T1 and T3 have fixed ratios, while T2 is a tap changing transformer.

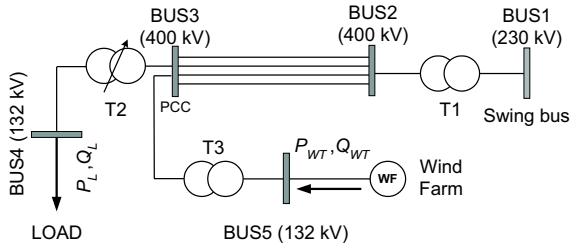


Figure 1. Single line diagram of the investigated power system.

#### 2.1.2 Load model

In this study, a 0.85 lagging *pf* static ZIP load model is considered consisting of 50%Z load, 25%I load and 25%P load. The active ($P_L$) and reactive power ($Q_L$) at any voltage $V$ are accordingly given by

$$P_L = zP_o\{0.5(\frac{V}{V_o})^2 + 0.25(\frac{V}{V_o}) + 0.25\} \quad (1)$$

$$Q_L = zQ_o\{0.5(\frac{V}{V_o})^2 + 0.25(\frac{V}{V_o}) + 0.25\} \quad (2)$$

where z is a demand variable which represents the total amount of equipment connected at the bus, $V_o$ is the nominal voltage of the load bus, $P_o$ and $Q_o$ are load active and reactive power demand at nominal voltage, respectively, when $z$=1.

#### 2.1.3 Wind farm model

In this paper the individual wind turbines are assumed to be equipped with full power converters. For the purpose of comparison, a traditional fixed speed wind turbine set-up (directly connected induction machine with only no-load fixed reactive compensation) is also considered. Four different types of wind turbine systems are investigated here (see Fig. 2),

System-*A* - traditional fixed speed wind turbine system with constant no load reactive power compensation.

System-*B* - variable speed wind turbine producing active power at unity power factor.

System-*C* - variable speed turbine with a full power grid side converter which has the same power rating as the turbine. While producing active power, this wind turbine system can inject/absorb reactive power into the grid as long as the current injection limit of the converter is not violated. During high wind speed operation, the system is able to reschedule its active production, to provide emergency reactive support to the grid.

System-*D* - with a larger grid side converter (over dimensioned). Reactive power support to the grid is possible during high wind speed operation without reducing the active production from the turbine.

Emphasis will be on systems *C* and *D* mainly.

Systems *B*, *C* and *D* are modelled as a negative load at the connection point with negative conductance and positive susceptance, as shown in Fig. 3. The wind farm acts like a constant MVA source within the converter's current limit. The conductance($G_{WT}$) and susceptance($B_{WT}$) are given by

$$\hat{Y}_{WT} = -G_{WT} + jB_{WT} = \frac{P_{WT} + jQ_{WT}}{\hat{V}_{WT}^2} \quad (3)$$

where $P_{WT}$ and $Q_{WT}$ are the wind farm's active and reactive power production, respectively, $V_{WT}$ is the wind farm connection point voltage. The injected current by the wind farm is

$$\hat{I}_{WT} = \sqrt{(P_{WT} + jQWT)\hat{Y}_{WT}}. \quad (4)$$

When the converter current limit is reached, it operates as a constant current source and conductance and susceptance varie according to

$$\hat{Y}_{WT} = -G_{WT} + jB_{WT} = \frac{I_{max}\angle arctan(\frac{Q_{WT}}{P_{WT}})}{\hat{V}_{WT}} \quad (5)$$

where $I_{max}$ is the converter maximum current rating. Current injection at this stage is

$$\hat{I}_{WT} = I_{max}\angle arctan(\frac{Q_{WT}}{P_{WT}}). \quad (6)$$

In the simulations, two different wind speed situations are considered: high and low. At high wind speed, the turbine operates at rated power and at low wind speed it operates at 30% of its rated production.

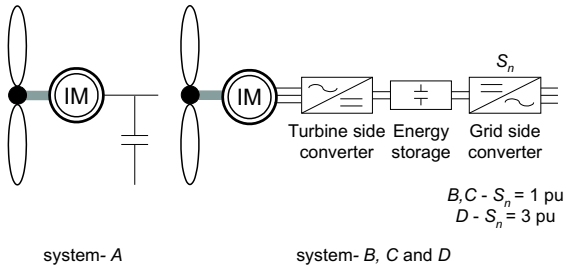


Figure 2. The wind turbine systems treated in this paper.

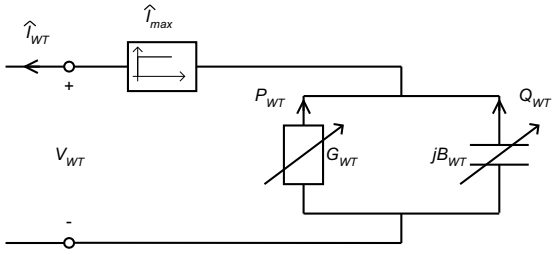


Figure 3. Variable speed wind turbine model.

## 2.2 PV diagram

Fig. 4 illustrates the definitions of the quantities $P_{allow}$, $P_{max}$ and $V_{maxP}$ using a *PV* diagram. $P_{allow}$ defines the allowed active load that can be drawn keeping the bus voltage at 0.95pu and $P_{max}$ is the maximum deliverable load. The voltage is defined as $V_{maxP}$ when the active load consumption is $P_{max}$. In the following sections, the results from the analysis will be presented in *PV* diagrams for BUS4, see Fig. 1.

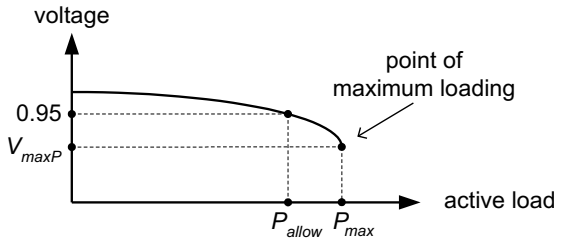


Figure 4. $PV$ diagram showing $P_{allow}$, $P_{max}$ and $V_{maxP}$.

## 2.3 Case studies

Simulations are carried out for two general cases. In the first case, the tap changing action of transformer T2 is blocked and the static voltage behavior is presented using a *PV* diagram. In the second case, the tap changing action is included to carry out different dynamic case studies. The above mentioned four types of wind turbine systems are investigated in both cases.

## 2.4 Simulation tool

The commercial power system simulation software PSS/E® is used for the simulations and analysis. Both the load flow module (psslf4) and the dynamic simulation module (pssds4) are used for simulations. The wind farm systems *B*, *C* and *D* are written as user-defined models in FORTRAN®, whereas the PSS/E® library model for the induction machine (CIMTR3) with a shunt capacitor is used to represent system *A*.

# 3 Voltage Stability Aspects of Systems *C* and *D*

The reactive power injection capability of the wind turbine systems *C* and *D* can be seen as a shunt compensation for the power grid. The power system in Fig. 1 can be simplified to the one shown in Fig. 5, where $B_l$ is the line charging susceptance and $X_l$ is the inductance of the line. The Thevenin equivalent seen by the load has the following emf and impedance

$$E_{th} = \frac{1}{1-a-jb}E \tag{7}$$

$$Z_{th} = R_{th} + jX_{th} = \frac{j}{1-a-jb}X_l \tag{8}$$

where $a = X_l(B_l + B_{WT})$ and $b = X_l G_{WT}$. The maximum deliverable power to the load for a given power factor $\cos\phi$ is

$$P_{max} = \frac{\cos\phi}{|Z_{th}| + Re\{Z_{th}\}\cos\phi + Im\{Z_{th}\}\sin\phi}\frac{{E_{th}}^2}{2}. \tag{9}$$

Replacing $E_{th}$ and $Z_{th}$ into (7) gives

$$P_{max} = \frac{\cos\phi}{\sqrt{(1-a)^2+b^2} - b\cos\phi + (1-a)\sin\phi}\frac{E^2}{2X_l} \tag{10}$$

and the corresponding voltage at this maximum load is

$$V_{maxP} = \frac{1}{1-a-jb}\frac{E}{\sqrt{2}\sqrt{1+\frac{(1-a)\sin\phi - b\cos\phi}{\sqrt{(1-a)^2+b^2)}}}}. \tag{11}$$

Equation (8) shows that with increasing reactive power injection from the wind turbine, which means in-

creasing $a$, the maximum deliverable power to the load increases. The load voltage at this maximum load also increases with increasing reactive power injection. The maximum deliverable load also depends on the active production of the wind turbine, which corresponds to $G_{WT}$. Similar calculations are shown in [2] for a pure capacitive shunt compensation.

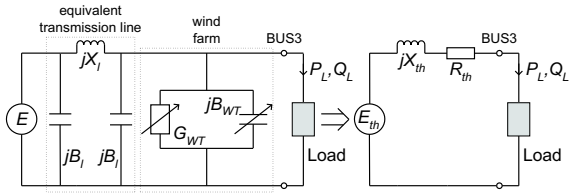


Figure 5. Shunt compensation by wind turbine system *C* and *D*.

## 4 Results (Tap Changer Locked)

### 4.1 Low wind speed situation

The operating point of the wind turbine system *C* during a low wind speed situation is shown in point $LW_1$ in Fig. 6, where the power factor is kept at unity. At this operating point, the wind turbine does not utilize the full capacity of its power electronic converter. Keeping the active power production at the same level, the wind turbine system can inject a substantial amount of reactive power into the grid until it reaches the operating point $LW_2$, shown in Fig. 6. The reactive power injection capability of this type of wind turbine system can be seen as a shunt compensation for the power system but with negligible additional cost.

Fig. 7 shows the *PV* curves at the load bus (BUS4) in the presence of the different wind turbine systems. It is clear from Fig. 7 that the maximum deliverable power ($P_{max}$) is increased by using the reactive power injection facility of the variable speed system *C*. In other words, the voltage stability margin can be increased by reactive power injection from system *C*. Fig. 7 shows one particular case where system *C* uses 50% of its available reactive power resource (operating point $LW_3$ in Fig. 6). In this case, $P_{allow}$ increases from 885MW to 960MW and $P_{max}$ increases from 916MW to 985MW. By using system *D* during low wind speed situations, however, these quantities can be increased even more.

Fig. 8 shows the allowed and maximum steady-state power obtained using different levels of reactive power injection from the wind farm. Both $P_{max}$ and $P_{allow}$ at the load bus (BUS4) increase with increasing reactive power injection by the wind farm at BUS6, which is to be expected. It can be noted that at a higher reactive power injection level of the wind farm, the normal operating point progressively approaches the nose point of the $PV$ curve (Fig. 8).

Fig. 9 shows the percentage improvement in $P_{max}$ and $P_{allow}$. These quantities increase up to 14% and 17%, respectively, when the reactive power injection capacity of the wind farm is fully used.

The above simulations show a grid stabilizing property of a wind farm based on system *C*. It is clear from the calculations that, at low wind speed the power electronic converter of the turbine can be utilized to increase the voltage stability limit of the nearby load bus. As mentioned above, this can be done with negligible extra cost.

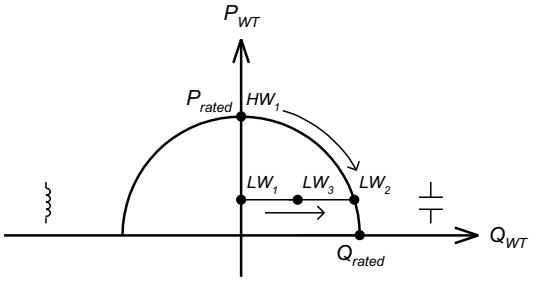


Figure 6. Variable speed wind turbine's capability curve at nominal voltage (system *B* and *C*).

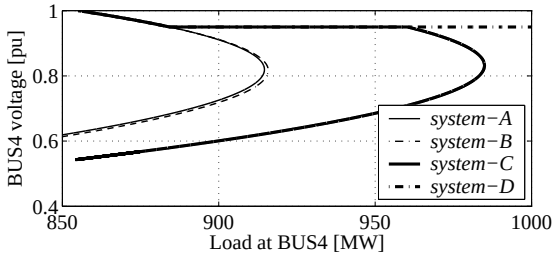


Figure 7. BUS4 $PV$ diagram considering the four types of wind turbine systems at BUS6. Low wind speed situation.

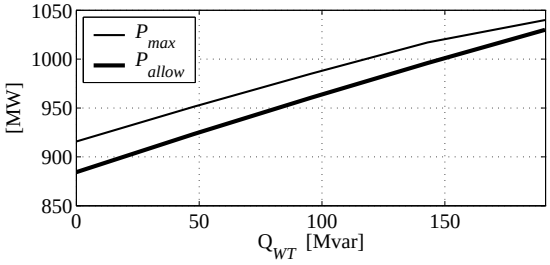


Figure 8. $P_{max}$ and $P_{allow}$ at BUS4 with different reactive injection levels of the wind turbine systems. Low wind speed situation.

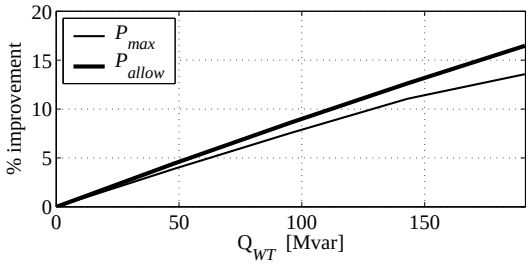


Figure 9. Percentage improvement in $P_{max}$ and $P_{allow}$. Low wind speed situation.

## 4.2 High wind speed situation

The power production from the turbine reaches rated value during high wind speed situations. The operating point shifts to $HW_1$, as shown in Fig. 6. The reactive power injection capability of the wind turbine system *C* is zero at this point. The grid reactive power requirement can be met at this stage of operation of the wind turbine system in the two ways below.

### 4.2.1 Reduction of active power production

A method for avoiding a voltage collapse event, due to the generator's armature current protection, by rescheduling the conventional generator, is illustrated in [11]. The possibility of such rescheduling of a modern wind farm is investigated here.

One way to provide emergency reactive power support to the grid during high wind speed situations is to reduce active power production from the wind farm system (*C*), and to utilize the relieved capacity of the existing power electronic converter to produce reactive power. Instead of operating at $HW_1$, the wind farm then will operate at any point in the first quadrant of the capability diagram, depending on the grid's need, observe the curved arrow in Fig. 6.

Fig. 10 shows the effect of shifting the operating point of the turbine, from the normal operation ($HW_1$), at $P_{max}$ and $P_{allow}$. As shown in the figure, both $P_{max}$ and $P_{allow}$ can be increased from their initial values (when, $P_{WT}$ = $P_{rated}$ and $Q_{WT}$ = 0) by reducing active power production from the turbine and utilizing the remaining capacity of the grid side converter to inject emergency reactive power into the grid. By employing this active power reduction mode of operation, both $P_{max}$ and $P_{allow}$ can be improved up to 12% and 15%, respectively, from their initial values.

The curves show that the proposed wind turbine system *C* can assist the grid even during high wind speed operation by reducing its active power production level and using the remaining capacity of the power electronic converter for injecting reactive power. Operation of the proposed system *C* in this active power reduction mode can be seen as a grid stabilizing property of the wind turbine. If the wind farm owner can be compensated for this *non-supplied production* as a form of *lost opportunity payment*, operation in this mode can be economically viable.

This active power reduction mode can also be employed during low wind speed operation if the reactive power needed by the grid is higher than the available reactive power injection capacity of the wind farm at this wind speed. Of course, operation of the wind farm in this *untraditional* mode depends on grid regulations and the level of compensation from the system operator.

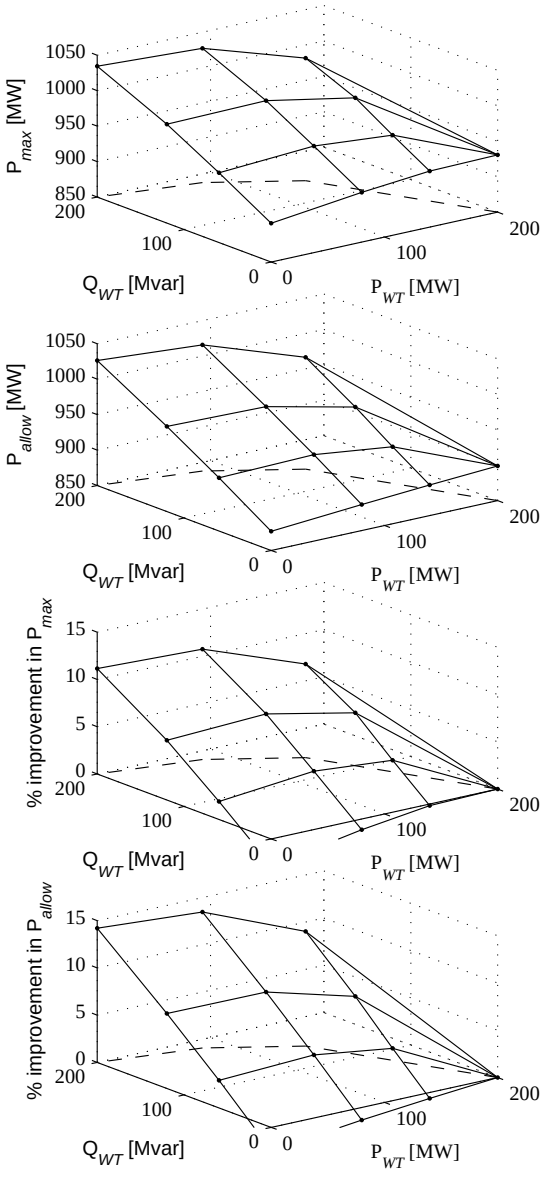


Figure 10. $P_{max}$, $P_{allow}$ and percentage improvement in $P_{max}$ & $P_{allow}$ at BUS4 during active power reduction mode of operation.

### 4.2.2 Over-dimensioning of grid side converter

Another way of providing reactive power support to the grid during high wind speed operation is to increase the size of the grid side converter (over-dimensioning). In this study, a three times larger grid side converter is considered. The active and reactive power production range of this type of wind turbine, system-*D*, is presented in Fig. 11. If a disturbance occurs in the grid, system *D* can maintain the active power production at high wind speed and still feed reactive power into the grid, reaching the point $HW_2$ (Fig. 11).

Fig. 12 presents the *PV* diagram of BUS4 considering a high wind speed situation. From this figure, it is clear that the maximum deliverable power to the load is increased when system *D* is used during a high wind speed situation without reducing active power production. One particular case is shown where system *D* utilizes 50% of its reactive power injection capability ($HW_3$). System *C* can also increase these quantities during high wind speed operation by reducing its active power production and utilizing the remaining capacity of the converter to inject reactive power. Fig. 12 shows one case where system *C* reduces its active production by 30% to allow for injecting reactive power and by doing so, increasing the $P_{allow}$ and $P_{max}$. It is interesting to note that, the standard variable speed system *B* does not provide much improvement in $P_{allow}$ and $P_{max}$ compared to the traditional fixed speed system *A*, while the use of systems *C* and *D* provides substantial improvement.

Fig. 13 presents $P_{max}$ and $P_{allow}$ for different reactive power injection levels of the wind farm. At higher reactive injection levels (near $HW_2$), the normal steady-state operating point ($P_{allow}$) is close to the maximum power transfer limit (nose point), which represents a highly compensated situation. But the high reactive power injection capacity of this type of wind turbine system can be valuable for maintaining the transient voltage stability of the system, as well as increasing the steady-state power transfer level.

Fig. 14 shows the percentage improvement in maximum and allowed power. By utilizing full reactive power injection capacity, the maximum and allowable power increases up to 38% and 43%, respectively.

Based on the results presented above, it can be said that the reactive power injection capability of the wind farm with this proposed over-dimensioned grid side converter can increase the voltage stability limit of the load bus substantially during high wind speed operation without reducing active power production from the farm, while a minor improvement is obtained if the converter rating is kept constant.

## 5 Results (Tap Changer Unlocked)

So far, results have been presented without considering the tap changing action, in order to purely see the effect of the

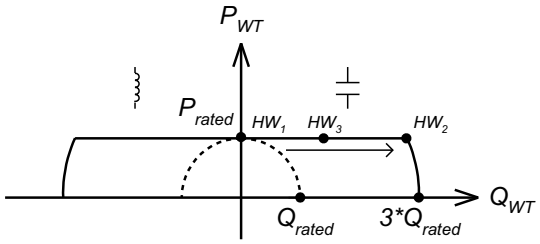


Figure 11. Capability curve of a modern variable speed wind turbine with an over dimensioned grid side converter (system-*D*).

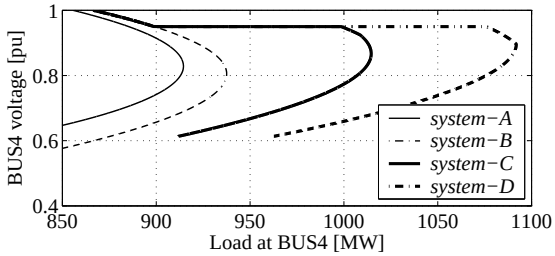


Figure 12. BUS4 $PV$ diagram considering the four types of wind turbine systems at BUS6. High wind speed situation.

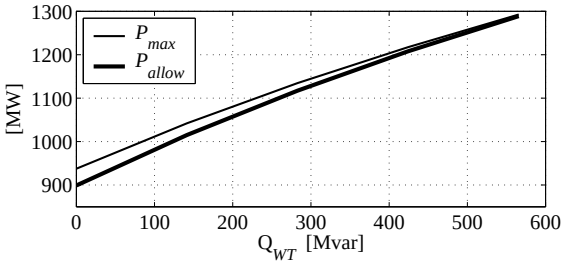


Figure 13. $P_{max}$ and $P_{allow}$ at BUS4 with different reactive power injection levels of the wind turbine systems. High wind speed situation.

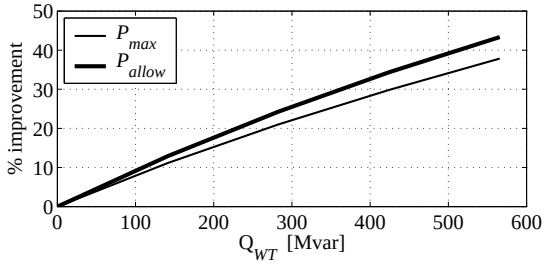


Figure 14. Percentage improvement in $P_{max}$ and $P_{allow}$. High wind speed situation.

reactive power injection from the wind turbine. However, tap changer action is an important issue, in fact, one of the driving forces of voltage instability [2,3]. By restoring the load side voltage to a predefined voltage range, the ULTC progressively degrades the transmission level voltage which can lead to a possible voltage collapse event. One possibility lies in utilizing the reactive power injection capability of the proposed wind turbine systems in a coordinated manner with the tap changing transformer, to avoid such destabilizing situations. For this purpose, some possible operational modes for the wind farm are discussed here.

## 5.1 Proposed wind farm control algorithms

### 5.1.1 Algorithm-1

With this strategy, the wind farm maintains steady-state voltage at the transmission level (BUS3), where it is integrated into the grid, within a predefined limit. This voltage regulation limit of the grid can be the same or may differ from the dead band of the tap changing transformer. Here, both limits are assumed to be the same ($\pm$5% deviation).

### 5.1.2 Algorithm-2

In this operational mode, the wind farm reacts in such a way that it utilizes its reactive power injection facility whenever the grid voltage deteriorates due to the tap changing action of the transformer. Here, the wind farm only counteracts the voltage reduction at the transmission level due to the tap movement of the transformer.

### 5.1.3 Algorithm-3

This algorithm states that, while integrated into the transmission level (BUS3), the wind farm uses its reactive power injection capability to regulate the distribution/load level voltage (BUS4). The constraint that is imposed in this algorithm is that the wind farm should meet the connection point (BUS3) voltage requirements set by the system operator.

Besides improving the transmission level voltage stability, the operation of the wind farm using algorithm *1* or *3* has a few additional advantages over operation using algorithm *2*. One is that, modes *1* and *3* enable the wind farm to prevent the tap of the transformer from operating. This is beneficial to the transformer in that excessive tap movement reduces the tap-changer's life-span. Another advantage is that algorithms *1* and *3* have better voltage stability performance than algorithm *2*. One drawback of algorithms *2* and *3* is that both algorithms require communication with other network equipment, while algorithm *1* can work on information based on the connection point voltage without communicating with other network equipment.

For a grid with wind power production, as considered in this study, the methods stated here can be seen as a better suited solution for emergency control of a tap changing transformer than the 'tap-reversing' method mentioned in [12]. 'Tap-reversing' decreases the load voltage and, hence, the load power when applied before the point of maximum loading (operation in upper part of the nose curve). The wind farm reactive power control strategies proposed in this paper restore the transmission level voltage, deteriorated by the tap changing action of the transformer, with a positive effect on load side voltage and, consequently, on the load.

The next subsection shows dynamic simulations employing algorithm *1*. A steady-state analysis has already been done in the previous section using algorithm *3*.

## 5.2 Case studies

Simulations are performed here using the tap changing action of the transformer $T_2$, applying algorithm *1* to the wind farm. The parameters for the tap changing transformer are given in Appendix I. Considering the wind speed situation and different load demands, four different cases are considered here. The four cases are:

| | Low demand | High demand |
|---|---|---|
| Low wind | Case 1 | Case 2 |
| High wind | Case 3 | Case 4 |

In Case 1, a low wind speed situation is considered at a wind turbine installation which implies 60 MW of wind power generation. The total load at the load bus (BUS4) is (910 MW, 560 Mvar). The grid disturbance is applied by disconnecting one of the high voltage transmission lines. The results are presented in Fig. 15. After the line disconnection, the BUS3 voltage drops due to the increasing reactive losses in the line and also due to the reduced line charging. With the passive type of wind farm (system *A* or *B*) integrated into the power system, the transmission level voltage (BUS3) drops further due to the tap changing action of the transformer. The tap changing action restores the load side voltage (BUS4), but one drawback is that it has a negative impact on grid side voltage and can initiate a voltage collapse event (Fig. 15). However, when considering the active wind turbine system *C*, the possible voltage collapse event is avoided. In this case, the wind turbine system utilizes its reactive power injection capability to maintain the voltage on the transmission level (BUS3) within the allowed limit ($\pm$5% deviation) after the grid disturbance. Most of the load side voltage (BUS4) is also restored by this action taken by the wind farm and part of the load side voltage is restored, in this case, by a few tap movements of the transformer. The voltage reduction at the transmission level due to this tap movement is counteracted by subsequent reactive power injection by the wind farm. These few tap movements can be eliminated either by reducing the voltage regulation dead band of the wind farm or by employing algorithm *1*.

In Case 2, a high load scenario is considered (1050 MW, 650 Mvar) when wind generation is low. The results are shown in Fig. 16. Using systems *A* and *B*, a voltage collapse event is evident. But with system *C*, the voltage collapse event can be delayed. In this case, system *C* hits its reactive power injection limit. The possible voltage collapse event is avoided by using system *D* which has a larger reactive power injection capability. A twice as large ($2\times$) grid side converter saved the system from a possible voltage collapse event.

A high wind generation and low load scenario is considered in Case 3. The results are shown in Fig. 17. Using wind turbine systems *A* and *B*, the power system approaches a voltage collapse event after the disconnection of one of the transmission lines. But with system *C*, employing the active power reduction mode during a high wind speed situation, by reducing the active power production from the turbine to allow for reactive power injection, the voltage collapse event is avoided. In this particular situation, a 50% reduction in the active power generation is needed. The voltage collapse event can also be avoided, as expected, by using system *D*. By employing system *D*, no reduction in active power production is required. In this case, a 25% over-dimensioning of the grid side converter is enough to avoid an emerging voltage collapse event.

Finally, a high wind speed and a high load situation are considered. The results are shown in Fig. 18. With the active wind turbine system *C*, the emerging voltage collapse event is delayed by employing the active power reduction mode, whereas the passive systems *A* and *B* fail to prevent the instability. However, the active wind turbine system *D* completely prevents the voltage collapse event due to the tap changing action of the transformer. Here, a twice as large ($2\times$) grid side converter is needed to prevent a possible voltage collapse event.

## 6 Discussion

The economic aspects associated with the active power reduction mode and the over-dimensioning of the grid side converter are beyond the scope of this study. However, it seems reasonable to guess that a grid side converter bridge having a capacity of twice the nominal power of the turbine should most certainly not exceed an additional cost of the turbine of 5%. Large hydro generators that have an agreement with the system operator trade their reactive power effort as an ancillary service, which the system operator uses to secure voltage stability of the system [13]. With increasing wind power penetration level, if the wind farm can trade its reactive power injection capability like large hydro generators, then over-dimensioning of the grid side converter can be economically viable. Also, if a wind farm owner could obtain compensation for *non-supplied production*, as a form of *lost opportunity payment*, the active power reduction mode of operation would be possible to implement.

The case studies considering the tap changing action of the transformer, presented in the paper, show that reactive power injection from wind turbine installations (systems *C* and *D*) can prevent a possible voltage collapse event due to tap movement. This can be seen as a global voltage

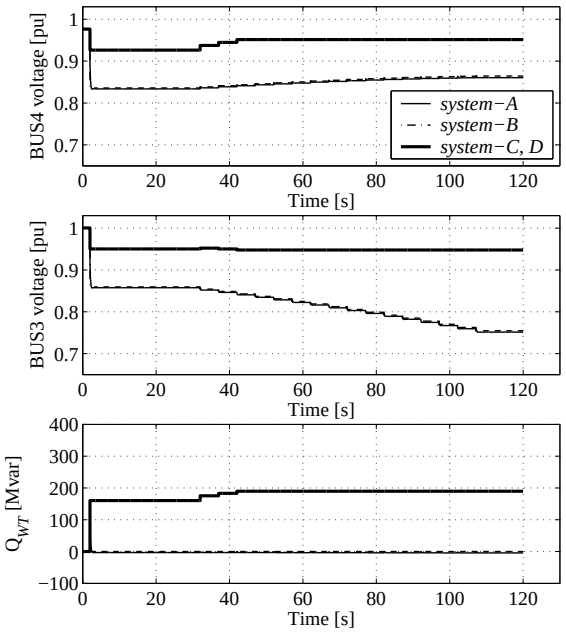


Figure 15. Case 1 (low wind, low demand): BUS3 and BUS4 voltage after the disconnection of one of the transmission lines and the response of different types of wind farms to this disturbance.

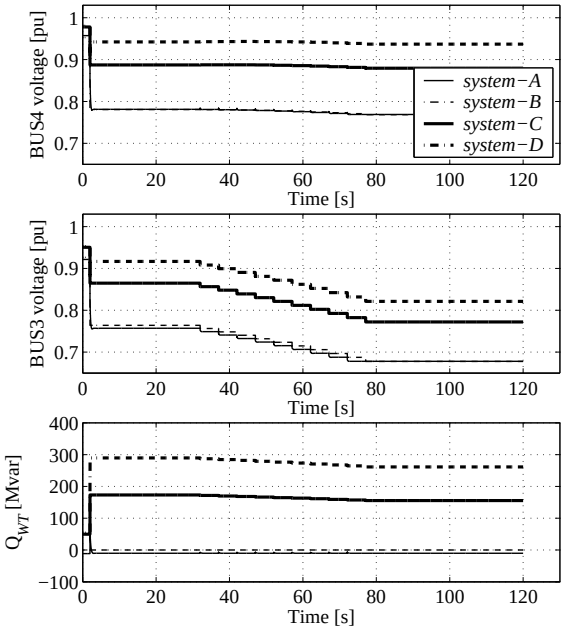


Figure 16. Case 2 (low wind, high demand): BUS3 and BUS4 voltage after the disconnection of one of the transmission lines and the response of different types of wind farms to this disturbance.

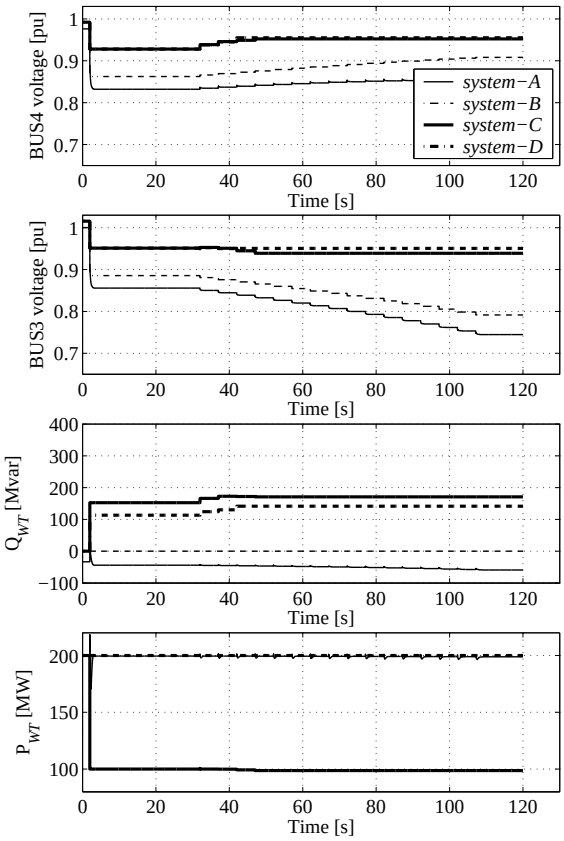


Figure 17. Case 3 (high wind, low demand): BUS3 and BUS4 voltage after the disconnection of one of the transmission lines and the response of different types of wind farms to this disturbance. Active power production ($P_{WT}$) from system *A*, *B* and *D* remains at 200 MW.

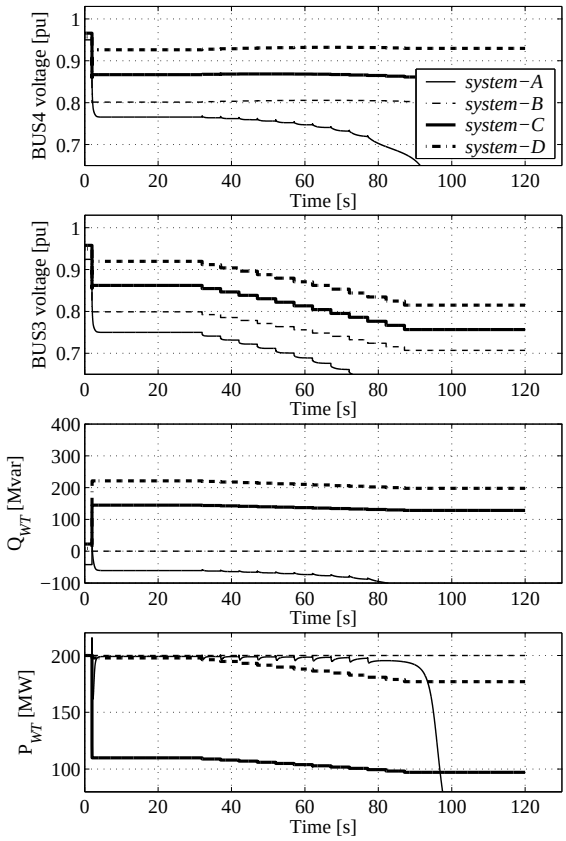


Figure 18. Case 4 (high wind, high demand): BUS3 and BUS4 voltage after the disconnection of one of the transmission lines and the response of different types of wind farms to this disturbance. Active power production ($P_{WT}$) from system *B* and *D* remains at 200 MW.

stabilizing property of the proposed wind turbine systems (*C* and *D*).

A recent draft version of a technical regulation for wind farms connected to the transmission grid in the Danish system, provides guidelines for reactive power control of wind farms [14]. This regulation requires wind farms to have the capability for altering active and reactive power production via remote control, and locally, on demand by the system operator, depending on the network situation. This implies that the system operator would have the potential to utilize the reactive power injection capability of the wind farms to increase system security and the wind farm owners would have the opportunity to trade for the built-in reactive power injection facility in the deregulated market environment. The results presented in this paper can give input to further investigation into such possibilities.

## 7 Conclusion

In this paper, the possibility of utilizing the reactive power injection capability of a modern wind turbine was investigated. It was shown that the grid voltage stability limit can be increased by utilizing the reactive power injection capability of a modern wind turbine.

The two proposed methods for giving reactive support to the grid during high wind speed situations were found to be beneficial to voltage stability. By reducing the active power production from the wind farm, to be able to inject reactive power, the allowed and maximum deliverable loads were increased up to 15% and 12%, respectively. By using a larger grid side converter ($2\times$), improvements were a substantial 29% and 25%, respectively.

It was also found that the standard variable speed system operating at unity power factor does not provide much improvement in allowed and maximum deliverable power, compared to the traditional fixed speed system unless the turbines operate at full power. Substantial improvement was achieved by using the reactive power from the wind farm.

The main idea of the proposed wind farm reactive power control algorithm was to regulate the voltage at the transmission level (point of connection into the grid) by using the reactive power injection facility of the wind farm.

It was found that, the proposed control algorithm for the wind farm improvesd the global voltage stability without communicating with other network equipment. In addition, it also prevented the transformer's tap from operating. This is advantageous for the transformer in the sense that excessive tap movement reduces the tap-changer's life-span.

## 8 Acknowledgments

In addition to the financial support provided by Sydkraft AB, the authors would also like to express their gratitude to Åke Juntti, Dan Andersson and Martin Randrup for their valuable technical assistance. Moreover, the authors would also like to thank Dr. Daniel Karlsson from Gothia Power AB, Göteborg, Sweden, for valuable comments.

## 9 Appendices

Values of different parameters of the investigated power system network are given in the following tables. System $S_{base}$ is 1500 MVA.

Table 1. Line data

| *Parameter* | *BUS2-BUS3 (four parallel lines)* |
|---|---|
| R [pu] | 0.13 |
| X [pu] | 1.30 |
| B [pu] | 0.18 |
| Line length [km] | 350 |

Table 2. Transformer data

| *Parameter* | *T1* | *T2* | *T3* |
|---|---|---|---|
| $SBASE_{1-2}$ [MVA] | 1500 | 1500 | 700 |
| $V_{N1}$ [kV] | 230 | 400 | 132 |
| $V_{N2}$ [kV] | 400 | 132 | 400 |
| $R_{1-2}$ [pu] | 0.0 | 0.0 | 0.0 |
| $X_{1-2}$ [pu] | 0.07 | 0.07 | 0.02 |
| No. of steps | - | $\pm 16$ | - |
| Step size | - | 15/16% | - |
| Dead band (pu bus voltage) | - | $\pm 5\%$ | - |
| Initial time delay [s] | - | 25 | - |
| Subsequent time delay [s] | - | 5 | - |

## 10 References

[1] C. W. Taylor, *Power System Voltage Stability*, New York: McGraw-Hill, Inc., 1994.

[2] T. V. Cutsem, C. Vournas *Voltage Stability of Electric Power Systems*, Boston: Kluwer Academic Publishers, 1998.

[3] P. Kundur *Power System Stability and Control*, New York: McGraw-Hill, Inc., 1994.

[4] (2005) Windpower Monthly website. [Online]. Available: http://www.windpower-monthly.com/ *Wind market status 2005*

[5] J. Matevosyan, T. Ackermann, S. Bolik and L. Söder "Comparison of International Regulations for Connection of Wind Turbines to the Network," *Proc. Nordic wind Power Conference*, Göteborg, Sweden 1-2 March 2004.

[6] N. G. Hingorani and L. Gyugyi *Understanding FACTS - Concepts and Technology of Flexible AC Transmission System*, New York: IEEE Press, 2000.

[7] M. Noroozian, Å. N. Petersson, B. Thorvaldson, B. A. Nilsson and C. W. Taylor "Benefits of SVC and STATCOM for Electric Utility Application," *Proc. IEEE Transmission and Distribution Conference and Exposition*, Sept. 2003, pp. 1143-1150.

[8] C. A. Cañizares, and Z. T. Faur, "Analysis of SVC and TCSC controllers in voltage collapse," *IEEE Trans. Power. Syst.*, vol. 14, no. 1, pp. 158-165, Feb. 1999.

[9] A. E. Hammad, "Comparing the voltage control capabilities of present and future var compensating techniques in Transmission systems," *IEEE Trans. Power. Delivery.*, vol. 11, no. 1, pp. 475-484, Jan. 1996.

[10] E. Larsen, N. Miller, S. Nilsson, S. Lindgren, "Benefits of GTO-based compensation systems for electric utility applications," *IEEE Trans. Power. Delivery.*, vol. 7, no. 4, pp. 2056-2064, Oct. 1992.

[11] S. G. Johansson, "Mitigation of voltage collapse caused by armature current protection," *IEEE Trans. Power. Syst.*, vol. 14, no. 2, pp. 591-599, May 1999.

[12] C. Vournas, and M. Karystianos, "Load tap changers in emergency and preventive voltage stability control," *IEEE Trans. Power. Syst.*, vol. 19, no. 1, pp. 492-498, Feb. 2004.

[13] K. Bhattacharya, M. H. J. Bollen and J. E. Daalder *Operation of Restructured Power Systems*, Boston: Kluwer

Academic Publishers, 2001.

[14] Elkraft System and Eltra Regulation TF 3.2.5 *Wind Turbines Connected to Grids with Voltages above 100 kV - Technical regulation for the properties and the regulation of wind turbines*, Draft version, Dec. 2004.

**Biography**

***Nayeem Rahmat Ullah*** was born in Khulna, Bangladesh in 1978. He received his Bachelor degree in Electrical and Electronic Engineering (EEE) from Bangladesh University of Engineering and Technology (BUET), Dhaka, Bangladesh in 2002. In 2004 he received his Master's in Electric Power Engineering from Chalmers University of Technology (CTH), Göteborg, Sweden. Currently he is working towards his Ph.D. degree at the same Division, in the Power Electronics and Wind Energy group.

***Torbjörn Thiringer*** received the Pd.D. degree in 1996 from Chalmers University of Technology. Currently, he is an Associate Professor at the Department of Energy and Environment, Division of Electric Power Engineering at Chalmers University of Technology, Göteborg, Sweden. His area of interest is power electronic applications as well as grid integration of wind energy converters.

# Effect of Operational Modes of a Wind Farm on the Transient Stability of Nearby Generators and on Power Oscillations: A Nordic Grid Study

Nayeem Rahmat Ullah and Torbjörn Thiringer
Department of Energy and Environment
Chalmers University of Technology
Göteborg-412 96, SWEDEN
email: {nayeem.ullah, torbjorn.thiringer}@chalmers.se

***Abstract*— In this work an operational mode of variable speed wind turbines to enhance the transient stability of nearby conventional generators is presented and investigated. This mode is then tested on the CIGRÉ Nordic32 test grid which is taken as a representation of the Swedish transmission network. It is found that by incorporating the suggested mode into the control of several planned wind farms in the souther part of the Swedish grid, the transient stability of nearby conventional generators can be increased compared to the base case where no wind farms were connected. It is also concluded that care has to be taken when selecting the control mode of a wind farm (constant power factor operation or voltage control operation) in a particular situation when it is connected together with a nearby conventional synchronous generator. The interaction between the operational mode of a wind farm and the overall synchronous generator control may interact with each other and could lead to a reduction of damping of power oscillations in nearby transmission lines instead of increasing the damping.**

***Index Terms*— Variable speed wind turbine, transient stability, voltage control, power oscillation.**

## I. Introduction

The wind generation penetration level is increasing day by day. The worldwide total installed capacity, by the end of 2005, was 58 GW of which over 40 GW was in Europe. The annual growth rate in 2005 was 20% [1]. By the end of 2005, the total installed capacity of wind power in Sweden was 500 MW [2]. The Swedish National Energy Agency has proposed a planning target of 10 TWh/year of wind energy expansion in 10-15 years [5]. Several large wind farm projects, totalling nearly 2GW of installed capacity, are under planning stage which could be realized in next few years [6], [7]. Geographically these large wind farms will be concentrated mostly in the southern coastal region.

Today wind turbines of variable speed type has become more common than traditional fixed speed turbines [8]. For a variable speed wind turbine, the generator is controlled by a power electronic converter. Fast control of active and reactive power can be achieved using these types of turbines.

It is presented in several research papers that the transient stability of conventional generators integrated in the electrical network increases when variable speed wind turbines of DFIG type are integrated instead of fixed speed turbines ([9][10]), which is due to the reactive current controllability of a DFIG system. A possibility using such a system is to control the voltage of the wind turbine terminal and in this way improve the voltage profile of nearby buses.

In this contribution a operational mode of a wind farm equipped with full scale frequency converter to improve the transient stability of other conventional generators in the grid is presented. This contingency operation mode is then incorporated with the control of the planned wind farm in the south of Sweden and tested. In addition, oscillations in the grid power are investigated under different operational modes of the wind farm. In this paper, two different integration level of the wind energy are investigated (3% and 12%).

## II. Investigated wind turbine systems

### A. System A

This system is a variable speed wind turbine system with the generator connected connected to the grid via a full scale frequency converter and is assumed to be equipped with voltage ride-through capability. The system layout is shown in Fig. 1. Enercon is the largest manufacturer of this type of wind energy conversion system (WECS) [8]. This system is capable of producing active power at a certain power factor. A preferable operation is at unity power factor. But in cases where a wind farm is connected to the grid by a large cable, it has to be operated at a lagging power factor angle to keep the reactive power exchange to zero at the grid connection point. In this case the grid side converter has to be overrated so that it can provide the necessary reactive power during high wind speed situations.

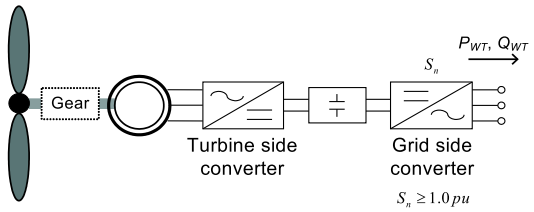


Fig. 1. Hardware set-up of wind turbine systems A and B.

### B. System B

The hardware set-up of a system B type turbine is similar to that of system A type turbine as shown in Fig. 1. But the control of the grid side converter is modified so that this wind turbine system can inject/absorb reactive power into/from the grid while producing active power depending on grid situations (observe the arrows in the capability diagram shown in Fig. 2), as long as the current rating of the grid side converter is not violated. So in principle system B is able to operate anywhere in the first and the fourth quadrant of the capability diagram.

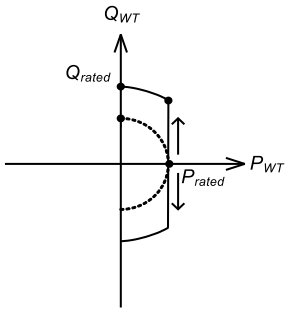


Fig. 2. Capability diagram of wind turbine system B at nominal voltage.

## III. Wind farm modeling

In this paper, variable speed wind turbines with full scale power electronic converters and with voltage ride through capability are considered. They are modeled as a negative load at the connection point with negative conductance and positive susceptance, as shown in Fig. 3. Due to the fact that almost instantaneous control of current could be achieved by converters of these type of wind turbines, they act like constant MVA sources within the converter's current limit. Accordingly, in this paper they are modeled as constant MVA source considering the current limitation of grid side converters. The conductance ($G_{WT}$) and susceptance ($B_{WT}$) are given by

$$\hat{Y}_{WT} = -G_{WT} + jB_{WT} = \frac{P_{WT} + jQ_{WT}}{\hat{V}_{WT}^2} \qquad (1)$$

where $P_{WT}$ and $Q_{WT}$ are the wind farm's active and reactive power production, respectively, $V_{WT}$ is the wind farm connection point voltage. The injected current by the wind farm is

$$\hat{I}_{WT} = \sqrt{(P_{WT} + jQWT)\hat{Y}_{WT}}. \qquad (2)$$

When the converter current limit is reached, it operates as a constant current source and the conductance and the susceptance vary according to

$$\hat{Y}_{WT} = -G_{WT} + jB_{WT} = \frac{I_{max}\angle arctan(\frac{Q_{WT}}{P_{WT}})}{\hat{V}_{WT}} \qquad (3)$$

where $I_{max}$ is the converter maximum current rating. Current injection at this stage is

$$\hat{I}_{WT} = I_{max}\angle arctan(\frac{Q_{WT}}{P_{WT}}). \qquad (4)$$

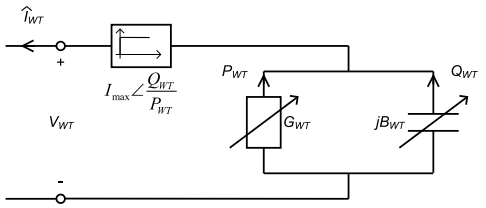


Fig. 3. Modeling representation of a variable speed wind turbine with a full scale power converter.

## IV. Transient stability improvement aspects

To illustrate the transient stability aspect of a variable speed wind turbine with a full scale frequency converter let us consider a simple network as shown in Fig. 4. $X_{GF}$ is the inductive reactance and $R_{GF}$ is the resistance seen by the generator when a solid three phase short circuit fault occurs at a position F without the presence of a wind farm. This network resistance $R_{GF}$ is the only resistance seen by the generator during a fault. The active loss associated with this resistance during a fault is supplied by the generator and this is the only way of transporting active power from a generator during a fault. The higher this active power transfer is during a fault, the less the accelerating energy gained by the generator during this faulted time is. But in presence of a wind farm, by injecting active current during a fault, the equivalent impedance seen by a generator can be changed.

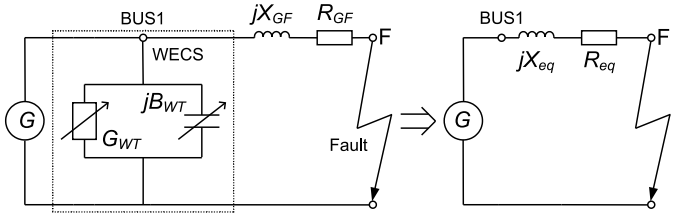


Fig. 4. Equivalent sketch of a simple power system including the WECS model near a conventional generator.

Let us examine the equivalent impedance seen by the generator in the presence of a wind farm. The equivalent impedance $Z_{eq}$ is given by the following equation

$$Z_{eq}=R_{eq}+jX_{eq}=\frac{(G_{GF}-G_{WT})}{(G_{GF}-G_{WT})^2+(B_{GF}-B_{WT})^2} + j\frac{(B_{GF}-B_{WT})}{(G_{GF}-G_{WT})^2+(B_{GF}-B_{WT})^2} \qquad (5)$$

where $G_{GF}$=$R_{GF}/(R_{GF}^2 + X_{GF}^2)$ and $B_{GF}$=$X_{GF}/(R_{GF}^2 + X_{GF}^2)$. Values of $G_{WT}$ and $B_{WT}$ are given by (3).

A wind farm located near a conventional generator, injecting active current at a fixed $pf$ (system A) during a network fault, will reduce the resistance seen by the generator (see Fig. 5) and can thus reduce the transient stability of the machine. On the other hand, system B has the possibility to control the active and reactive current injection during a grid fault. So, in principle, these systems can change the active current injection to zero ($G_{WT}$=0) and in this way keep the resistance seen by the generator to its initial value. They also have the possibility to inject reactive current during a fault (making the value of

$(B_{GF} - B_{WT})$ lower, i.e. reduce the reactive impedance seen by the generator).

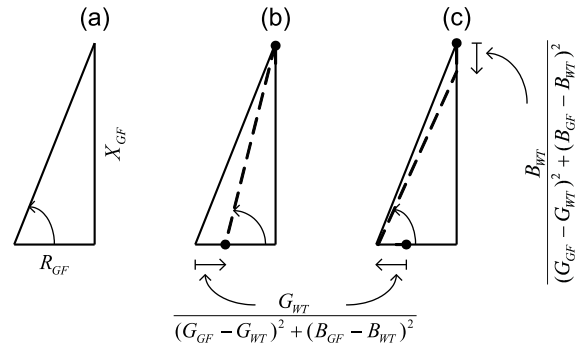


Fig. 5. The impedance seen by a generator during a fault at F, (a) no nearby WECS, (b) a system A type WECS and (c) WECS of type B.

Combining these two possible operations during a grid fault, the combined effect of which is a reduced $X_{eq}/R_{eq}$ ratio seen by the generator (see Fig. 5), a nearby WECS can increase the active power transfer from a conventional generator and can thus increase the transient stability of the machine.

## V. Operational modes of a wind farm

### A. Constant power factor operation

In this mode of operation, a wind farm operates at a certain power factor to maintain a zero reactive power exchange with the grid. This is the classical way to control a wind farm today. In the case where a wind farm is connected to the grid by a long cable, the wind farm has to absorb some reactive power generated by the cable to keep the reactive power exchange to zero at the grid connection point.

### B. Voltage control mode operation

In this mode of operation, the wind farm operation is modified so that it controls its terminal voltage to a predefined value that makes the reactive power exchange with the grid to zero. When the voltage deviates from this set value, the wind farm controls the exchanged reactive power to keep the voltage to the set value as long as the converter current capacity is not exceeded. The set point value is calculated from steady state analysis. So in principle, the SVC/STATCOM function has been incorporated into the control of the wind farm.

### C. Transient stability enhancement mode operation

In this mode of operation the wind farm operates according to the principle discussed in the previous section. When a fault is detected i.e. when the bus voltage goes down to a low value, the wind farm enters into this mode of operation. As long as there is no grid disturbance, it operates in the voltage control mode described in the previous subsection VB.

## VI. Modified Nordic32 grid

The CIGRE Nordic32 test system [11] is used as a representation of the Swedish transmission grid in this paper. The total installed capacity of this test system is 16.5 GW and the load is 10.9 GW. Accordingly, it is assumed in this paper that this test system is a 50% scaled down version of the Swedish system (33.5 GW installed capacity). The original Nordic32 grid has been modified in this work to incorporate the current network situation into account. Two thermal generating units at bus 4063 (530 MW each) have been taken out from operation and two new generating units (530 MW each) have been added at bus 4062 (Fig. 6). The reason for this modification is due to the fact that, two units of the nuclear power plant Barsebäck, situated near Malmö, are no longer in operation now [12].

A 320 MW wind farm is connected at the southwest region as shown in Fig. 7. This corresponds to a 3% wind energy penetration level (the ratio between the wind power and the total load).

To simulate a high wind energy penetration scenario, another large wind farm (1 GW) is connected in the central region as shown in Fig. 7. Two thermal units connected at bus 4062 are in this work taken out of operation from the southwestern region (530 MW each) to accommodate the new wind power. This situation corresponds to a 12% penetration level of wind power. To provide voltage support in the southwestern region, 2 synchronous condensers are connected in place of the two generators at bus 4062.

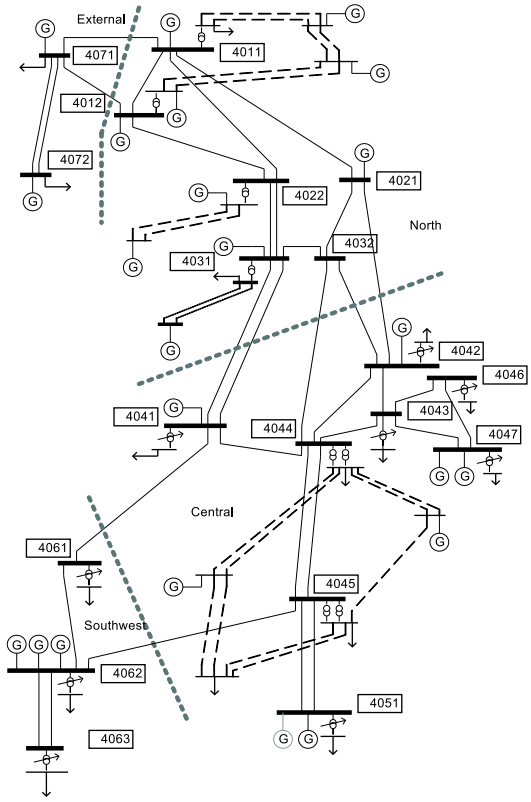


Fig. 6. Modified Nordic32 grid.

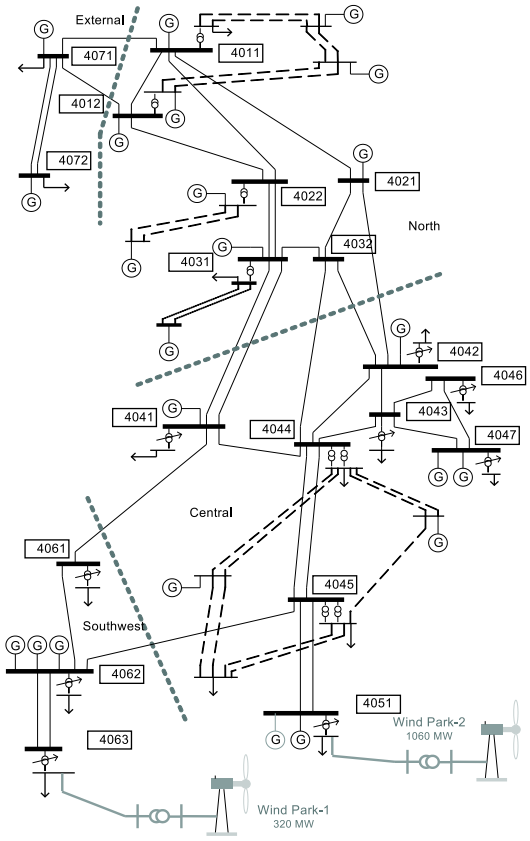


Fig. 7. Modified Nordic32 grid augmented with wind farms.

## VII. 3% WIND PENETRATION SCENARIO

As mentioned earlier, wind park-1 of 320 MW connected at the southwestern region corresponds to a 3% penetration scenario. The load and generation balance of the system is kept by increasing the system load by 320 MW. As the wind farm is connected to the grid by a long cable, the wind farm has to be operated at a lagging power factor to assure a zero reactive power exchange with the grid. Wind park-1 operates at a lagging power factor of 0.98 which corresponds to 65 MVAr of reactive power absorbtion at the wind farm. The operating voltage at the wind turbine terminal is 0.95 pu.

In following subsections the effects of different operational modes of wind park-1 on the transient stability of a nearby generator and on power oscillations are presented.

### A. Effect on transient stability

A very common indicator of the transient stability of a synchronous generator is the critical fault clearing time ($t_{critical}$), which is defined as the maximum duration of a given fault that will not lead to the loss of synchronism of the generator [13].

To determine the transient stability limit of the system in the presence of wind park-1, a three phase to ground fault is applied at bus 4062, which is the nearest bus to the wind farm that has conventional generators connected. When the wind farm is operating in the constant power factor mode, which resembles system A, the critical fault clearing time is 263 ms. When the suggested transient stability enhancement mode is incorporated, which resembles system B, the new critical fault clearing time is 317 ms. For the purpose of comparison, the critical fault clearing time of the system without any wind farm is also calculated which is 312 ms. So a new wind farm of type A will endanger the system transient stability while wind farm of system B, which incorporated the suggested transient stability enhance mode, will increase the system transient stability.

Fig. 8 shows rotor angles of generators connected at 4062 and 4051 when a fault is applied at 4062 for 150 ms. As shown in the figure, the rotor angle swing of the generator connected at bus 4062 has been reduced when system B is utilized, compared to system A. It can be noted that the rotor angle of the generator at bus 4051 has not been affected significantly which is natural since it is electrically far away from wind park-1. So it is concluded that generators in other regions of the network, which are even further from the wind farm, will not be influenced by this modified operation of wind park-1.

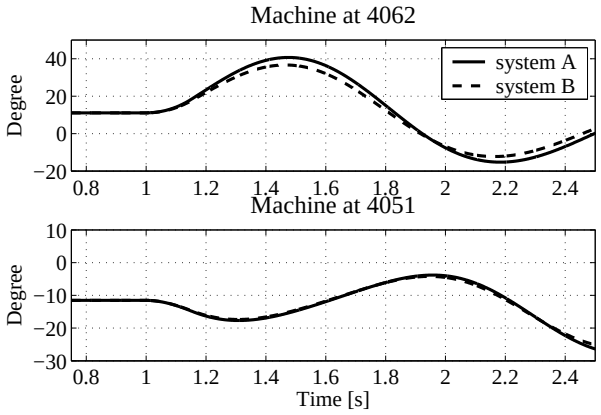


Fig. 8. Rotor angle swing of generators connected at bus 4062 and 4051 when a fault is applied at 4062.

### B. Effect on power oscillations

The transmission line between bus 4062 and 4045 is disconnected which results in power oscillation in different parts of the network. The power oscillations in lines 4063-4062 and 4062-4061 are monitored. It is assumed that system B is operating in the voltage control mode. In Fig. 9, the power oscillations are shown. In the figure, transmission loadings are presented as a percentage of the respective SIL (serge impedance loading) of the line, which is 550 MW for all the monitored lines. An increased damping in power oscillations is observed in line 4063-4062 when the wind farm is operated in the voltage control mode. The wind farm terminal voltage and reactive power are shown in Fig. 10. By controlling its bus voltage by changing the reactive power, the wind farm manages to increase the damping of power oscillations in the transmission line 4063-4062. As can be noticed from Fig. 9, due to the disconnection of line 4062-4045, the other transmission line 4062-4061, which connects the southwest region with the rest of the system, gets severely overloaded and the line will be tripped.

Another contingency situation is investigated where a generating unit at bus 4062 is disconnected. The resulting power oscillations in different transmission lines in the southwest region are shown in Fig. 11. An increased damping in power oscillations is observed in line 4063-4062 when system B is utilized instead of system A. No significant change is power oscillations are observed in the other two lines which are electrically far away from wind park-1.

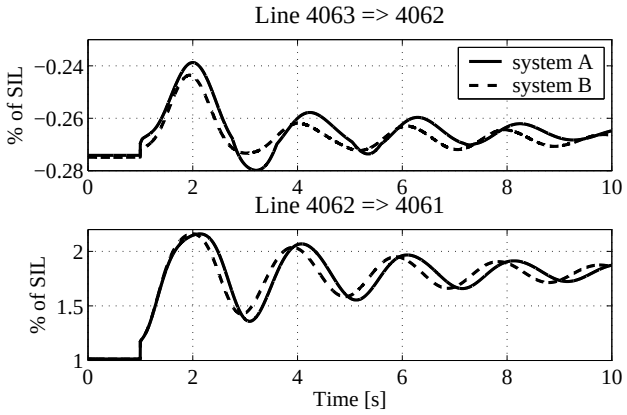


Fig. 9. Power oscillations in lines 4063-4062 and 4062-4061 when the line 4062-4045 is disconnected.

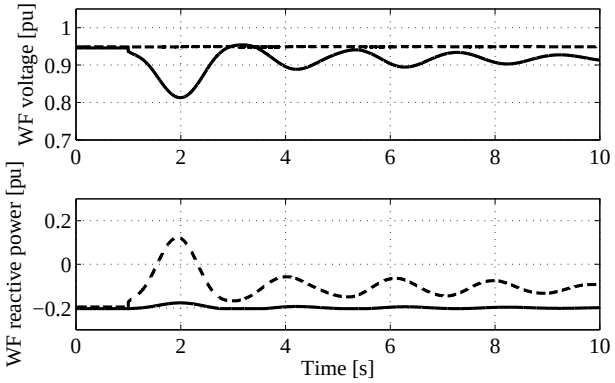


Fig. 10. Voltage at the wind farm terminal and the wind farm reactive power when line 4062-4045 is disconnected.

So it is concluded from this low penetration scenario analysis that by incorporating the transient stability enhancement mode in the operation of the planned wind farm in south of Sweden, the transient stability of the conventional generators operating in that region can be increased. It is also found that the damping of power oscillations in transmission line 4063-4062 are increased when this wind farm is operated in the voltage control mode instead of the constant power factor mode although no significant change in power oscillations are observed in other transmission lines which are far away from the location of the wind farm.

## VIII. 12% WIND PENETRATION SCENARIO

A higher wind penetration scenario is also investigated. In this case it is assumed that another large wind farm (1

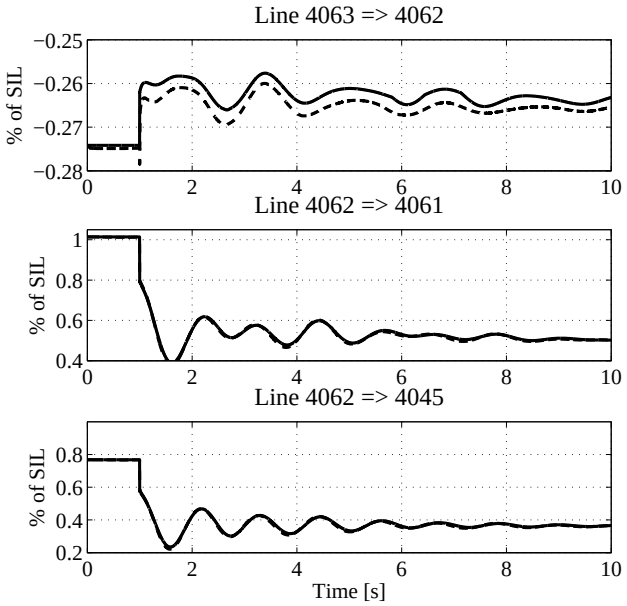


Fig. 11. Power oscillations in different transmission lines in the southwest region when one unit at bus 4062 is disconnected.

GW) is connected to the network near bus 4051. Two thermal generator units of equivalent size from the southwest region (at bus 4062) has been decommissioned in this case. To provide enough voltage support at in the southwest region, two synchronous condensers are added in bus 4062. Their total capacity is 600 MVAr. This new wind park, wind park-2, operates at a lagging power factor of 0.93 to maintain zero reactive power exchange with the grid in the pcc. The operating voltage of the wind farm is 0.97 pu.

Similar analysis of the transient stability and power oscillations are performed for this high wind penetration scenario as have already been done for the low wind penetration scenario, and the results are shown in the next subsections.

### A. Effect on transient stability

To determine the transient stability of the system in presence of several wind farms, a three phase to ground fault is applied at two different locations. First a fault is applied at bus 4062, which is near to wind park-1. The critical fault clearing time is 414 ms when system A is employed in wind park-1. When system B is employed, the critical fault clearing time is increased to 432 ms.

Another fault is applied at bus 4051 near wind park-2. Bus 4051 is the grid connection point of wind park-2 and a conventional generator is connected at this bus. The critical fault clearing time is 375 ms when system A is employed in wind park-2. When system B is employed, which incorporates the suggested transient stability enhancement mode, the critical fault clearing time increases to 676 ms. The critical fault clearing time of the system without any wind farm for a fault at bus 4051 is 539 ms.

### *B. Effect on power oscillations*

Like the previous scenario, transmission line 4062-4045 is disconnected which results in power oscillations in different parts of the system. Power oscillations in transmission lines 4051-4045, 4063-4062, 4062-4061 and 4045-4044 are monitored. Fig. 12 shows the results. From the figure, it is noted that the damping of power oscillations in line 4051-4045 reduces in the presence of a system B type wind farm which is located near bus 4051 and is operating in voltage control mode. Wind farm of a system A type, which is operating at constant power factor, shows better performance in this case. It is due to the fact that two conventional synchronous generators are connected at bus 4051 which also is the connection point of the second wind farm. The interaction between the wind farm's simple voltage control mode of operation and the generator overall control may cause the reduced damping in power oscillations in line 4051-4045. Slightly reduced damping in power oscillations are also observed in line 4062-4061 and 4045-4044 when a wind farm of type B is employed compared to the case when system A is employed. But interesting to note is that increased damping in power oscillations are observed in line 4063-4062. Note that wind park-1 is connected at the end of line 4063-4062 where no conventional generating unit is in operation. Therefore a simple voltage control mode operation of this wind farm increased the damping in power oscillations in line 4063-4062.

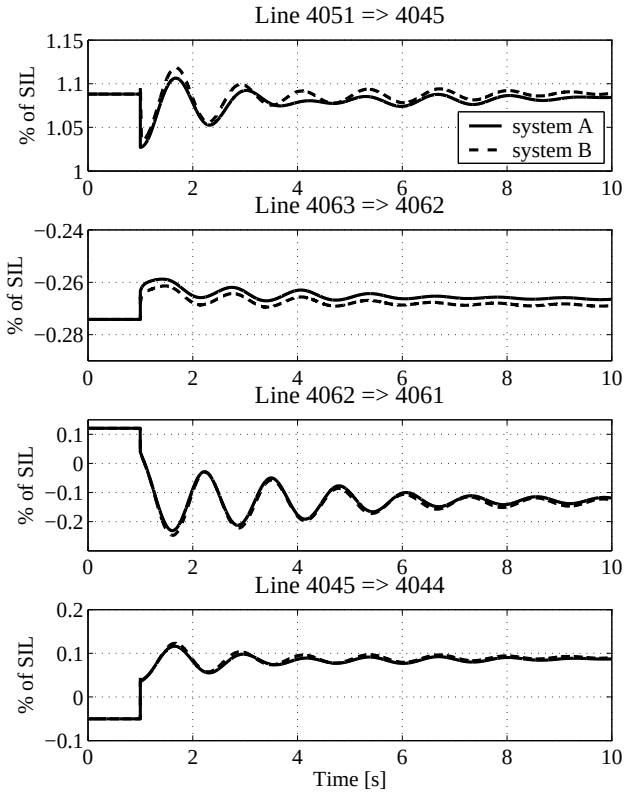


Fig. 12. Power oscillations in different lines when the line 4062-4045 is disconnected.

Another contingency situation is also investigated in this paper where the generating unit at bus 4062 is tripped. The resulting power oscillations in lines 4051-4045, 4063-4062, 4062-4061, 4062-4045 and 4045-4044 are shown in Fig. 13. A reduced damping in power oscillations are observed in line 4051-4045 when wind park-2 operates in voltage control mode (system B) compared to the case when the wind farm operates in fixed power factor mode (system A). A reduction in the damping of power oscillations are also observed in other lines except line 4063-4062. Damping in power oscillations are increased in line 4063-4062 when wind park-1 operates in the voltage control mode.

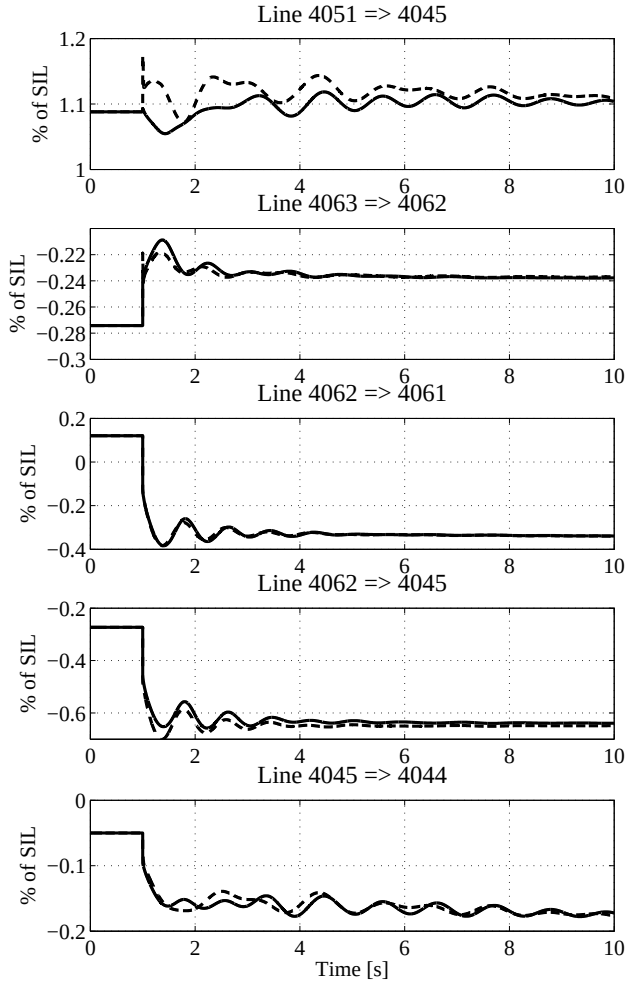


Fig. 13. Power oscillations in lines 4061-4062 and 4062-4061 when the line 4062-4045 is disconnected.

It is concluded from the high penetration scenario analysis that the transient stability of nearby conventional generators are increased from the base case when the proposed transient stability enhancement operation mode is incorporated into the control of the planned wind farms. It is also observed that using the simple voltage control mode of operation of wind park-2 did not increase the damping in power oscillations of the nearby transmission lines compared to the constant power factor mode operation. But the damping in power oscillations are increased in line 4063-4062 when wind park-1 operates in voltage control mode. Wind park-1 is connected at the end of line 4063-4062 where no conventional generators are in

operation.

## IX. Conclusion

In this paper, an operational mode of variable speed wind turbines equipped with full scale frequency converter is presented to enhance the transient stability of nearby conventional generators. The method is then tested on the CIGRE Nordic32 grid. Two different wind energy penetration scenarios are investigated. For both the scenarios it is found that by incorporating this transient stability enhancement operation mode in the control of several planned wind farms in the nordic grid, the transient stability of nearby conventional synchronous generators can be increased.

The effect of various control modes of a wind farm, namely, constant power factor operation and voltage control mode operation, on transmission line power oscillations are also investigated in this paper. In both the investigated wind penetration scenarios it is found that damping of power oscillations in line 4063-4062 are increased when wind park-1 operates in voltage control mode. While, this simple control mode employed in wind park-2 did not increase the damping of power oscillations in line 4051-4045. Interesting to note is that no conventional synchronous generator is connected at the connection point of wind park-1 while two synchronous generators are in operation at bus 4051 where wind park-2 is also connected. So care must be taken while designing the control of a large wind farm, in the particular situation where conventional synchronous generators are in operation near the wind farm. A voltage control mode of operation could in these situations reduce the damping of power oscillations.

## Acknowledgments

In addition to the financial support provided by E.ON Sverige, the authors would also like to express gratitude to Åke Juntti and Dan Andersson for their valuable technical assistance.

## References

[1] (Feb. 2006) German wind energy association (BWE) website. [Online]. Available: http://www.wind-energie.de/index.php?id=166

[2] (Feb. 2006) The European wind energy association website. [Online]. Available: http://www.ewea.org/

[3] (Feb. 2006) Svensk Energi website. [Online]. Available: http://www.svenskenergi.se/ Energy in Sweden - 04

[4] (2005) Elåret 2005: Starket år för vattenkraft och kärnkraft gav elexport (in Swedish) [Online]. Available: http://www.svenskenergi.se/media/underlag/prm051228.pdf

[5] The Swedish National Energy Agency, Tech. Rep. no.: ER 6 2002. The Climate Report 2001. [Online]. Available: http://www.stem.se/web/biblshop.nsf/FilAtkomst/ER62002.pdf/$FILE/ER62002.pdf?OpenElement

[6] (Feb. 2006) Vattenfall [Online]. Available: http://www.vattenfall.se/om_vattenfall/var_verksamhet/lokal/

[7] (Feb. 2006) E.ON Vindprojektering Sverige AB. [Online]. Available:http://www.eon.se/templates/InformationPage.aspx?id=42453

[8] T. Ackermann, Ed., *Wind Power in Power Systems.* West Sussex: John Wiley and Sons Ltd., 2005

[9] M. V. A. Nunes, J. A. P. Lopes, H. H. Zürn, U. H. Bezerra and R. G. Almeida, "Influence of the Variable -Speed Wind Generators in Transient Stability Margin of the Conventional Generators Integrated in Electrical Grids", *IEEE Trans. Energy. Conversion.*, vol. 19, no.4, pp. 692-701, Dec. 2004

[10] F. W. Koch, I. Erlich, F. Shewarega and U. Bachmann, "Dynamic Interaction of large Offshore Wind Farms with the Electric Power System", in *Proc. IEEE Bologna PowerTech Conference*, June 2003.

[11] K. Walve "Nordic32-A CIGRÉ Test System for Simulation of Transient Stability and Long Term Dynamics", Svenska Kraftnat, Sweden, 1993.

[12] (March 2006) Ringhals AB website. [Online]. Available: http://www.ringhals.se/index.asp?ItemID=1291

[13] P. Kundur, *Power System Stability and Control* New York: McGraw-Hill Inc., 1993

# Small Scale Integration of Variable Speed Wind Turbines into the Local Grid and Its Voltage Stability Aspects

Nayeem Rahmat Ullah
Department of Energy and Environment
Chalmers University of Technology
Göteborg-412 96, SWEDEN
email: nayeem.ullah@chalmers.se

***Abstract*— The effect of small scale variable speed (VS) wind energy integration into the local grid is investigated in this paper. In particular, the effect of reactive power control from wind turbines on the local voltage stability considering different types of load is analyzed here. Both steady-state and dynamic analysis have been done. It is found that integration of wind power in several feeders of a sub station could influence the operation of the tap changing transformer at the substation. With the high level of integration of wind turbines at the local grid, mixed with different critical loads, high load-low wind condition is the most critical situation from a load power quality point of view when lost voltage-time area at the load bus will be higher for a given disturbance at the grid. To overcome a relatively low voltage disturbance (grid voltage dip higher than 85%) by utilizing the fast power electronic converter of the nearby wind turbine, keeping the active power production from the wind turbine at the pre-disturbance value, it is the high wind-low load situation which is the difficult case to handle from the wind turbine side. Mitigation of a larger voltage disturbance in this way requires a larger grid side converter. Instead, injecting reactive current into the grid keeping the active current injection from the wind turbine at the pre-fault level, gives satisfactory contingency performance of the wind turbine from the grid point of view.**

## I. Introduction

The wind generation penetration level is increasing day by day. Economic utilization of wind resources requires the wind turbines to be connected at remote sites with high average wind speed. Such sites are often situated far from a strong grid. Maximization of small scale integration of wind farms (<10 MW) in such grids requires overcoming technical constraints like flicker, steady-state voltage variation limit, thermal overloading of the feeder etc. The flicker emission constraints is no longer a problem for VS wind turbines [1]. Existing distribution grids are usually designed with a higher thermal capacity than needed to maintain an acceptable voltage profile and also to make room for future network expansion. So, generally the thermal rating of a distribution feeder does not limit the amount of wind energy integration level into the local weak grid.

Today wind turbines of VS type with power electronic converters has become more common than traditional fixed-speed turbines. In 2002, the total market share of VS turbines with power electronic based converter was 67%[2]. Fast control of active and reactive power can be achieved from these types of turbines.

It is quite common that wind turbines are to be connected at the feeder mixed with other loads. Typical substation loading types are of housing, commercial and industrial type, of which commercial and industrial loading are sensitive to voltage disturbances i.e. critical loads. Good supply voltage quality is a demand for these loads. High level of wind power integration into the distribution feeders with such critical loads may, in future, require the wind turbines to have voltage control capability to some extent and could also require contingency operation of wind turbines during grid disturbances. In principle, with the help of the built in power electronic converter of the variable speed wind turbine, it will be quite possible to do so.

The main purpose of this work is to investigate the short term voltage stability aspects of distributed VS wind generation mixed with voltage sensitive loads at weaker parts of the network. In particular, another goal is to investigate the possibility of utilizing the reactive power from the wind turbine's grid side converter during network disturbances. In addition to this, another objective is to find limiting factors in the integration level by steady-state calculations.

## II. Investigated System

The investigated power systems are shown in figs.1 and 2. For both the systems, the short circuit capacity at the substation secondary is 70 MVA. Three different feeders have been investigated. The parameters for the feeders are given in the appendix. The steady state wind integration limit is calculated for the system shown in fig.1 considering the three different feeders separately. Later the three different feeders are considered connected to the sub-station and the integration limit is re-calculated for the system shown in fig.2 and the effect of the tap changing transformer is investigated. In the dynamic simulation, different types of load-wind combinations at feeder-2 during network disturbances are investigated with the system shown in fig.1. Office load, residential load and industrial load are considered. Later in a case study simulation,

the system shown in fig.2 is considered with all the three feeders with different types of loads mixed with wind turbines.

### A. Load model

In the dynamic simulations, residential loads, which are mainly heating load, are modeled as constant impedance loads. Commercial loads are here all considered to have an UPS and are accordingly modeled as constant power loads. The industrial loads are modeled as induction motors. The parameters for the induction motors are chosen based on the typical value from [3]. In both static and dynamic calculations, the load power factor is taken 0.98.

### B. Wind turbine modeling assumption

Throughout the whole work, VS wind turbines with full power converter are considered, which have a voltage dip ride-through capability. The presence of the full power converter isolates the generator from the rest of the grid. Only the converter characteristic is seen by the grid [4]. An ideal converter is assumed in this work. In the dynamic simulation, the wind speed is considered to be constant as we are interested in short term voltage stability and the time frame we are interested in is $<$1s. Variable speed wind turbines equipped with power electronics based reactive power injection capability can either inject or absorb reactive power. The control of active and reactive power from the wind turbine is done separately. Fast control of active and reactive current from the turbine is realized by the power electronic converter. In this work, VS wind turbine is modeled in such a way that it acts as an intelligent constant power source.

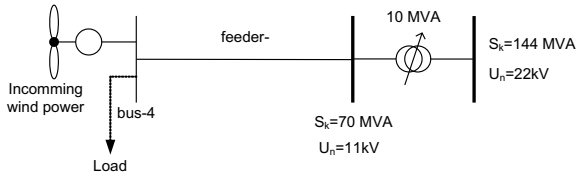


Fig. 1. Single line diagram of the investigated power system, setup-1.

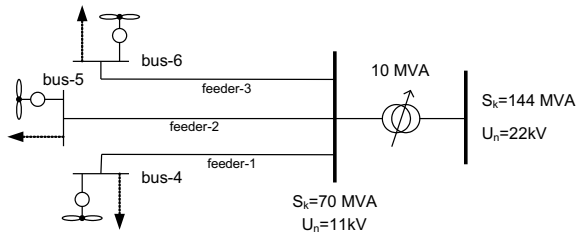


Fig. 2. Single line diagram of the investigated power system, setup-2

## III. Wind Power Integration into the Existing Feeders

### A. Feeder effect

The steady-state voltage span is one of the factors that limits the wind power integration limit into a distribution feeder where the local loads are connected. The allowed steady state voltage variation limit at the load bus depends on the operator of the local grid. In this work the highest permissible voltage is assumed to be 1.025 pu and the lowest allowed value is assumed to be 0.96 pu.

The short circuit capacity at the sub-station is 70 MVA. Feeder-1 is first considered. The load level is assumed to be zero which gives the most conservative value of the integrated wind power for a given static voltage variation limit. Depending on the loading profile of the feeder, the minimum feeder loading could be added to this value to determine the amount of maximum wind power that could be integrated into this feeder. Fig.3a shows the results. The amount of integration is limited to 3.6 MW due to the voltage variation limit. The integration limit for feeder-2 and 3 are 4.8 MW and 3.9 MW respectively, as shown in fig.3b and c.

Feeder-1 is a 6 km over head (OH) line with an $X/R$ ratio equals 3. Feeder-2 is also an OH line of 4 km with the same $X/R$ ratio. Feeder-3 is a 4 km cable with an $X/R$ ratio 0.75. All the feeders have the same ampacity (500 A). From the results shown in fig.3a and b, the voltage variation limit is reached first in feeder-1 which has a longer length than the feeder-2. On the other hand, although feeder-2 and 3 have the same length, the voltage variation limit is first reached at feeder-3 which has a lower $X/R$ ratio. In neither case, the thermal limit of the feeders is reached since the original system is designed to handle the maximum load situation considering the voltage variation limit. Maximum current carrying capacity of a feeder could be a limiting factor when the integrated wind power is higher than the maximum loading of the feeder.

### B. Effect of tap changers

From the previous subsection an observation is that the tap changing transformer has not influenced the wind energy integration limit as the sub station voltage remains within its permissible value ($\pm$1.25%). Comparing the wind energy integration results, fig.3, it is noticed that substation voltage is higher for feeder-2 than for feeder-1. These two feeders considered here have the same $X/R$ ratio but feeder 2 is shorter in length. The short circuit capacity of the grid at the end of feeder-1 and 2 are 30 MVA and 37 MVA respectively. On the other hand feeder-2 and feeder-3 have the same length but different $X/R$ ratios. The short circuit capacity of the grid at the end of feeder-3 is 53 MVA. And as expected, the voltage at the sub station is higher for feeder-3 than feeder-2. So a conclusion could be that, the tap changing transformer will influence the wind energy integration level when the short circuit capacity at the integration point is comparable to the short circuit capacity at the low voltage side of the sub station. A situation like this could arise when the turbine is connected closer to the substation. But in real situation where the wind turbines will be connected at the far end of a feeder, the tap changing transformer will merely influence the integration level.

In practice it may happen that wind turbines could be integrated in several feeders of a sub station due to the high

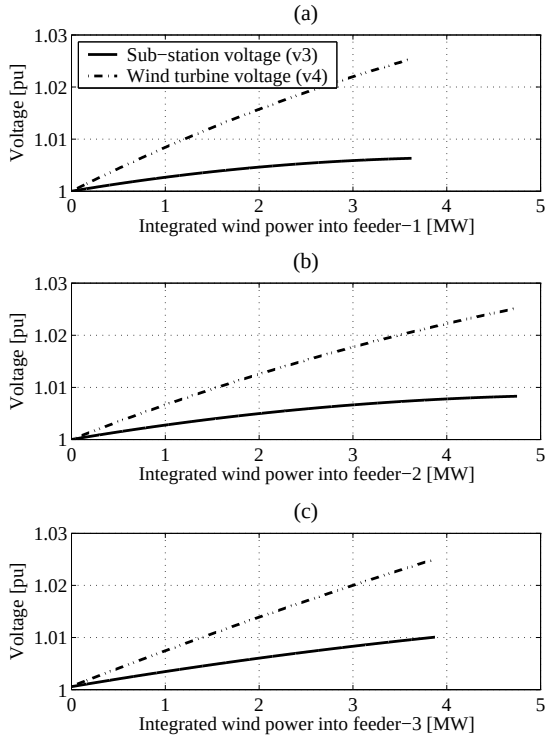


Fig. 3. Wind power integration into - (a) feeder-1, (b) feeder-2 and (c) feeder-3.

availability of the wind and/or the interest from the wind farm owners. A power system shown in fig.2 is considered in this case where all the three different feeders are present at the substation. Feeder loadings are assumed zero here as well, which will give the most conservative value. Neglecting the tap changing action of the transformer, the total integration limit is 7.5 MW (fig.4a) which is less than the sum of the limits of the three feeders calculated in the previous section. The total active power loss and the reactive power support needed to transport this wind power into the grid is 3% and 12% respectively.

Now the tap changer is considered in the calculation. The wind power absorption in different feeders are shown in fig.5a. The total absorption limit is increased up to 15 MW. The total active power loss and the reactive power support needed in this case is 7% and 25% respectively. The increasing reactive power support needed to transport the wind power generated at the far end of the distribution network, into the grid, could limit the wind production due to the net reactive power exchange requirement of the local distribution grid with the transmission grid. A situation like this could arise when the power production from the wind turbines exceeds the local consumptions. By providing the reactive power support needed to transport the surplus of wind power, at the node where the bulk amount is exchanged into the grid, this limit could be overcome.

We can draw a conclusion that, tap changing transformer will influence the wind integration limit when several feeders of the substation have the possibility to absorb incoming wind power. As concluded earlier, when the short circuit capacity at the wind turbine connection point is comparable with the substation short circuit capacity, the tap changing transformer could influence the integration limit. In this case, where we have considered wind power integration at several feeders, the combined short circuit capacity of the grid is 57 MVA (calculated by considering three simultaneous faults at the wind turbine connection points) which is comparable with the sub station's short circuit capacity.

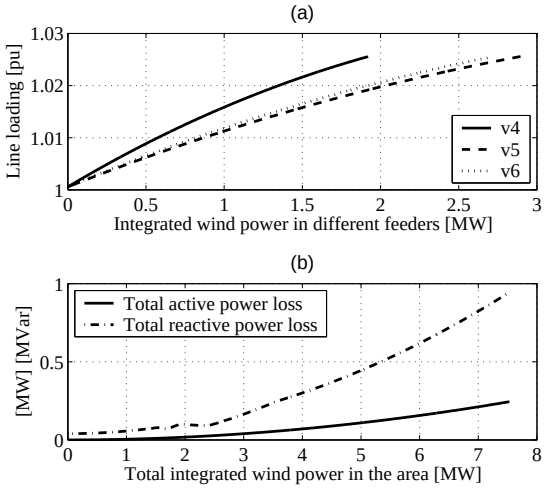


Fig. 4. Wind power integration into all the existing feeders - (a) voltage profile of the different wind turbines pcc, (b)total active and reactive power loss in the system. Tap changer locked.

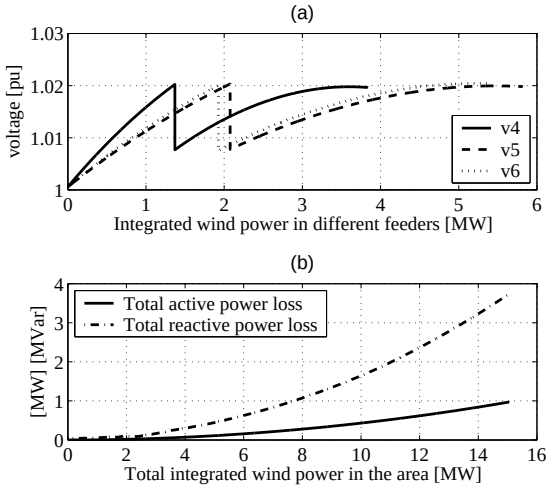


Fig. 5. Wind power integration into all the existing feeders - (a) voltage profile of the different wind turbines pcc, (b) line (bus-2 - bus-1) loading (c) total active and reactive power loss in the system. Tap changer unlocked.

While integrating wind energy into several feeders of a sub-station, another limiting factor could arise at the transportation level of the surplus wind power into the grid. In the previous case where the voltage variation limit was pushed towards

the thermal limit of the feeder, the total integration possibility was increased up to 15 MW. The original local network and the substation was designed to comply with the maximum load demand. When the amount of wind power integration is higher than the substation capacity, the sub transmission lines connecting the substation to the grid could be overloaded after the grid disturbances. In those situations some of the wind turbines should be disconnected or the integration limit should be reduced to avoid such situations.

The conclusions drawn from the steady state calculations are:

1) the steady-state voltage variation limit could limit the integration of wind energy when wind turbines are integrated into one single feeder of thesubstation where the short circuit capacity is low compared to that of the substation, provided no bottle neck is present in the feeder.
2) the tap changer's action could enhance the integration limit of the wind energy when wind energy is integrated into several or all of the existing feeders of the substation. In this situation the equivalent short circuit capacity at the wind integration points is comparable to the sub station short circuit capacity.
3) while transporting the surplus wind energy from the local grid to the next higher grid, another limiting factor could be the thermal limit of the sub-transmission line.

## IV. Voltage Stability Enhancement by Distributed Wind Generation

### *A. Voltage disturbance response of different types of load-wind combinations*

A typical distribution feeder load types could include residential, commercial and to some extent industrial load. These loads behave differently towards different voltage disturbances. For example, housing loads which are mainly heating loads, behave as a constant power load in long term because of the thermostatic control associated with it which has time constant of several minutes [3,5]. During short disturbances they behave like a constant impedance load. On the other hand commercial or office loads consists of mainly computer loads fed by electronic power supply and fluorescent lighting with electronic control. The control associated with these loads make them constant power load [5]. When the grid disturbance is over, the voltage recovers immediately when these types of loads are connected. The situation is different in case of an industrial load which, here is assumed to have a large amount of induction machines. The voltage sag duration is larger in this case due to the high amount of reactive power consumed by the motor immediately after the fault to build up its magnetizing flux. This makes a post disturbance voltage sag at the bus.

Parts of commercial loads which are supplied by electronic power supply for example, computer, is sensitive to voltage dip less than 85% for a 500 ms voltage dip [6,7]. 500 ms is a typical breaker operating time in the distribution grid. In this respect this types of loads are sensitive load. Motor using power electronics for variable speed control are becoming common. In [8] it is stated that adjustable speed drive cannot tolerate less than 80% voltage dip with 500 ms duration. For a local grid, a voltage dip less than 80% for a duration of 500 ms is a severe disturbance from load point of view when sensitive loads will be disconnected.

In fig.6, the response of different types of load to a 80% voltage dip (500 ms duration) at the swing bus is shown. The voltage reduction at the load bus is higher when the load is an office load compared to the heating load case, as expected. In case of an industrial load, post disturbance or secondary voltage reduction is present. The post disturbance effect is higher with decreasing dip for a given dip duration.

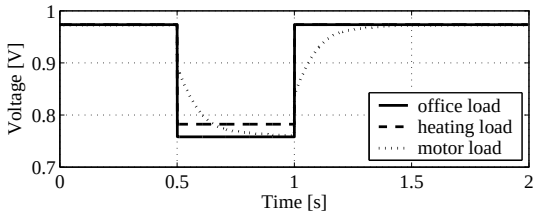


Fig. 6. Response of different types of load to a grid disturbance of 500 ms duration 80% voltage dip

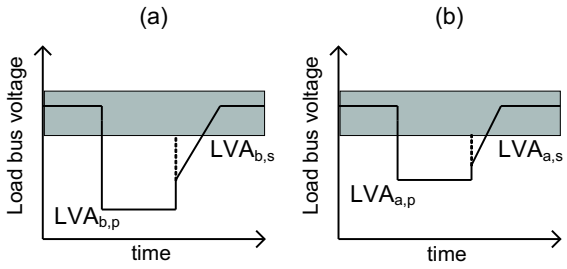


Fig. 7. Lost Voltage Area (LVA) at the load bus due to a disturbance at the grid (a) no remedial action taken (b) reactive power injection action taken. Shaded area indicates the acceptable voltage variation limit.

For a given disturbance duration, the voltage area that is lost at the load bus due to the voltage dip at the higher voltage grid, is an index of the disturbance severity. The lost voltage area (LVA) as calculated in this work, is shown in fig.7. Fig.7a shows the primary ($p$) and secondary ($s$) LVA at the load bus due to a disturbance at the grid when no remedial action has been taken. Fig.7b shows the LVA when reactive power injection is done at the load bus to counteract the dip. The lost voltage area recovery is calculated as:

$$LVA\ recovery,\ p = LVA_{b,p} - LVA_{a,p}. \tag{1}$$

$$LVA\ recovery,\ s = LVA_{b,s} - LVA_{a,s}. \tag{2}$$

Referred to the set-up shown in fig.1, feeder-2 is considered supplying the load. The load power factor is assumed to be 0.98 lagging. Different types of loads, namely, housing,

commercial and industrial, are considered separately. In the calculation two different load/wind combinations have been considered: high load-low wind situation and high wind-low load situation. In the former situation the power flow direction is from the substation to he load end and the later situation refers to a net power transfer to the grid from the turbines. The maximum loading on this feeder is 3.5 MW and the total installed wind power on this feeder is 5 MW. For both the load and wind, 20% of the rated value is taken as the low level value.

In fig.8 the primary and secondary LVA for different types of load is shown for different voltage dip magnitudes, where a high load-low wind situation is considered. From the figure it is clear that the primary LVA is higher for commercial load than the other two types of loads, which means that these types of load will have higher effect on the voltage stability during grid disturbance. On the other hand, industrial load has a significant secondary LVA.

Fig.9 presents the LVA for a high wind-low load situation. As expected, the LVA is less than the high load-low wind case. In this case, industrial load shows negligible secondary LVA which makes all the three types of load responses similar.

From the remedial action point of view, high load-low wind situation is harder to handle where the LVA is higher than the high wind-low load case and it will require higher reactive support.

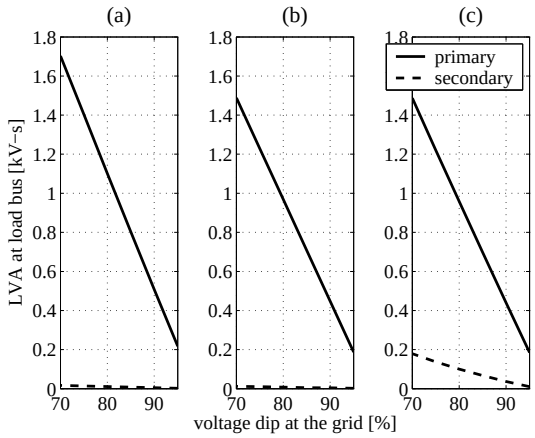


Fig. 8. Load bus LVA due to a 500 ms duration of grid voltage disturbance with different dip magnitude for (a) commercial and office load, (b) residential load and (c) industrial load. High load-Low wind situation.

### *B. Requirement for wind turbine's converter current capacity*

The wind turbines today are mostly variable speed wind turbines with power electronic converter capable of controlling the reactive power to produce active power at unity power factor. To be able to provide reactive power support to the grid during high wind operation, the grid side converter should be over rated to some extent. In this section, the following assumptions have been made for the wind turbine operation:

1) wind power availability remains constant during the short disturbance

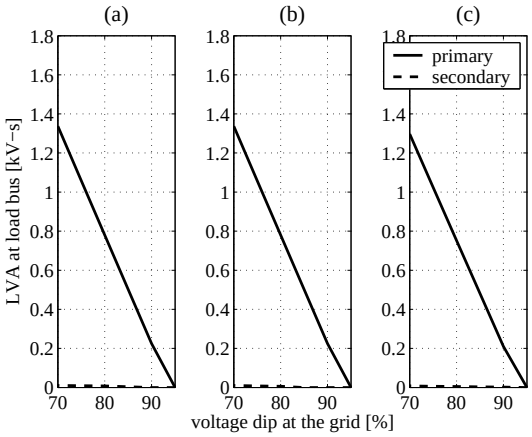


Fig. 9. Load bus LVA due to a 500 ms duration of grid voltage disturbance with different dip magnitude for (a) commercial and office load, (b) residential load and (c) industrial load. High wind-Low load situation.

2) active power production from the turbine is kept the same as the pre-disturbance value by controlling the active component of the current depending on the current rating of the grid side converter
3) during voltage disturbance, reactive current is injected into the grid to provide voltage support keeping the active power production at the pre disturbance value.

In fig.10 high wind-low load situation with a 85% voltage dip at the grid is presented considering an industrial load. Fig.10a shows the load bus voltage and active and reactive power production from the turbine. During the voltage dip, active power injected by the wind turbine into the grid is reduced due to the converter current limitation. With the help of a larger converter, reactive power support could be provided, as shown in fig.10b. In this occasion 3.25 MVar reactive power support is provided by the wind turbine to restore the voltage level into the permissible limit. Which means, a 20% over-rated grid side converter (or rated at 0.84 power factor) is required.

The required wind turbine grid side converter's rated power factor to handle grid voltage disturbances of different magnitude for the two load-wind combinations discussed above, are calculated and shown in fig. 11 and 12.

In fig.11 the wind turbine's converter capacity requirement for high load-low wind situation is presented for three different types of load as discussed earlier. It is noticed that for a given level of disturbance at the grid, industrial load (fig.11c) puts higher requirement on wind turbines. With commercial (fig.11a) and residential (fig.11b) load connected, the requirements on wind turbines are relatively less than the industrial load case. A grid voltage disturbance down to 90% could be handled by the wind turbine without the need to over rate the grid side converter. It is due to the fact that during low wind operation, the converter current is far below the rated current. But in a high wind-low load situation (fig.12), the grid side converter has to be over rated to handle even a 90% dip in the grid for all the load types. So, to handle a

relatively low voltage disturbance (grid voltage dip higher than 85%) by the reactive power injection of the wind turbine, high wind-low load situation is the critical load/wind condition that determines the required sizing of the converter. On the other hand, a high load-low wind situation is the critical load/wind condition to handle by the reactive power injection from the wind turbine during severe voltage disturbance (dip less than 85%).

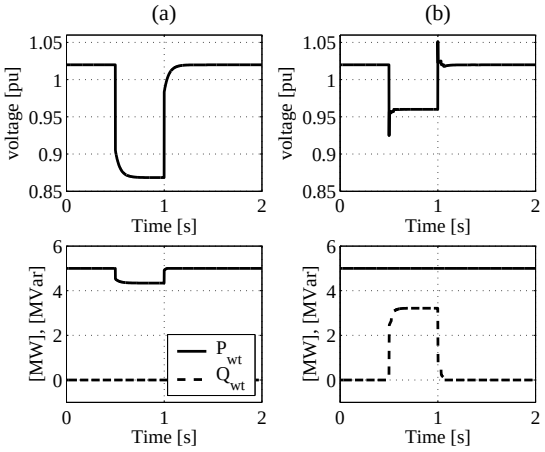


Fig. 10. High wind-low load (industrial load) situation and 85% dip of 500 ms duration at the grid. Load bus voltage and the active and reactive power from the wind turbine when (a) no reactive power is injected by the wind turbine and (b) reactive power support provided by the wind turbine's over-rated converter.

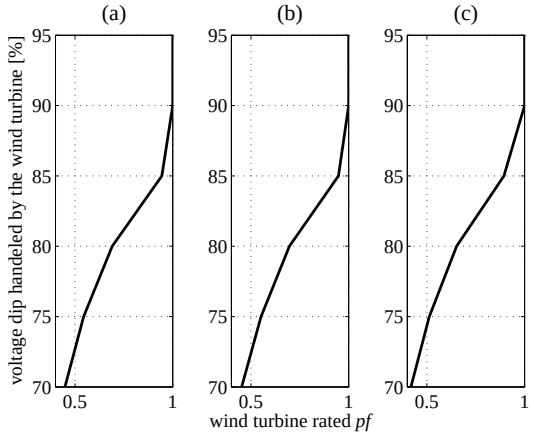


Fig. 11. High load-low wind situation. Wind turbine's converter capacity requirement to handle different grid voltage dip (a) commercial and office load, (b) residential load and (c) industrial load.

### C. Contingency operation of wind turbines at the local grid

In the previous subsection it was shown that a relatively small disturbance of the grid voltage could be handled by the wind turbine's grid side converter which is slightly over rated. In those situations, the active power production from the wind turbine is kept to the pre-disturbance value and the remaining capacity of the grid side converter is utilized to inject reactive

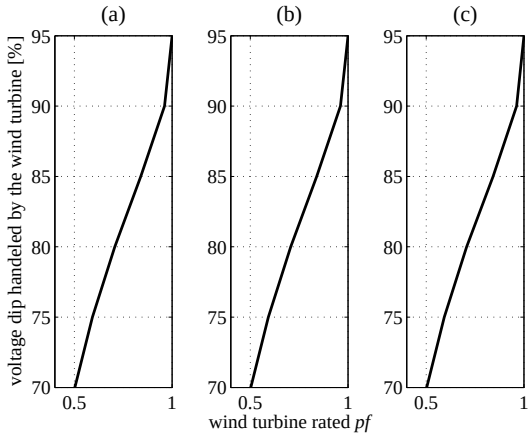


Fig. 12. High wind-low load situation. Wind turbine's converter capacity requirement to handle different grid voltage dip (a) commercial and office load, (b) residential load and (c) industrial load.

power to assist the grid. During severe grid disturbance, this mode of operation is not feasible as the required converter size becomes larger.

In this subsection, we will address some alternative contingency modes of operations of the wind turbine with a reasonable size of the grid side converter (5% over rated) which can assist the grid during disturbance. Grid setup-2 (fig.2) is considered where the substation has three different types of feeder with different types of loadings and all the feeders have high level of wind energy integration. The maximum load and the installed wind power for different feeders are - 2.5 MW - 4.3 MW (feeder-1), 3.5 MW - 6.5 MW (feeder-2) and 3.5 MW - 5.9 MW (feeder-3). Low level value of the load and the wind power is assumed to be 20% of their respective values. Load power factors are assumed to be 0.98 lagging. Feeder-1 loading is of commercial type, feeder-2 loading is of industrial type and feeder-3 loading is of residential type.

A particular contingency case is considered here. Feeder-3 has surplus of wind power (high wind and low load) while other two feeders (feeder-1 and 2) have a opposite situation (high load and low wind generation). At this state, a three-phase to ground fault with certain fault resistance occurs at bus-6 and after 500 ms, the faulted feeder is removed from the rest of the grid by the protection system at the substation. During this network contingency, four different modes of contingency operations of the wind turbine are investigated. Different operational modes are:

*1) mode-1 inactive mode:* During network disturbance, the gate signals to the PWM converter is blocked, so the production from the turbine is zero during the disturbance period and when the disturbance is removed, the turbine resumes is pre-fault production.

*2) mode-2 normal mode or* $\cos\varphi = 1$ *mode:* The turbine behaves like a constant power source with current limitation. During the fault the turbine will inject the rated active current and the power production from the wind installation depends on the remaining voltage of the grid.

*3) mode-3 reactive current injection mode:* During the fault, the turbine will keep injecting pre-fault active current like the normal operation and depending on the converter size, will inject reactive current.

*4) mode-4 pure reactive mode:* In this mode, the turbine will stop injecting any active current, instead it will inject pure reactive current into the grid. When the normal grid operation is restored, the turbine starts injecting the pre-fault active current.

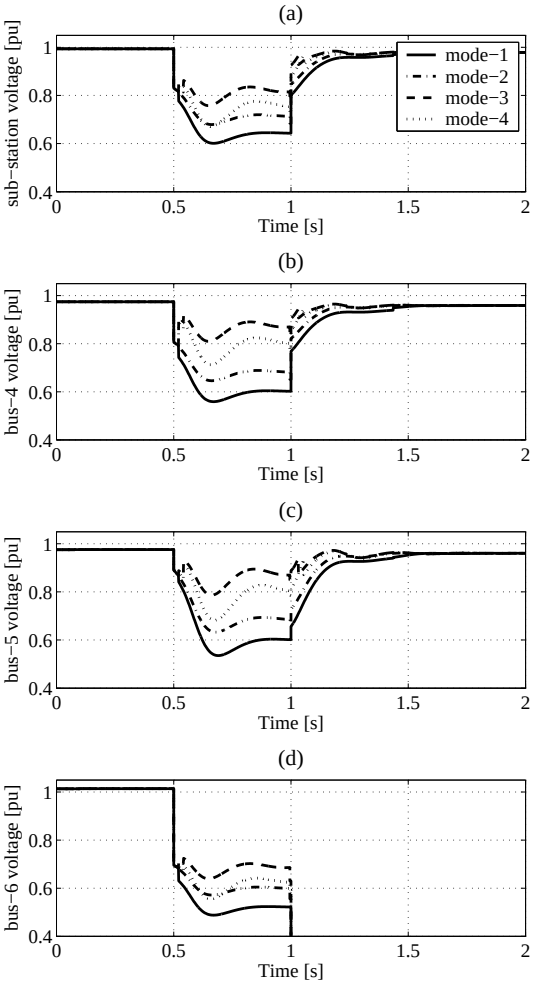


Fig. 13. Voltage profile for the four different operational modes of the wind turbines (a) substation, (b) bus-4, (c) bus-5 and (d) bus-6.

In fig.13, the substation voltage and the three feeder end voltages are shown for the four different operational modes of the wind turbines. From the figure, it is clear that the inactive mode or the mode-1 operation of the wind turbine during grid disturbances is the worst case when the non faulted load voltages go down up to 0.5 pu. In this situation critical loads connected at feeder-1 and 2 (mainly commercial and industrial load) will be disconnected. Mode-2 operation which is the normal operation of the wind turbine is also not an attractive operation from grid point of view. The remaining voltages at the critical loads are around 0.6 pu which will also lead to a load disconnection. Mode-3 operation or the reactive current

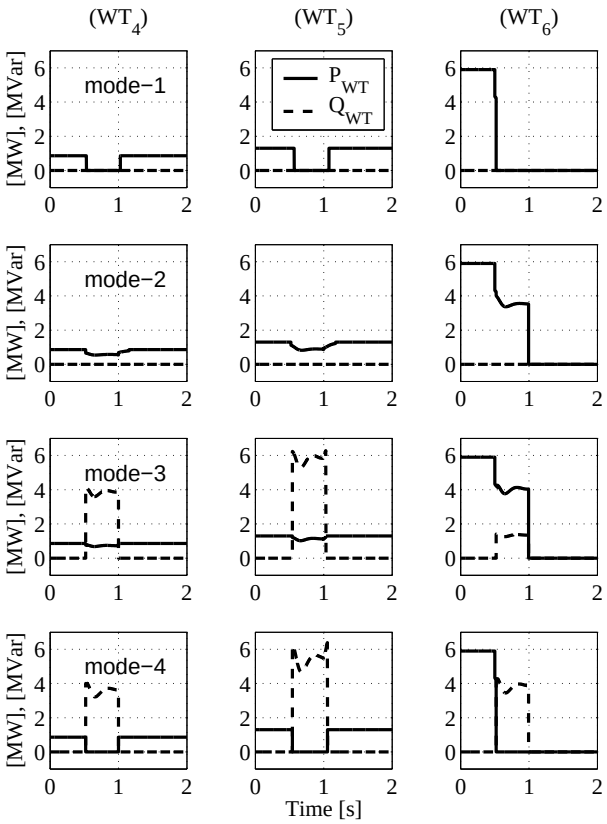


Fig. 14. Active and reactive power of different wind turbines for the four different operational modes.

injection operation seems to be the best suited contingency operational mode of the wind turbine during grid disturbance for this particular case considered here. Non faulted feeders voltages during the fault remain within 0.8 pu and the critical loads interruption is avoided. Finally mode-4 or the pure reactive mode where the wind turbine injects only reactive current, couldn't improve the situation better than the mode-3 operation. The remaining voltages in the critical feeders are around 0.7 pu which means that some of the critical loads will be interrupted.

In fig.14 different wind turbine's active and reactive power production are shown under different contingency operation modes.

The conclusions drawn from the dynamic simulations are:

1) High load-low wind case is the worst case from the load point of view when the primary and secondary voltage lost areas at the load buses are higher for a given voltage dip at the grid.
2) From the remedial action point of view, high wind-low load is a critical case to handle with the reactive power injection by the over-rated grid side converter of the wind turbine keeping the active power production from the wind turbine at the pre-disturbance value, when the voltage disturbance is relatively low (grid voltage dip higher than 85%). During larger voltage disturbance, the required grid side converter capacity becomes larger.

3) A suitable contingency operation of the wind turbine could be to keep the active current at the pre-disturbance value and to inject the reactive current until the grid side converter's current limit is reached.

## V. CONCLUSION

The main conclusions drawn from this work are:

1) Integrating wind power into one feeder of a substation will hardly effect the substation's tap changing transformer. But integration of wind power into several or all of the existing feeders of a substation could influence the tap changing transformer. High penetration of wind power into the local grid can cause thermal overheating of the feeder and the transformer if the integration level is higher than the maximum predicted load.
2) With the high level of wind power integration at the local grid mixed with different critical loads, high load-low wind situation is the worst case from load point of view when the voltage lost area at the load buses will be higher for a given voltage disturbance at the grid. To maintain an acceptable voltage profile at the critical load bus during less severe voltage disturbance (grid voltage dip higher than 85%) by utilizing the reactive power injection capability of the near by wind turbine, the critical situation is the high wind-low load condition where a 20% over-rated grid side converter was required to over come this voltage disturbance keeping the active power production from the wind turbine at the pre-disturbance value. To over come a larger voltage disturbance in this way requires a even larger grid side converter which is not realistic.
3) During a network disturbance, injecting reactive current keeping the active current injection at rated level from the turbine gives the best contingency performance of the wind turbine from the network point of view.

## APPENDIX I

TABLE I
FEEDER AND X-FORMER DATA

| | |
|---|---|
| feeder-1 | R=0.12,X=0.36[$\Omega/km$] L=6$km$ A=250$mm^2$ |
| feeder-2 | R=0.12,X=0.36[$\Omega/km$] L=4$km$ A=250$mm^2$ |
| feeder-3 | R=0.12,X=0.09[$\Omega/km$] L=4$km$ A=250$mm^2$ C=0.26[$\mu$F/$km$] |
| X-former | $S_n$=10$MVA$ $x$=8% |

## ACKNOWLEDGMENTS

In addition to the financial support provided by E.ON Sverige, the author would also like to express gratitude to Åke Juntti, Dan Andersson and Martin Randrup for their valuable technical assistance.

## REFERENCES

[1] T. Thiringer, T. Petru and C. Liljegren, "Power quality impact of a sea-located hybrid wind park," *IEEE Trans. Energy Conv.*, vol. 16, no. 2, pp. 123-127, June. 2001.
[2] T. Ackermann, *Wind Power in Power Systems*, West Sussex: John Wiley and Sons, Ltd., 2005.
[3] P. Kundur *Power System Stability and Control*, New York: McGraw-Hill, Inc., 1994.
[4] T. Gjengedal "Integration of Wind Power and The Impact on Power System Operation," *Proc. Power Engineering, 2003 Large Engineering Systems Conference on*, May. 2003, pp. 76-83.
[5] C. W. Taylor, *Power System Voltage Stability*, New York: McGraw-Hill, Inc., 1994.
[6] ANSI/IEEE Std 446-1987, *IEEE Recommended Practice for Emergency and Standby Power Systems for Industrial and Commercial Applications*, (IEEE Orange Book) 1987.
[7] J. Lamoree, "How utility faults impact sensitive loads," *Electrical World*, pp. 60-63, April 1992.
[8] Math H. J. Bollen, *Understanding PowerQuality Problems*, Piscataway: IEEE Press, 2000.

# The Use of a Combined Battery/Supercapacitor Storage to Provide Voltage Ride-Through Capability and Transient Stabilizing Properties by Wind Turbines

N. R. Ullah*, J. Groot**, T. Thiringer*
* CHALMERS UNIVERSITY OF TECHNOLOGY
Department of Electric Power Engineering
SE-412 96 Gothenburg, Sweden
Tel:0046-31-772 1644 Fax: 0046-31-772 1633
E-mail:{nayeem.ullah, torbjorn.thiringer}@elteknik.chalmers.se
** VOLVO TECHNOLOGY CORPORATION
Dept 06120, Alternative Drivetrains, CTP 9D
SE-412 88 Gothenburg, Sweden

## Acknowledgements

The financial support provided by Sydkraft Research Foundation is gratefully acknowledged.

## Keywords

Transient stability marginal, Power system stability, Wind energy, Fault ride-through, Electrochemical Supercapacitor, EDLC, Ultracapacitor, Energy Storage.

**Abstract** In this paper a dc-link energy storage system for wind turbines is investigated. The purposes of the energy storage are: To use the wind turbine to damp power oscillations occurring in the grid, and to improve the transient stability margin for conventional power production units connected to the grid nearby. In addition, the energy storage system can also be used to provide voltage fault-ride through capability for a wind energy installation. In this paper only modern variable-speed wind turbines with pitch control and a power electronic converter are considered. Two types of energy storage systems will be investigated: Supercapacitors and combined NiMH / Supercapacitor storage system. The batteries will provide the long-term power while supercapacitors (Electrochemical capacitor) will be used for the rapid power transients.

## I. Introduction

Wind turbines will in the future have higher requirements than today regarding their grid performance during network disturbances. Today wind turbines disconnect rather quickly if there is a grid voltage problem. Earlier, when the number (and size) of wind energy installations were fewer (lower), this did not matter so much, but today when certain areas have a substantial wind energy production it can no longer be accepted that wind turbines disconnect unless it is absolutely necessary. Manufacturers are today dealing with this issue. The most commonly proposed method is to use a breaking resistor on the dc-link, which can dissipate the power during a voltage dip. There is an alternative method, if we assume that the turbine is equipped with a modern control system, and that is to adjust the turbine rotor to the new operating situation, which would mean that the turbine shortly overspeeds and then the pitch actuator brings the turbine to a standby situation. The drawback, which most likely is the reason for that this solution is not chosen, is that when the voltage returns, it might not be possible to immediately come back to full power production. In [1] it was demonstrated using experiments on a laboratory set-up that a variable speed wind turbine with a full-power converter can handle various types of voltage dips with only a standard dc-link capacitor. Using more energy storage capacity on the dc-link just facilitates the ability to control the turbine during voltage disturbances.

Another issue that has grown in importance is that the wind turbines apart from staying on-line also should make a contribution to the stability of the grid. Today the installation requirement is usually that the power factor should be one if possible. However, there is a possibility to use the wind turbines to control the voltage level by using another reactive power control strategy. Furthermore, there is an ongoing discussion if wind turbines could be used also for active power efforts, for instance to improve the transient stability margin or to damp power oscillations. This requires a rapid active power control facility of the wind turbine.

A suggestion proposed in this paper is to use a combination of supercapacitors (Electrochemical Capacitors, EC) and batteries as energy storage on the dc-link in order to enhance the stability of the grid during power transients and to improve power oscillation damping. Such a system was investigated both theoretically as well as experimentally for a hybrid electric vehicle system in [2]. Such an energy storage system could also be used to obtain a ride-through function of a variable-speed turbine and give it a limited, quick, but short term active power control ability.

The purpose of this paper is to investigate a battery-supercapacitor energy storage system for a variable speed wind turbine and to study what kind of improvements that such a wind turbine can have on the damping of grid power pulsations as well as on the transient stability margin of a hydro generating unit located nearby.

## II. New Demands on Wind Turbines

### A. Voltage Ride-Through Facility

In Fig. 1 the Swedish voltage ride-through reference curve for larger wind turbine installations suggested by the national grid operator, Svenska Kraftnät is presented.

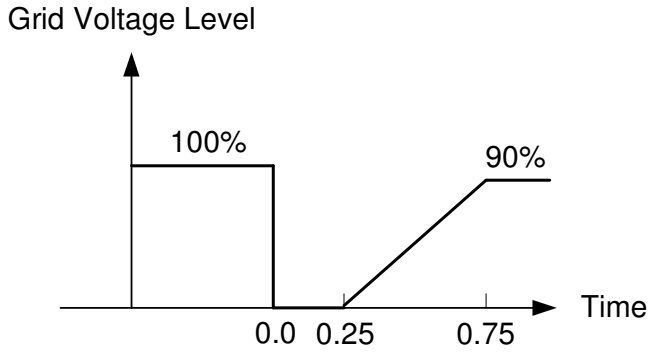


Fig. 1. Reference voltage dip proposed by Svenska Kraftnät.

The voltage dip that wind turbines should be able to handle differs from country to country, but in general the wind turbines should be able to withstand a 0-15 % remaining voltage for 0.1-3 seconds. In Sweden the suggestion is down to 0 % during 250 ms and then up to 90 % during the following 500 ms, as Fig. 1 shows. If the voltage dip is less severe then the reference curve, the demand is that the turbine must stay on-line and may not be disconnected. Since the voltage is low during the dip, it might be necessary to reduce the power flowing out to the grid. This leads to a surplus of energy over the dc-link capacitor and then either the power coming from the turbine must be limited or the power on the dc-link must be dissipated or moved into another storage (thyristor with breaking resistor, battery/EC system).

### B. Active power control

To store energy in a supercapacitor/battery system for the utilisation as spinning reserve is extremely expensive. Spinning reserve means that a power system must have power sources that quickly can make up for the loss of the largest power producing unit in the system. In the Nordic system it is 1200 MW that must be found automatically within a few seconds and last for a quarter of an hour up to a couple of hours until other production units have been started up.

However, there is another feature, that is more realistic that wind turbines with a dc-link energy storage could be used for and that is to increase the transient stability margin. A fairly similar idea was presented in [3], where active load control (switching of resistors connected to a power system node) was utilised to damp oscillations and in this way the transient stability margin was improved. In the same way, a wind turbine equipped with a supercapacitor/battery system could be used. Moreover it is also possible to damp other types of power oscillations that may occur in the grid.

For weak grids and in particular for autonomous grids, the ability to contribute with some part of active power control will definitely be of a great value.

## III. Wind Turbine System Description

In Fig. 2 the proposed modification of the DC-link of the wind turbine is presented. Today the energy storage system for a variable speed wind turbine is a conventional dc-link capacitor.

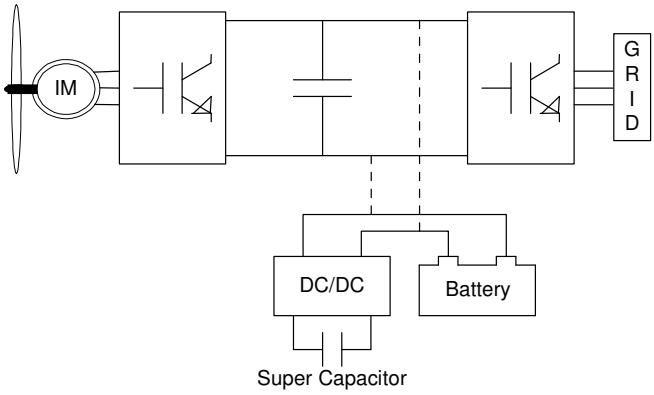


Fig. 2. Proposed energy storage system for a wind energy installation.

## IV. Electric Energy Storage System

### A. Electric Energy Storage System

Any electric storage system [ESS] is designed from application specific constraints. To start with, the usable energy content and the maximum output power determine together with the operation temperature span, the possible topologies. Secondly, the desired lifetime and cyclelife of the system must be taken into consideration. In this reasoning the particular load cycle of the application is vital. In addition, the cost in terms of initial cost, maintenance and lifetime may put another restriction to the design. The design process can then finally be summarized as a series of trade-off relations where the key issue is to determine which property is most important to the particular application.

This section briefly discusses the main electric storage components aimed for use in windpower systems.

## B. Battery

If a battery is used as a main energy storage component, it could typically be connected directly to the DC-bus. Even if the open circuit voltage profile for most batteries are flat compared to capacitors, the minimum voltage at rated power may be too low to ensure proper operation of the DC/AC converter. Therefore, power-optimised batteries with low internal resistance will be the natural choice for this particular application. The restriction of the DC-link voltage also rules out the some potential battery technologies even though they may be able to deliver both desired power and energy.

Low self-discharge is favourable, but on the other hand not a cost driver; a small maintenance charging will be insignificant from an energy efficiency point of view.

Since the batteries will be used to deliver energy during the comparably sparsely occurring voltage disturbances and grid power pulsations, they will be kept fully charged and ready for discharge at rated power. This load cycle will reduce the battery lifetime compared to any low power discharge, but with respect to the high power and energy needed and the relatively low cyclelife desired (see section IV-D), the overall cost may still be acceptable.

Compared to the supercapacitor, any battery is complicated to model. Internal temperature and state of charge (Relative charge level) are two examples of important parameters difficult or practically impossible to measure. Nevertheless, the simplified model presented in Figure 3 can provide sufficient accuracy for the overview simulations made in this paper.

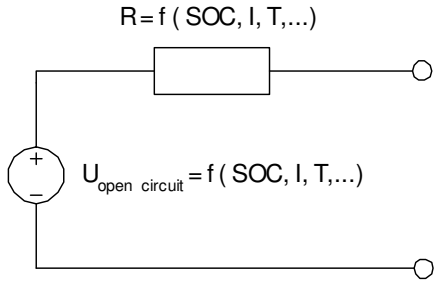


Fig. 3 Battery model used in simulations.

The battery specific parameters used in the model are calculated from measurements on a power optimised NiMH-battery cell operated at +20°C.

## C. Electrochemical Capacitor

The supercapacitor is a far more ideal component than the battery. Lifetime and cyclelife is superior to batteries, and they have extremely high specific power and high current capability at a wide temperature range. The voltage profile is however not favourable, implying that an extra DC/DC converter is needed if power and energy are to be efficiently utilised. On the other hand, if supercapacitors are merely used to provide very short pulses of high power, the limited power and energy available at low working voltage will be of minor interest and the DC/DC converter redundant.

Compared to any battery technology, the energy content is low or very low, but if used together with batteries as a high power supplier the total performance of the energy storage system will be superior compared to using batteries or supercapacitors only.

The self-discharge rate is high, but put in relation to the small energy content (if supercapacitors are *not* used as a primary energy source) it has small impact on the overall performance.

Simulation of supercapacitor performance is simpler than that of batteries. The only vital parameters for an overview simulation, the capacitance and the internal series resistance, are easy to measure and they have an insignificant temperature dependency. A simplified equivalent circuit is shown in Fig. 4. Balancing circuitry has not been taken into account in the simulations, but is represented as a 30% increase in the total cost.

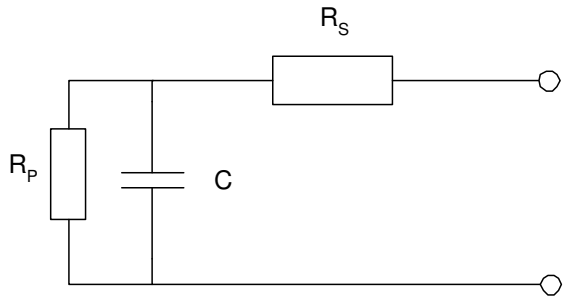


Fig. 4 Simplified equivalent circuit of the supercapacitor.

## D. DC/DC Converter

Even though it is possible to connect supercapacitors directly in parallel with batteries, it is not a favourable solution of several reasons. First of all, the fundamentally different charge and discharge profiles of batteries and supercapacitors limit the maximum usable energy. Secondly, the current and power distribution between the two components is a direct function of internal parameters (internal impedance and voltage), current rate, time, lifetime and operating temperature. Consequently, an estimation of the power distribution and total lifetime is complicated and too uncertain.

Adding a DC/DC converter between the supercapacitors and the DC-link (see Figure 2) solves these potential problems, and also implicate the possibility to separately control the power flow from/to both supercapacitors and batteries. On the other hand, it adds complexity and cost to the electric storage system. In this work the DC/DC-converter will be treated and modelled as an ideal component with a fixed efficiency over the entire voltage and current range.

## E. Cost and Life-cycle

Generally, the prices for complete energy storage system of this size are hard to estimate since the prices are most dependent on the order size and the result of an exclusive business deal. Consequently, the costs presented in this paper should only be seen as brief estimations. Supercapacitor prices have recently reached the long term goal of €0.01 / F. To this figure the cost for a balancing circuitry, which is likely to be vital in this application due to the large charge currents, should be added, 30 % is the figure used in this paper.

In general, battery prices are harder to estimate and depend strongly on technology, order size and manufacturer. A cost of 50€ / cell (NiMH, ≈25Ah) is used in this paper. The DC/DC converter are assumed to follow the approximate price / power relation of 100€ / kW.
When the lifetime of the components is compared, the only general conclusion to be drawn is that the lifetime measured in calendar life or number of cycles at a specified depth is 10-100 times higher for supercapacitors compared to that of batteries.

Estimated cost and life time for the complete energy storage systems discussed are presented in sections VI-A and VI-B.

The occurrence of the faults discussed in this paper, voltage dip, power transients, oscillation damping and long-term power supply is presented in Table-I.

**Table-I Fault cases**

| Fault | Occurrence |
|---|---|
| Voltage dip | 3 / year |
| Oscillation Damping | 1-5 Hz, rated power, < 30 min /day |
| Rated Power Output | 1 / day, < 60s |

### F. Composition of Electric Storage System

In a previous work [2] a combined battery/supercapacitor system was successfully implemented and verified experimentally for a hybrid electric vehicle system. For the implementation in a wind turbine some modifications are needed. The control of the dc-link voltage now becomes more complicated. The dc-link voltage is governed by the grid side converter, generator side converter and the supercapacitor system, apart from the passive control from the battery. The control algorithm for the battery current has also been changed and simplified. Energy is delivered / absorbed to full extent by the supercapacitors as long as the voltage is kept within the permitted range. This strategy is chosen in order to divert as much cycling to the supercapacitors as possible and in this way the lifetime of the battery is increased. It should be stated clearly that the aim of the simulations is to give an overview of the performance rather than to investigate optimal control strategies or to optimise the composition of the electric storage system.

Two main topologies are investigated in this paper; pure supercapacitor storage without DC/DC converter and combined battery-supercapacitor storage system. If supercapacitors are used as the only energy storage component, damping of power oscillations and voltage ride-through facility will be possible, but with limited rated power output capacity due to the low energy content. The use of a combined battery-supercapacitor system will not only make full power performance possible for a somewhat longer time, it will also extend the maximum ride-trough time for any of the faults discussed. In either case the design is based on the permitted voltage range and minimum ride-trough time for the discussed fault types.

## V. Analysis of Wind Turbine System with a Large DC-link Storage

### A. Investigated Power System

A one machine – infinite bus system has been employed to analyze the impact of the active wind turbine on a grid disturbance. The generator bus (BUS1) is equipped with a phasor measurement unit (PMU). The phasor measurement unit is used to get the voltage phasor angle of the bus voltage. More detailed information about a phasor measurement unit can be found in [4]. A three-phase to ground fault (250 ms duration) is applied at the end of the first pi-link of the line (BUSA – BUS2) as grid disturbance, resulting in a power oscillation. The energy storage system of the active wind turbine is assumed to have the same power rating as the wind turbine. This means that in case that the wind turbine should be able to feed out a power increase of 1 pu when it is already operating at rated power, the grid side converter needs to be overdimensioned by a factor of two. The cost for such an

overdimensioning is most likely only 1-2 % of the total cost of the wind turbine [5], especially if only a very short-term power peak is needed. Typically it is for the improvement of the transient stability margin that the power needs to exceed 1 pu. For the damping of power pulsations and the voltage dip ride-through function there is no need for an overdimensioning. In this paper we refer to this system as 'active WECS' (Wind Energy Converter System). The layout of the investigated system is shown in Fig. 5. The control of the power flow from the energy storage system uses the voltage phase angle of BUS1 relative to the voltage phase angle of the swing bus (BUS2). When the angle difference signal is outside a dead band region (+/- 20% of the average value), energy starts to flow between the grid and the energy storage system. The average power of the hydro generator is 62 MW and the generator bus voltage phase angle difference towards the swing bus is 44$^o$ before the disturbance occur. The active WECS absorbs energy from the bus when the derivative of the angle difference signal is positive and it injects energy into the bus when the derivative is negative.

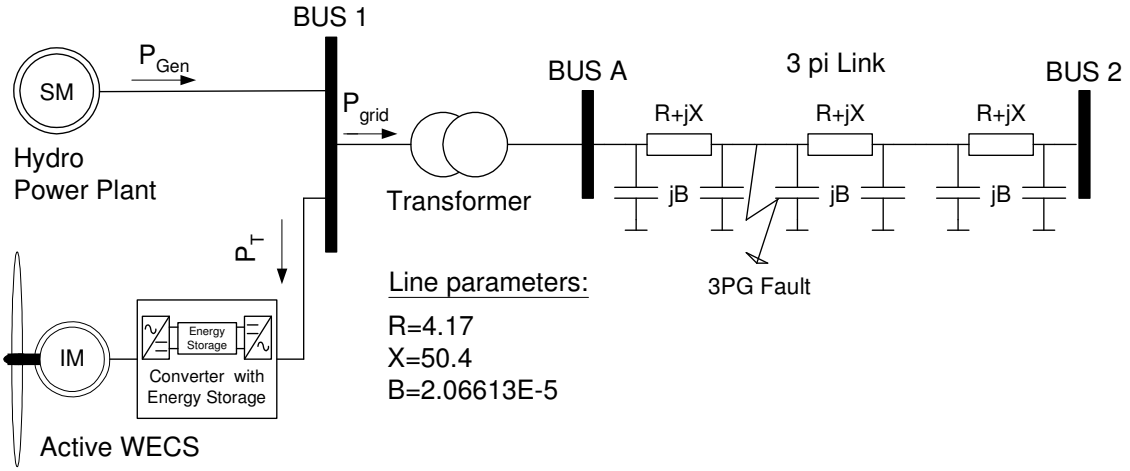


Fig. 5 Layout of the investigated power system with an active WECS

When a fault occurs on a line, the electrical output from the generator is greatly reduced during the fault and may even reach zero for a fault close to the generator. Assuming that the mechanical power input remains constant during the first transient swing, the excess mechanical power during the transient period will accelerate the generator rotor. As the machine speed increases, the generator rotor angle also increases. When the fault is cleared, the generator rotor starts decelerating and the rotor angle reaches a maximum value. At this operating point the generator electrical power output is higher than the mechanical input power of the generator. So the rotor angle will start decreasing from this value and it will reach a minimum value. This oscillation persists until it dies out by the system inherent damping. If a load is connected near the generator during the transient period then the excess mechanical power could be used by the load instead of accelerating the generator rotor. The proposed energy storage system could be used for this purpose. When the generator rotor angle starts increasing immediately after the fault, the energy storage system of the active WECS is switched to the bus (BUS1) and some of the excess mechanical power of the turbine is used to charge the energy storage system and the rest is used to accelerate the generator rotor. As could be expected, the maximum generator rotor swing will be less when the energy storage system is active because in this case less amount of power is available for accelerating the generator rotor [6].

The impact of the active WECS during and after a transient disturbance has been studied in this section using various relative power rating of the WECS. The proposed battery/supercapacitor energy storage system has been employed for two main purposes: 1. to improve the transient stability margin (TSM) and 2. to improve the damping of the power oscillation. The definition of transient stability margin is shown in Fig. 6. When the power into the grid ($P_{grid}$) exceeds the average value, the energy

storage system of the WT absorbs the energy and when it is below the average value, the energy storage system injects the energy. In this way the system can provide damping of the grid power oscillation and improve the TSM.

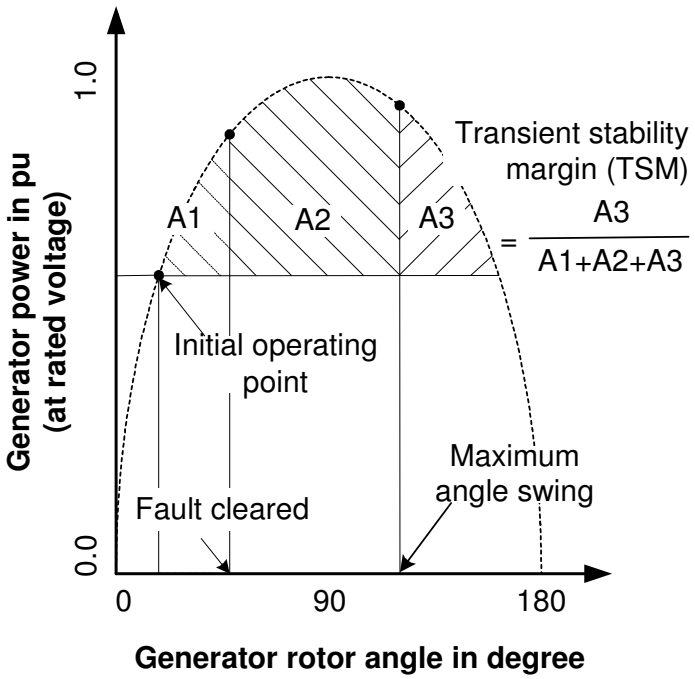


Fig. 6 Transient stability margin.

**B. Impact of the Active WECS on Transient Stability Margin:**

The definition of transient stability margin used in this paper is shown in Fig. 6. The area under the power-angle curve indicated by 'A2+A3' is the area available for the generator to dissipate the accelerating energy that has been gained during the transient period. The area indicated by 'A3' is the margin available for the generator depending on the present operating point and the severity of the fault. The ratio between area 'A3' and 'A1+A2+A3' is defined as the transient stability margin.

Fig. 7 shows the angle difference signal with the active WECS connected where it is shown that maximum transient angle swing is reduced with increased WECS rating. Fig. 8 shows the percentage gain in TSM with different WECS rating. As is expected, the TSM increases with the rating of the WECS system. An active WECS with rated power of 10% of the hydro generator power can improve the TSM by 17% and one with 20% power of the hydro generator can improve it by 28%.

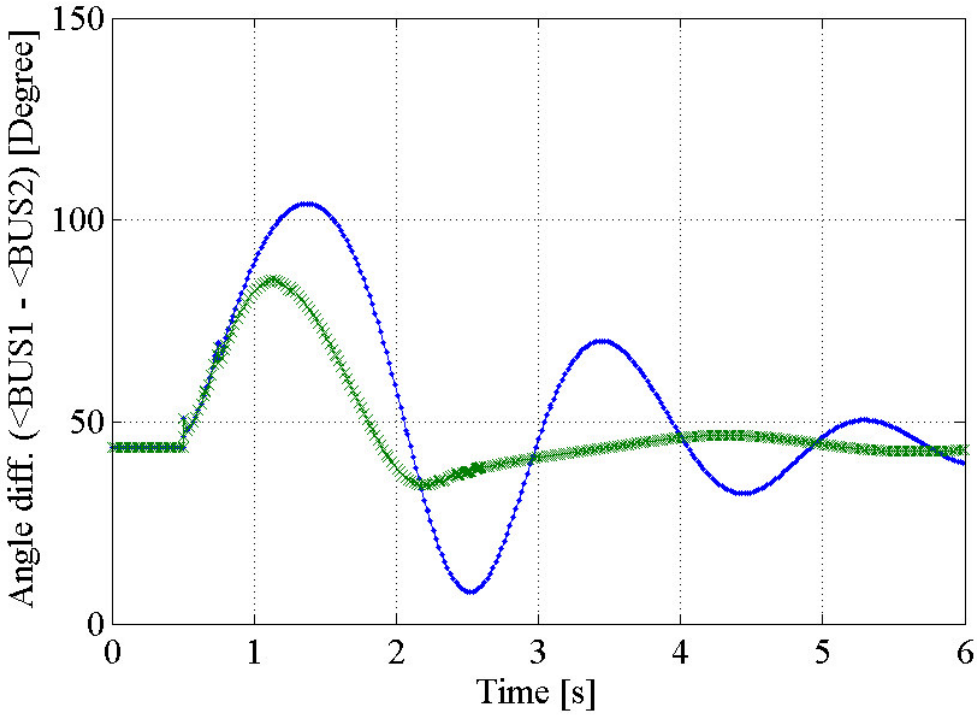


Fig. 7 Hydro generator voltage phase angle relative to the swing bus [dot – no WECS connected, cross –WECS connected (20% of the hydro generation)]

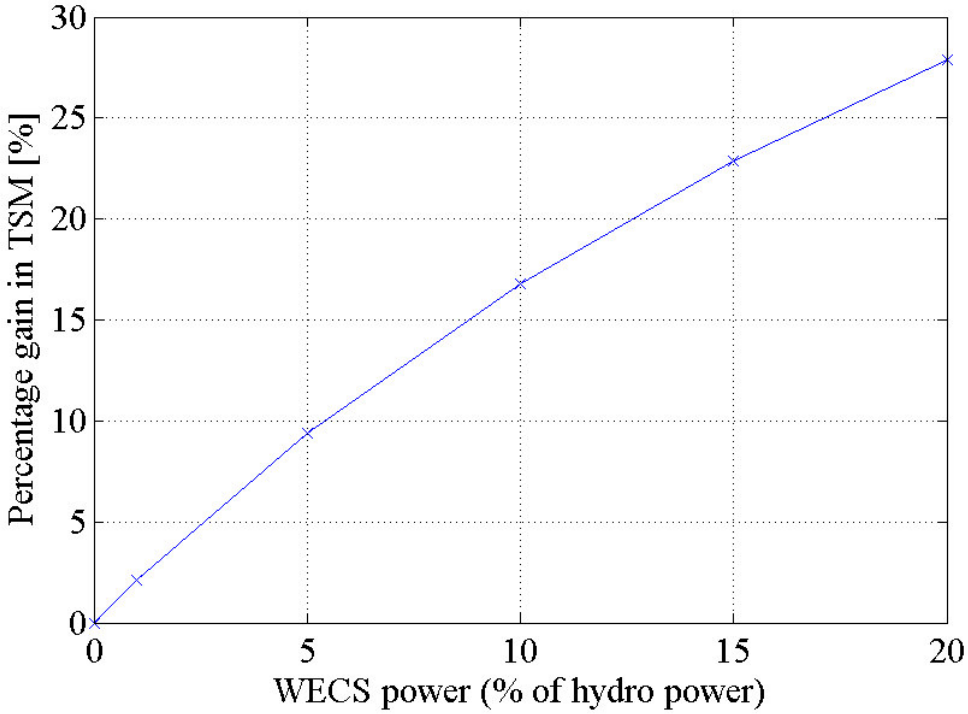


Fig. 8 Percentage gain in TSM with different relative WECS

**C. Impact of the Active WECS on Damping Constant:**

Besides improving the TSM, the active WT could be used to increase the damping of the power oscillation. This is accomplished by subsequent charging and discharging of the energy storage system. When the derivative of the angle difference signal or the speed deviation signal is positive, the energy storage system stores energy and when the speed deviation signal is negative, the energy storage system delivers the energy back to the grid in order to counteract the speed variation of the turbine-generator. In this way it could assist in damping of the power oscillation. In Fig. 9 the response to the grid disturbance is presented for two cases – one with a passive WECS and one with an active WECS with a rating of 20% of the hydro generator. From Fig. 9 it is obvious that a rapid damping of the dynamic power oscillation could be achieved using an active WECS. The percentage gain in damping constant of the power oscillation with varying WECS power is shown in Fig. 10. The percentage gain in damping constant increases with the increasing wind energy installation power. A wind energy installation with 10% of the hydro generator power increases the damping by 48% and one with 20% of the hydro generator power increases it by 73%.

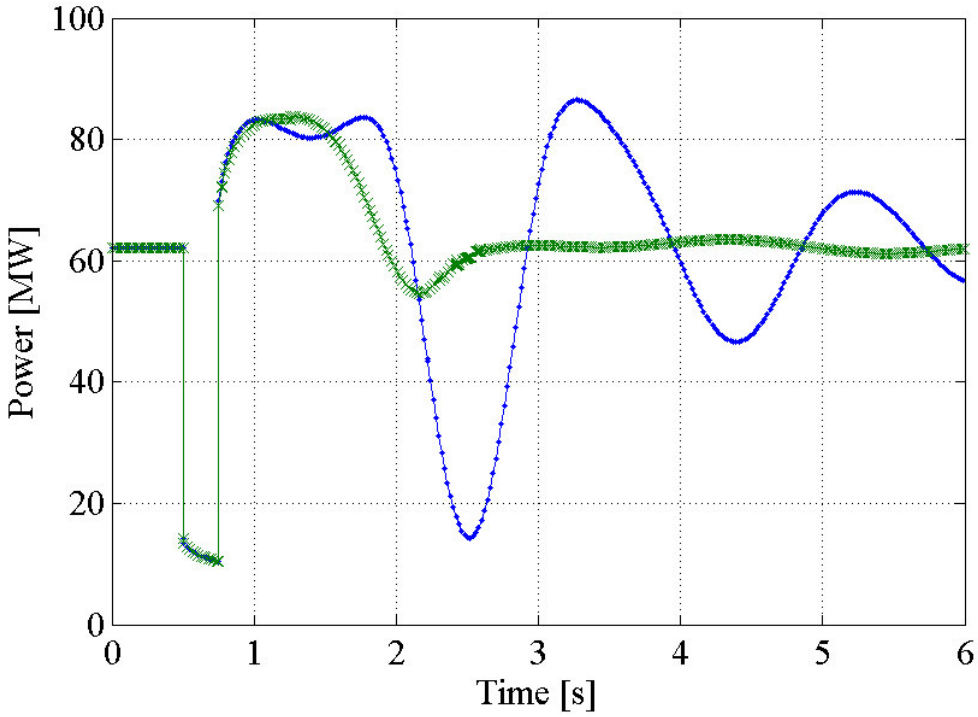


Fig. 9 Grid power from the hydro generator – WECS system [dot – no WECS connected, cross – WECS connected (20% of the hydro generation)]

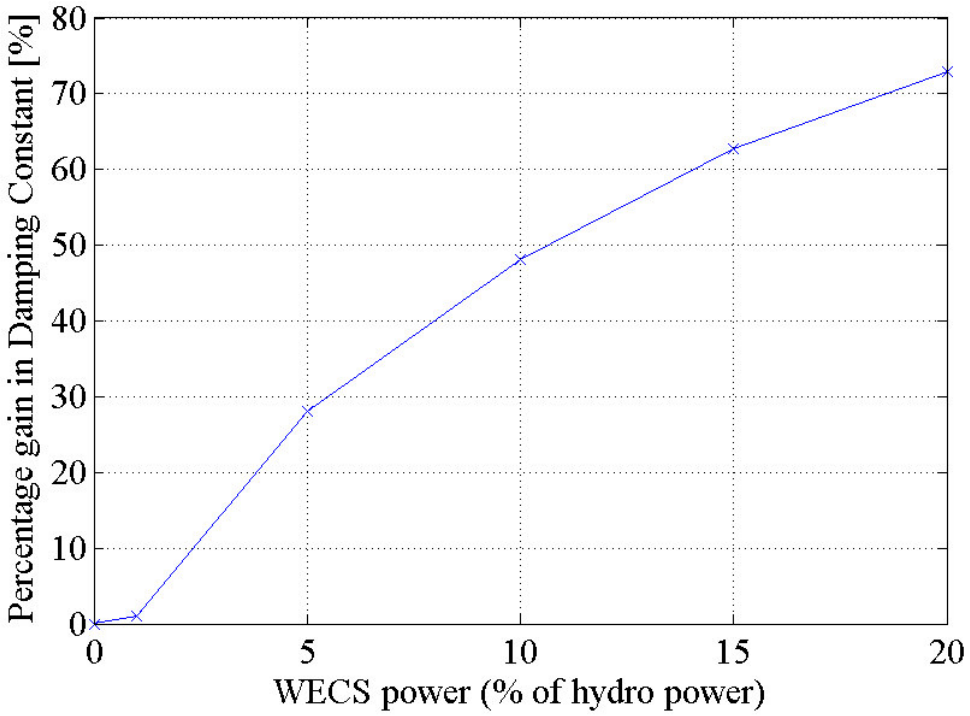


Fig. 10 Percentage gain in damping constant with relative WECS

Finally the value of maximum angle swing and damping constant with varying active WT power is shown in table-II.

**Table-II List of maximum angle swing and damping constant.**

| | **No WECS connected** | **WECS connected [ - % of hydro generator power]** | | | | |
|---|---|---|---|---|---|---|
| | | **1%** | **5%** | **10%** | **15%** | **20%** |
| **Maximum angle swing** | 104° | 103° | 97° | 92° | 88° | 85° |
| **Damping constant** | 0.20 | 0.21 | 0.29 | 0.40 | 0.55 | 0.76 |

## VI. Investigated Energy Storage System

In this section, the two discussed energy storage systems are simulated and their operation properties and performance is highlighted, followed by a summary with selected performance parameters and cost / life-time estimations. A short presentation of the initial conditions and operation limits are presented in table-III below.

**Table -III Initial conditions and operation limits**

| Parameter | Value | Unit |
|---|---|---|
| Nominal DC-link Voltage | 1200 | V |
| Maximum DC-link Voltage | 1300 | V |
| Minimum DC-link Voltage | 1000 | V |
| Nominal Power [Pn] | 1 | MW |
| Maximum Current | 1000 | A |
| Maximum DC/DC Current (EC side) | 1500 | A |
| DC/DC Efficiency | 95 | % |
| Initial battery SOC | 100 | % |
| Initial EC SOC | ≈ 85 | % |
| Voltage Dip | 0% in 250ms, 0-0.9 Pn in following 500ms | |
| Power Damping | 1-5 Hz, rated power output | |
| Rated Power Output | < 60 s, 1.0 Pn discharge power | |
| Lifetime | 30 years | |

When the energy storage system is used to damp power oscillations, the time specified in the results tables represents the maximum time per day that the system can withstand without additional replacement or maintenance during the desired 30 year lifetime.

During voltage dips, only the supercapacitors are active since the batteries are fully charged to be ready for rated power output. An active balancing circuitry is included in the EC prices.

## A. Supercapacitor Storage System

In table-IV and table-V, the simulation results are shown for the different fault cases and the two design topologies. Estimated costs are also presented.

**Table -IV Results with supercapacitor storage system**

| **Size & Limits** | | |
|---|---|---|
| EC bank size | 15.6 | F |
| | 1800 | A |
| | 1000-1300 | V |
| | 500 000 | Cycles at 70% usage |
| | 13 | MJ (total energy) |
| | 11 | MJ (available at 85% SOC) |
| **Performance** | | |
| Voltage Dip | 250 ms at 1.0 Pn | |
| Power Damping | 22 min / day | |
| Rated Power Output | EC bank only, U > 1000 V: 1.2s | |
| | EC bank only, U > 900 V: 2.5s | |
| | EC bank and DC/DC: 4.2s | |

| Cost | | |
|---|---|---|
| Initial Cost | 55 000 | € |
| with DC/DC | 155 000 | € |

### B. Combined Supercapacitor / Battery Storage System

**Table -V Results with combined supercapacitor / battery storage system**

| Size & Limits | | |
|---|---|---|
| EC-bank size | 15.6 | F |
| | 1800 | A |
| | 400-1300 | V |
| | 500 000 | Cycles at 70% usage |
| | 13 | MJ (total energy) |
| | 11 | MJ (available at 85% SOC) |
| NiMH battery size | 100 | Ah |
| | 1200 | A |
| | 1130 | V (nominal) |
| | 1000 | Cycles at 100% usage |
| | 4.1 | MJ (total energy) |
| DC/DC Converter | 1 | MW |
| | 1500 | A |
| | 1300 | V |
| **Performance** | | |
| Voltage Dip | 250 ms at 1.0 Pn | |
| Power Damping | 22 min / day | |
| Rated Power Output | EC only: 4.2s | |
| | EC & NiMH, U > 1000V: 56s | |
| | EC & NiMH, U > 900V: 133s | |
| **Cost** | | |
| Initial Cost | 336 000 | € |

In Fig. 11, the power coming from the storage system during a situation where the grid needs as much active power as possible is presented. Initially the power is delivered by the supercapacitor system, but as the supercapacitor voltage decreases (see Fig. 12), the current is increased (see Fig. 13) until the DC/DC current limit is reached. At this point, the battery is used to deliver the residual power until the lower voltage limit of the supercapacitors is reached and the battery is forced to deliver the full power.

The limited efficiency of the DC/DC converter is shown in the time period 1-5s in Fig. 11, where the supercapacitors will have to deliver more power than the desired output power.

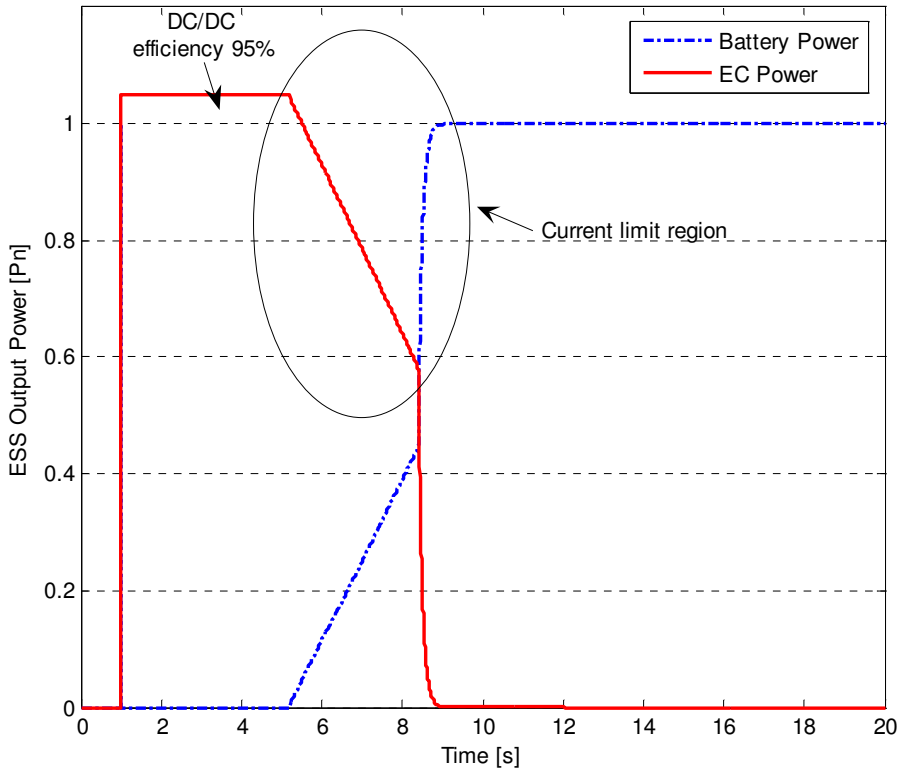


Fig. 11 Combined supercapacitor / battery output power during "Rated Power Output" operation.

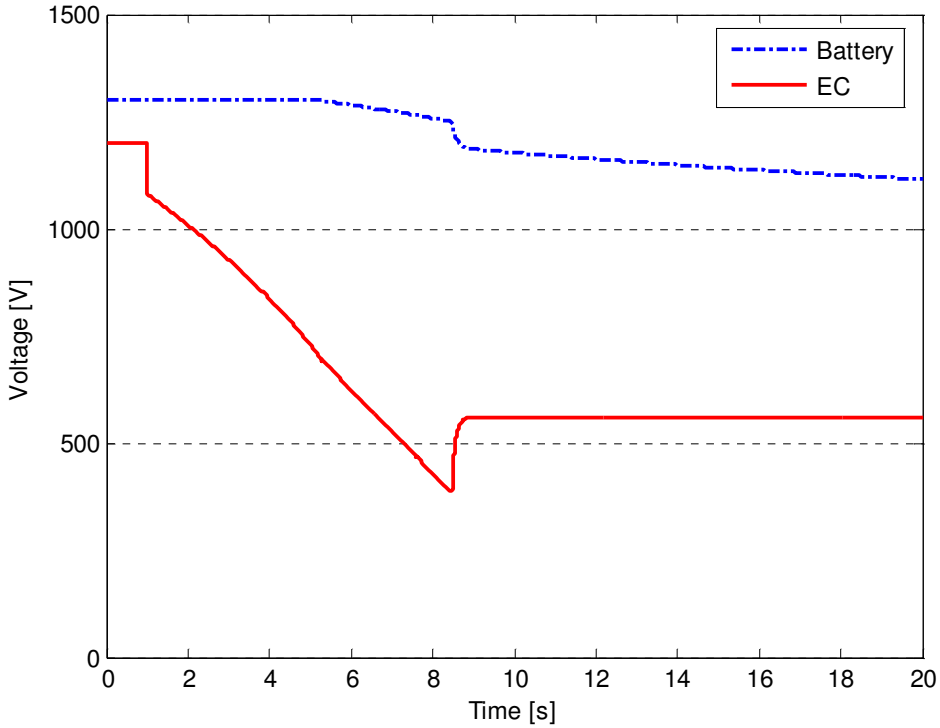


Fig. 12 Combined supercapacitor / battery voltage during "Rated Power Output" operation.

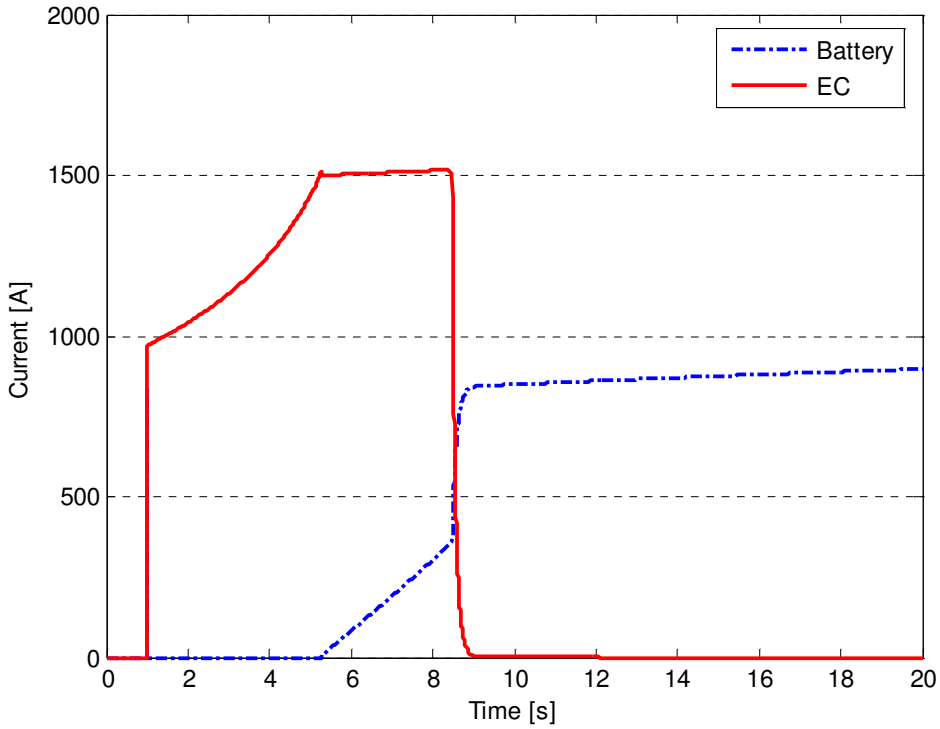


Fig. 13 Combined supercapacitor / battery output current during "Rated Power Output" operation.

### C. Discussion on the DC-Link Energy Storage System

With supercapacitors as the primary energy storage component directly connected to the DC-link, performance is strongly restricted by the voltage limits. In addition to the 60% non-used energy at 1000V open circuit voltage, the voltage drop caused by the internal resistance, limits the energy even further. Performance is significantly enhanced when a dc/dc-converter as well as when a combination of both battery and EC's are used.

When the energy storage system is used to deliver power during transients and long-term power output, the operation is significantly limited by the voltage limits of the dc/dc-converter. If a lower DC-link voltage could be accepted during extreme conditions, performance is enhanced for both EC-system and the combined supercapacitor / battery system. The lifetime cost is estimated for 30 years of operation, where the batteries and supercapacitors are replaced after delivering energy corresponding to the maximum cyclelife.

It should be mentioned that the price for a 1 MW wind turbine including grid connection is about 0.8 M€. This means that although the costs of the energy storage systems are high, they are not at all unrealistic. Depending on the grid situation at the site, an assessment must be made regarding if it is worth to invest in dc-link storage capacity.

## VII. Conclusion

A battery/supercapacitor energy storage system for a variable speed wind turbine has been investigated in this paper. This new energy storage system has been found to give wind turbines the possibility to increase the transient stability margin and to damp grid power oscillations. For instance, the transient stability margin of a nearby located hydro power generating unit was increased by 28 % by utilising the suggested solution on a wind power installation with a rating of 20 % of the hydro power. Moreover it was found that the damping ratio of a grid power oscillation could be improved by 73 % using this system. In addition, this energy storage system also gives the wind turbine a voltage ride-through function. It has been found that performance is significantly enhanced when this combined energy storage system is used instead of the supercapacitors alone.

## VIII. References


[1] Ottersten, R., Petersson, A., Pietiläinen, K., "Voltage sag response of PWM rectifiers for variable-speed wind turbines", 2004 Nordic Workshop on Power and Industrial Electronics (NORpie 2004), Trondheim, Norway, June 13-16, 2004

[2]. Andersson, T., Groot, J., Berg, H., Lindström, J., Thiringer, T., "Alternative Energy Storage System for Hybrid Electric Vehicles". 2004 Nordic Workshop on Power and Industrial Electronics (NORpie 2004), Trondheim, Norway, June 13-16, 2004

[3]. Ullah, N.R., Olasumbo, O., Daalder, J., "PMU based damping algorithm of power oscillation by resistive load switching", 4th IASTED International Conference on Power and Energy Systems - EuroPES 2004, June 28 - 30, 2004, Rhodes, Greece

[4] http://www.abb.com/substationautomation

[5] Petersson, A., Lundberg, S., Thiringer, T., "A DFIG wind-turbine ride-through system influence on the energy production", Nordic Wind Power Conference 2004, 1-2 March 2004, Gothenburg, Sweden.

[6] Narain G., Hingorani, Laszlo Gyugyi, "Understanding facts : concepts and technology of flexible AC transmission systems" (Piscataway, NJ: IEEE Press, 2000).